ผลของขนาดอนุภาคและการปรับปรุงพื้นผิวของอนุภาคนาโนซิลิกาต่อสมบัติของพอลิเบนซอกซาซีนคอมพอสิท

นายณัฐพล เลียวธัญญรัตน์

วิทยานิพนธ์นี้เป็นส่วนหนึ่งของการศึกษาตามหลักสูตรปริญญาวิศวกรรมศาสตรมหาบัณฑิต
สาขาวิชาวิศวกรรมเคมี ภาควิชาวิศวกรรมเคมี
คณะวิศวกรรมศาสตร์ จุฬาลงกรณ์มหาวิทยาลัย
ปีการศึกษา 2558

EFFECTS OF PARTICLE SIZE AND SURFACE TREATMENT OF SILICA NANOPARTICLE ON PROPERTIES OF POLYBENZOXAZINE COMPOSITES

Mr. Nutthaphon Liawthanyarat

A Thesis Submitted in Partial Fulfillment of the Requirements
for the Degree of Master of Engineering Program in Chemical Engineering
Department of Chemical Engineering
Faculty of Engineering
Chulalongkorn University
Academic Year 2015

Thesis Title	EFFECTS OF PARTICLE SIZE AND SURFACE TREATMENT OF SILICA NANOPARTICLE ON PROPERTIES OF POLYBENZOXAZINE COMPOSITES
By	Mr. Nutthaphon Liawthanyarat
Field of Study	Chemical Engineering
Thesis Advisor	Associate Professor Sarawut Rimdusit, Ph.D.

Accepted by the Faculty of Engineering, Chulalongkorn University in Partial Fulfillment of the Requirements for the Master's Degree

.....Dean of the Faculty of Engineering

(Associate Professor Supot Teachavorasinskun, D.Eng.)

THESIS COMMITTEE

.....Chairman

(Associate Professor Siriporn Damrongsakkul, Ph.D.)

.....Thesis Advisor

(Associate Professor Sarawut Rimdusit, Ph.D.)

.....Examiner

(Associate Professor Varong Pavarajarn, Ph.D.)

.....External Examiner

(Assistant Professor Chanchira Jubslip, D.Eng.)

ณัฐพล เลียวธัญญรัตน์ : ผลของขนาดอนุภาคและการปรับปรุงพื้นผิวของอนุภาคนาโนซิลิกาต่อสมบัติของพอลิเบนซอกซาซีนคอมพอสิท (EFFECTS OF PARTICLE SIZE AND SURFACE TREATMENT OF SILICA NANOPARTICLE ON PROPERTIES OF POLYBENZOXAZINE COMPOSITES) อ.ที่ปรึกษาวิทยานิพนธ์หลัก: รศ. ดร. ศราวุธ ริมดุสิต, 109 หน้า.

คอมพอสิทที่เติมสารเติมปริมาณสูงจากนาโนซิลิกาและเบนซอกซาซีนถูกวัดสมบัติทางกลและทางความร้อนตามปริมาณการเติม, ขนาดของอนุภาคและการปรับปรุงพื้นผิวของอนุภาค โดยนาโนคอมพอสิทถูกเตรียมด้วยการผสมแบบแรงเฉือนสูงตามด้วยการใช้แรงอัด เบนซอกซาซีนมอนอเมอร์ซึ่งมีความหนืดต่ำทำให้ความสามารถในการอาบนาโนซิลิกาดีเยี่ยม ซึ่งสามารถเติมนาโนซิลิกาที่ไม่ปรับปรุงพื้นผิวได้สูงถึง 20, 25, 40 และ 45 เปอร์เซ็นต์โดยน้ำหนักตามขนาดของอนุภาค 7, 14, 20 และ 40 นาโนเมตรตามลำดับ ในขณะที่ปริมาณการเติมสูงสุดของอนุภาคที่ทำการปรับปรุงพื้นผิววัดที่ 30 เปอร์เซ็นต์โดยน้ำหนัก นอกจากนี้การเพิ่มขึ้นของสมบัติทางกล (มอดูลัสสะสมและค่าความแข็ง)ของคอมพอสิทจากเบนซอกซาซีนและนาโนซิลิกาพบว่าเพิ่มขึ้นมากกว่าคอมพอสิทของอีพอซีและนาโนซิลิกาอย่างมีนัยสำคัญที่ปริมาณการเติมสูงสุดของแต่ละขนาดของอนุภาคนาโนซิลิกา ความสัมพันธ์ของค่ามอดูลัสของนาโนคอมพอสิทกับปริมาณของอนุภาคนาโนซิลิกาได้ถูกทำให้เข้ากันได้ดีโดยใช้สมการทั่วไปของ Kerner นอกจากนี้ ค่าความแข็งของอนุภาคนาโนซิลิกาที่เติมลงในพอลิเบนซอกซาซีนคอมพอสิทที่ปริมาณการเติมสูงสุดที่สูงถึง 625 MPa ซึ่งผลการทดลองเข้ากันได้กับแบบจำลองของ Halpin-Tsai มากกว่านั้นการเพิ่มขึ้นอย่างมากของอุณหภูมิการเปลี่ยนสถานะคล้ายแก้วของคอมพอซิทของอนุภาคนาโนซิลิกาที่เติมลงในพอลิเบนซอกซาซีนที่ปริมาณการเติมสูงสุดได้ถูกพบที่ 203 $^{\circ}$C ในขณะที่อุณหภูมิการเปลี่ยนสถานะคล้ายแก้วของพอลิเบนซอกซาซีนถูกวัดได้ที่ 185 $^{\circ}$C อุณหภูมิการสลายตัวทางความร้อนที่การสูญเสียมวล 5 เปอร์เซ็นต์โดยน้ำหนักของนาโนคอมพอซิทเปลี่ยนอย่างมีนัยสำคัญต่ออุณหภูมิที่สูงขึ้นตามปริมาณของนาโนซิลิกาและขนาดที่เล็กลงของนาโนซิลิกา นาโนคอมพอสิทแสดงการลดลง 89 เปอร์เซ็นต์ของค่าอัตราการสึกหรอที่ปริมาณการเติมสูงสุดของนาโนซิลิกา สัมประสิทธิ์การเสียดทานของนาโนซิลิกาที่เติมลงในพอลิเบนซอกซาซีนคอมพอสิทถูกพบว่าเพิ่มขึ้นตามปริมาณนาโนซิลิกา นอกจากนี้สมบัติทางกลและทางความร้อนของนาโนคอมพอซิทที่เติมนาโนซิลิกาที่ไม่ทำการปรับปรุงพื้นผิวจะดีกว่านาโนคอมพอสิทที่เติมนาโนซิลิกาที่ทำการปรับปรุงพื้นผิว ซึ่งเป็นเพราะนาโนคอมพอซิทที่เติมนาโนซิลิกาที่ไม่ทำการปรับปรุงพื้นผิวสามารถเกิดพันธะระหว่างนาโนซิลิกาที่ไม่ปรับปรุงพื้นผิวกับพอลิเบนซอกซาซีน

ภาควิชา วิศวกรรมเคมี ลายมือชื่อนิสิต .....

สาขาวิชา วิศวกรรมเคมี ลายมือชื่อ อ.ที่ปรึกษาหลัก .....

ปีการศึกษา 2558

5670199721 : MAJOR CHEMICAL ENGINEERING

KEYWORDS: POLYBENZOXAZINE; NANOCOMPOSITES; NANOSILICA; THERMOMECHANICAL PROPERTY; HIGHLY FILLED COMPOSITE.

NUTTHAPHON LIAWTHANYARAT: EFFECTS OF PARTICLE SIZE AND SURFACE TREATMENT OF SILICA NANOPARTICLE ON PROPERTIES OF POLYBENZOXAZINE COMPOSITES. ADVISOR: ASSOC. PROF. SARAWUT RIMDUSIT, Ph.D., 109 pp.

Highly filled polybenzoxazine nanocomposites filled with nanosilica particles were investigated for their mechanical and thermal properties as function of filler loading, particle size and surface treatment. The nanocomposites were prepared by high shear mixing followed by compression molding. A very low viscosity of benzoxazine monomer gives it excellent processability having maximum untraeted nanosilica loading as high as 20, 25, 40 and 45 wt% with nanoparticle size of 7, 14, 20 and 40 nm, respectively, while the maximum loading of treated nanosilica was measured to be 30 wt%. In addition, the enhancement in mechanical properties (storage modulus and microhardness) of the nanosilica filled polybenzoxazine composites was found to be significantly higher than that of the recently reported nanosilica filled epoxy composites at maximum loading of each particle size of nanosilica. The dependence of the modulus value of nanocomposite on the nanosilica content is well fitted by the generalized Kerner equation. Furthermore, the microhardness of the nanosilica filled polybenzoxazine composites at maximum loading of nanosilica up to 625 MPa was achieved, which the experimental data agree with Halpin-Tsai model. Moreover, the substantial enhancement in glass transition temperature (T_g) of the nanosilica filled polybenzoxazine composites at maximum loading of nanosilica was observed to be 203 $^{\circ}$C, while the T_g of neat polybenzoxazine was mesured to be 185 $^{\circ}$C. The degradation temperature at 5 % weight loss ($T_{d,5}$) of the nanocomposites shifted significantly to higher temperature as a function of the nanosilica contents and smaller size of nanosilica. The nanocomposite shows reduction in specific wear rate by 89% at maximum loading content of nanosilica. Coefficient of friction (COF) of nanosilica filled polybenzoxazine composites was found to increase with nanosilica content. In addition, the mechanical and thermal properties of nanocomposite with untreated nanosilica was better than that of nanocomposite with treated nanosilica, which it was due to nanocomposites filled untreated nanosilica can form chemical bonding between the untreated nanosilica and the polybenzoxazine matrix.

Department: Chemical Engineering Student's Signature .....

Field of Study: Chemical Engineering Advisor's Signature .....

Academic Year: 2015

ACKNOWLEDGEMENTS

I am sincerely grateful to my advisor, Assoc. Prof. Dr. Sarawut Rimdusit, for his invaluable guidance and valuable suggestions including constant encourage throughout this study.

I am also grateful to my committee members, who provided constructive and scientific advices for the completion of this thesis. This includes, Assoc Prof. Dr. Siriporn Damrongsakkul and Assoc Prof. Dr. Varong Pavarajarn, from the Department of Chemical Engineering, Faculty of Engineering, Chulalongkorn University and Asst. Prof. Dr. Chanchira Jubsilp from the Department of Chemical Engineering, Faculty of Engineering, Srinakharinwirot University.

I am very thankful for every inspiration that they have made throughout my difficult years. They are more than my best friends. Thank are also extended to every polymer engineering research laboratory member for every constructive discussion they contributed and all their help.

Finally, my deepest regard to my beloved family and parents, who have always been the source of my support and encouragement. There is never a single day without them standing by me. It is why I can journey this far. I am lifetime beholden.

CONTENTS

Page

Page

Page

LIST OF FIGURES

Figure Page

LIST OF TABLES

Table Page

CHAPTER I
INTRODUCTION

1.1 General introduction

Polymer nanocomposites have been studied by of various past investigations due to their unique properties and much potential applications. It is well known that polymer nanocomposites have excellent mechanical properties due to their extremely high interface area between nanoparticles and polymer [1-8]. Their high interface leads to a potentially great bonding between the two phases and hence great strength and/or toughness properties. Specifically, when the nanoparticles become part of the friction layer, they will increase the nominal area of the contact resulting enhances mechanical properties, coefficient of friction and reduction of wear of the components [9]. Therefore, various good characteristics of neat polymers, such as low weight, ductility, good process ability, as well as transparency will be obtained after the addition of nanoparticles in the mixture. In recent years, nanosilica [1-6], carbon nanotube [7], and carbon black [8] mostly commonly used as additives to achieve overall performance of polymer substantially.

Nanosilica is a very versatile reinforcement for thermoplastic [8, 10] and thermosetting matrices [1-3]. Thermosetting polymers such as epoxies [1, 3] and phenolic resins [11] finds great usage as component material for electronic packaging, coatings and similar processes. For industrial applications, nanosilica particles find

major use in improving mechanical and thermal properties of polymers. Additionally, nanosilica particles can reinforce polymer matrices to lower shrinkage upon curing, decreasing coefficient of thermal expansion [12], increasing fracture toughness, impact strength, and modulus [1], additives for friction materials [4-6] and improving adhesion property [3]. In addition, it is a relatively light ceramic material because its density is of about 2.203 g/cm^3 [13]. Highly dispersed precipitated silica exhibit specific chemical affinity to various polymers, resins and components of paints and varnishes. Initially, they are hydrophilic and chemical affinity to typical hydrocarbon polymers is restricted [14, 15]. For this reason it is very important to conduct surface modification of silicas so that they can be used more effectively [16]. Selection of suitable modifying substances [17] and the method in modification of the surface of the highly dispersed silicas is performed and seems to be very important. For this purpose various types of surface treatment chemical compounds can be used including surfactants [18], silane coupling agents [19-21]. Following modification, silicas exhibit specific physicochemical and surface properties. In particular case, their surface becomes more hydrophobic, exhibiting more affinity to organic compounds.

Polybenzoxazines are a new class of thermosetting polymers that have achieved much attention due to their reported excellent performance and high flexibility in molecular design [22]. Polybenzoxazines have the attractive properties of the traditional phenolic resins, such as cost effectiveness, heat resistance and flame

resistance. In addition, they have advantageous characteristics over the traditional phenolic resins such as no catalysts or initiators are required for the polymerization and no by-products are created during the polymerization. Moreover, polybenzoxazines have additional unique characteristics including low water absorption, high dimensional stability and near-zero shrinkage or expansion upon curing [23, 24]. In recent years, many researchers focused on investigating and improving thermal stability, structural morphology, and mechanical properties of benzoxazine-based materials. However, there is limited information of friction and wear properties of polybenzoxazines and their composites are in the literatures [25-31]. In recent years, there have been exist limited reports on the use of polybenzoxazine composites [25, 26], polybenzoxazine filled with nanoparticles of ZnO_2 [27, 28], and SiO_2 [29] for an application as brake pad or friction materials. The use of polybenzoxazine based friction materials as had also been recently reported in a US patent from Akebono Co., Ltd. [30, 31]. Friction materials should maintain a stable friction coefficient and low wear at a wide range of pressure, speed, temperature and other operating parameters [32]. The variation of friction coefficient (COF) under different operating conditions is a very important issue as it can be affected by many factors, such as mechanical behaviors, surface topography, particle size [5], particle surface treatment [33], and contents of filler [27].

Therefore, the present study will examine effects of particle size and surface

treatment of fumed silica filled with polybenzoxazine on the friction and wear characteristics. Other essential properties such as mechanical, thermal and physical properties of the obtained fumed silica filled with polybenzoxazine composite specimens will also be investigated.

1.2. Objectives

To study effects of particle sizes and surface treatments of silica nanoparticle on properties of polybenzoxazine nanocomposites as friction materials

1.3 Scopes of the study

1. Synthesis of benzoxazine rasin based on bisphenol-A by a solventless method.

2. Preparation of silica nanoparticles filled in polybenzoxazine at various nano-SiO2 contents. (0-45 wt%).

3. Preparation of polybenzoxazine filled hydrophilic silica nanoparticles with different of primary particle size (7, 14, 20 and 40 nm).

4. Preparation of polybenzoxazine filled hydrophobic silica nanoparticles with different surface treatment i.e. polydimethylsiloxane and dimethyldichlorosilane.

5. Evaluation of functional groups of fumed silica on polybenzoxazine nanocomposites using Fourier Transform Infrared Spectroscope (FTIR).

6. Evaluation of physical properties of fumed silica filled-polybenzoxazine nanocomposites using

- Density

- Scanning Electron Microscope (SEM)

7. Evaluation of thermal properties of fumed silica on polybenzoxazine nanocomposites by

- Thermogravimetric analysis (TGA)

- Differential scanning calorimeter (DSC)

8. Evaluation of mechanical properties of fumed silica filled-polybenzoxazine nanocomposites using

- Dynamic mechanical analysis (DMA)

- Friction test (CHASE machine)

1.4 Procedures of the study

1. Reviewing related literature.

2. Preparation of chemicals and equipment for using in this research.

3. Synthesis of benzoxazine resin based on bisphenol-A by a solventless method.

4. Preparation of polybenzoxazine filled hydrophilic and hydrophobic silica nanoparticles.

5. Determination of physical, thermal and mechanical properties of polybenzoxazine filled with silica nanoparticle as follows:

5.1 Glass transition temperature (T_g)

5.2 Decomposition temperature (T_d)

5.3 Coefficient of friction (μ)

6. Analysis of the experimental results.

7. Preparation of the final report.

CHAPTER II
THEORY

Many composite materials are composed of just two phases; one is termed the matrix, which is continuous and surrounds the other phase, often called the dispersed phase. The properties of composites are a function of the properties of the constituent phases, their relative amounts, and the geometry of the dispersed phase. “Dispersed phase geometry” in this context means the shape of the particles and the particle size, distribution, and orientation; and structural composites; also, at least two subdivisions exist for each. The dispersed phase for particle-reinforced composites is equated (i.e., particle dimensions are approximately the same in all directions); for fiber-reinforced composites, the dispersed phase has the geometry of a fiber (i.e., a large length-to-diameter ratio). Structural composites are combinations of composites and homogeneous materials [34].

They combine the advantages of the inorganic material (e.g., rigidity, thermal stability) and the organic polymer (e.g., flexibility, dielectric, ductility, and processability). Moreover, they usually also contain special properties of nanofillers leading to materials with improved properties. A defining feature of polymer nanocomposites is that the small size of the fillers leads to a dramatic increase in interfacial area as compared with traditional composites. This interfacial area creates a significant volume fraction of interfacial polymer with properties different from the

bulk polymer even at low loadings [35]. In fact, among the numerous inorganic/organic nanocomposites, polymer/silica composites are the most commonly reported in the literature. They have received much attention in recent years and have been employed in a variety of applications. The preparation, characterization, properties, and applications of polymer/silica nanocomposites have become a quickly expanding field of research.

2.1 Nanosilica

Nanosilica was first developed in 1941 by Dr. Harry Klopfer, as he was trying to develop white reinforcing filler comparable to channel blacks in rubber properties. Nanosilica is widely used in industry as an active filler for reinforcement of elastomers, as a rheological additive in fluids and as a free flow agent in powders. Typical BET specific surface areas of nanosilica range from 50-400 m^2/g. Some specific properties of nano-SiO_2 are shown in Table 2.1 [36]. Nanosilica is a synthetic amorphous silicon dioxide produced by hydrothermal hydrolysis of chlorosilanes in an oxygen-hydrogen flame as followed in Eq. (3).

The first step, nanosilica molecules are formed which collide and react to nano-size proto particle, which by further collision in a second step form primary particles of around 5-40 nm in size. The flame process itself leads to the formation of smooth particle surfaces, which provides nanosilica with a high potential for surface interactions as present in Figure 2.1. At the high temperatures of the flame

primary particles are not stable but are fused together to form space-filling aggregates. Leaving the flame, at lower temperatures, the silica agglomerates stick together by physic-chemical forces building up large micron-sized agglomerates and finally fluffy flocks [37].

$$2H_2 + O_2 \longrightarrow 2H_2O \quad (1)$$

$$SiCl_4 + 2H_2O \longrightarrow SiO_2 + 4HCl \quad (2)$$

$$2H_2 + O_2 + SiCl_4 \xrightarrow{> 1000°C} SiO_2 + 4HCl \quad (3)$$

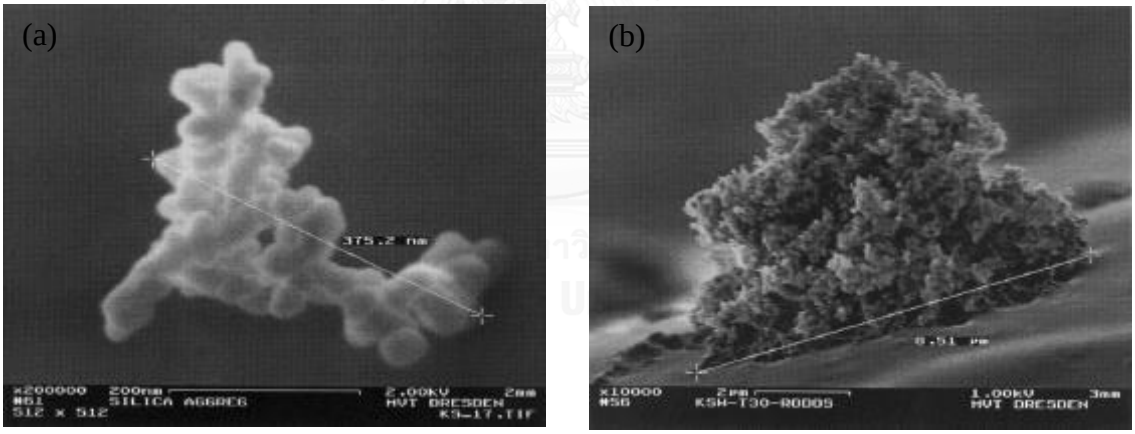

Figure 2.1 SEM images of (a) nano-SiO_2 aggregates and (b) agglomerates.

Nanosilica has been attracting attention as a reinforcing material for polymer because it exhibits a high transparency to light, outstanding electrical properties, and chemical resistance. Nanosilica has been used as a thixotropy or thickening agent in plastic, adhesives and paints. On these importance properties, nanosilica is widely used in many industries. The physical properties of nanosilica are shown in Table 2.1

Table 2.1 Properties of nano-SiO_2 **[36]**.

Property	**Value**
Chemical formula	SiO_2
Density	2-2.2 g/cm^3
Decomposition temperature	> 2000°C
Particle size primary	5-40 nm
Specific surface area	50-400 m^2/g
Refractive index	1.46

At present, nanosilica is evaluated as a reinforcement to improve materials properties including increase in mechanical strength, modulus, ductility and flame retardant. The structure of nanosilica shows a three-dimensional network. Silanol and siloxane groups are created on the silica surface, leading to hydrophilic nature of the particles. The surfaces of the silica are typically terminated with three silanol types: free or isolated silanols, hydrogen-bonded or vicinal silanols and geminal silanols (Figure 2.2) [38]. The silanol groups residing on adjacent particles, in turn, form hydrogen bonds and lead to formation of aggregates, as shown in Figure 2.3. These bonds hold individual nanosilica particles together and the aggregates remain intact even under the best mixing conditions if stronger filler-polymer interaction is not present [39].

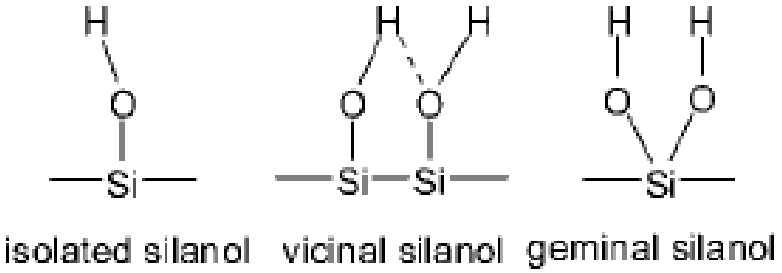

Figure 2.2 Schematic illustrations of three types of surface silanol.

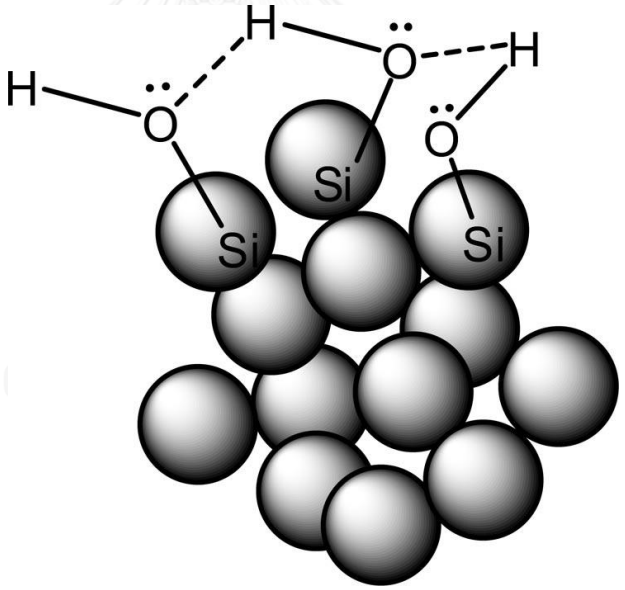

Figure 2.3 Schematic of aggregate formation between adjacent nano-SiO_2 particles through hydrogen bonding among the silanol groups.

The dispersion of nanometer-sized particles in the polymer matrix has a significant impact on the properties of nanocomposites. A good dispersion may be

achieved by surface chemical modification of the nanoparticles or physical methods such as a high-energy ball-milling process and ultrasonic treatment. The great differences in the properties of polymer and silica materials can often cause phase separation. Therefore, the interfacial interaction between two phases of nanocomposites is the most decisive factor affecting the properties of the resulting materials. A variety of methods have been used to enhance the compatibility between the polymer (hydrophobic) and nanosilica. The most frequently used method is to modify the surface of silica nanoparticles (especially for the blending and in situ method), which can also improve the dispersion of nanosilica in the polymer matrix at the same time. In general, surface modification of nanosilica can be carried out by either chemical or physical methods [40].

2.1.1 Modification by chemical interaction [35]

Much attention has been paid to modification of the surface of the nanosilica by chemical interaction since it can lead to much stronger interaction between modifiers and silica nanoparticles. Chemical methods involve modification either with modifier agents or by grafting polymers. Silane coupling agents are the most used type of modifier agents. They generally have hydrolyzable and organofunctional ends. Hydrophobic silica can thus be obtained. Some typical silane coupling agents used for surface modification of nanosilica are listed in Table 2.2.

Grafting of polymer chains to silica nanoparticles is also an effective method to increase the hydrophobicity of the particles and to bring about tunable interfacial interactions in nanocomposites. It was found that modification of nanoparticles through graft polymerization was very effective to construct nanocomposites because of (i) an increase in hydrophobicity of the nanoparticles that is beneficial to the filler/matrix miscibility, (ii) an improved interfacial interaction yielded by the molecular entanglement between the grafting polymer on the nanoparticles and the matrix polymer, and (iii) tailorable structure-properties relationship of the nanocomposites provided by changing the species of the grafting monomers and the grafting conditions since different grafting polymers might bring about different interfacial characteristics.

2.1.2 Modification by physical interaction

Surface modification based on physical interaction is usually implemented by using of surfactants or macromolecules adsorbed onto the surface of silica particles. The principle of surfactant treatment is the preferential adsorption of a polar group of a surfactant to the surface of silica by electrostatic interaction. A surfactant can reduce the interaction between the silica particles within agglomerates by reducing the physical attraction and can easily be incorporated into a polymer matrix [37]. Most of the widely used organosilanes have one organic substituent and three hydrolyzable substituents. In the vast majority of surface treatment applications, the

Table 2.2 Typical silane coupling agents used for surface modification of silica nanoparticles [37].

Abbreviation	Name	Chemical structure
APMDES	Aminopropylmethydiethoxysilane	$H_2N(CH_2)_3(CH_3)Si(OC_2H_5)_2$
TESPT	bis(triethoxysilylpropyl)tetrasulfane	$(C_2H_5O)_3Si(CH_2)_3S_4(CH2)_3Si(OC_2H_5)_3$
DDS	Dimethyldichlorosilane	$(CH_3)_2SiCl_2$
ICPTES	3-isocyanatopropyltriethoxysilane	$OCN(CH_2)_3Si(OC_2H_5)_3$
MMS	Methacryloxymethyltriethoxysilane	$CH_2=C(CH_3)COOCH_2Si(OC_2H_5)_3$
MPTES	Methacryloxypropyltriethoxysilane	$CH_2=C(CH_3)COO(CH_2)_3Si(OC_2H_5)_3$
MPTS	mercaptopropyl triethoxysilane	$SH(CH_2)_3Si(OC_2H_5)_3$
PDMS	Polydimethylsiloxane	$CH_3[Si(CH_3)_2O]_nSi(CH_3)_3$
MTES	Methyltriethoxysilane	$CH_3Si(OC_2H_5)_3$
PTMS	Phenyltrimethoxysilane	$PhSi(OCH_3)_3$
VTES	Vinyltriethoxysilane	$CH_2=CHSi(OC_2H_5)_3$
VTS	Vinyltrimethoxysilane	$CH_2=CHSi(OCH_3)_3$

alkoxy groups of the trialkoxysilanes are hydrolyzed to form silanol-containing species. Reaction of these silanes involves four steps. Initially, hydrolysis of the three labile groups occurs. Condensation to oligomers follows. The oligomers then hydrogen bond with OH groups of the substrate. Finally, during drying or curing, a covalent linkage is formed with the substrate with concomitant loss of water (Figure 2.4). Although described sequentially, these reactions can occur simultaneously after the initial hydrolysis step. At the interface, there is usually only one bond from each

silicon of the organosilane to the substrate surface. The two remaining silanol groups are present either in condensed or free form. The R group remains available for covalent reaction or physical interaction with other phases [41].

2.2 Polybenzoxazine

Polybenzoxazine is a newly developed class of thermosetting resin with interesting properties that are based on the ring opening polymerization of benzoxazine precursors. As a novel class of phenolic resin, it has been developed and studied to overcome several short comings of conventional novolac and resole-type phenolic resin. Polybenzoxazine resins are expected to replace traditional phenolic, polyesters, vinyl esters, epoxies, BMI, cyanate esters and polyimides in many respects [42]. The mechanical and physical properties can be tailored to various needs. The material can be synthesized using the patented solventless technology to yield a relatively clean precursor without the need of solvent elimination or monomer purification [43].

Polybenzoxazine can be synthesized from inexpensive raw materials and can be cured without the use of strong acid or base catalyst. The crosslinking reaction of the resin is through thermally activated ring-opening reaction; therefore, it does not release by-products during the polymerization. The material has excellent properties commonly found in traditional phenolic resins such as high thermal stability, flame retardance, dimensional stability, low viscosity, near-zero shrinkage upon

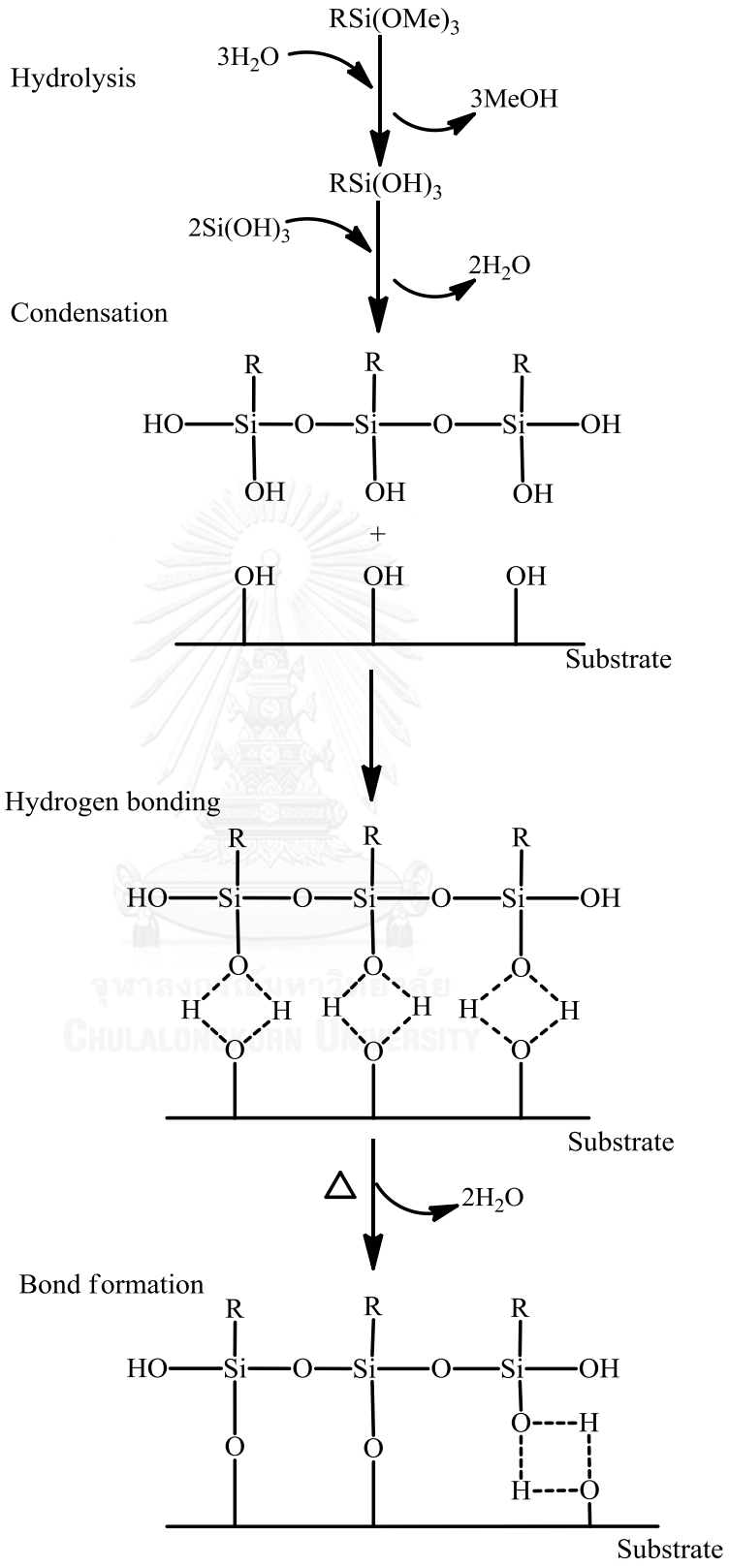

Figure 2.4 Hydrolytic depositions of silanes.

polymerization, low water absorption, excellent electrical properties, high mechanical integrity, glass transition temperatures much higher than cure temperature, fast mechanical property build-up as a function of degree of polymerization, high modulus and high char-yield. Furthermore, the ability of benzoxazine resin to be alloyed with other polymers renders the resin with even broader range of applications [44, 45].

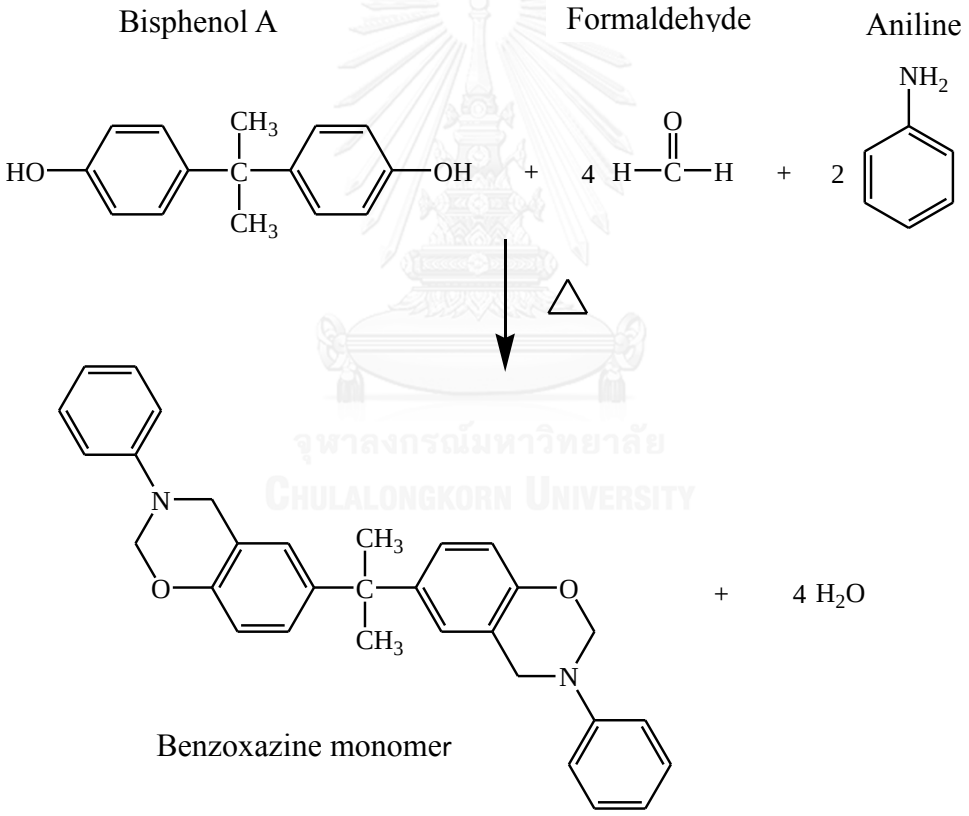

Figure 2.5 Synthesis of bifunctional benzoxazine monomer.

Benzoxazine resin based on bisphenol-A and aniline is synthesized according to the following reaction scheme as shown in Figure 2.5 [46]. The properties of

polybenzoxazines compared with those of the state of art matrices were depicted in Table 2.3. Polybenzoxazines present the highest tensile properties. Their results from dynamic mechanical analysis reveal that these candidate resins for composite applications possess high moduli and glass transition temperatures, at low cross-link densities. Long-term immersion studies indicate that these materials have a low rate of water absorption and low saturation content. Impact, tensile, and flexural properties are also outstanding [47].

2.3 Tribology

2.3.1 Friction

The earliest works on polymer tribology probably started with the sliding friction studies on rubbers and elastomers [48]. Further work on other polymers (thermosets and thermoplastics) led to the development of the two-term model of friction [49]. The two-term model proposes that the frictional force is a consequence of the interfacial and the cohesive works done on the surface of the polymer material. This is assuming that the counterface is sufficiently hard in comparison to the polymer-mating surface and undergoes only mild or no elastic deformation. Figure 2.6 shows a schematic diagram of the energy dissipation processes in the two-term model [50]. The interfacial frictional work is the result of adhesive interactions and the extent of this component obviously depends upon factors such as the hardness of the polymer, molecular structure, glass transition temperature and crystallinity of the

polymer, surface roughness of the counterface and chemical/electrostatic interactions between the counterface and the polymer. For example, an elastomeric solid, this has its glass transition temperature below the room temperature and hence very soft, would have very high adhesive component leading to high friction. Beyond interfacial work is the contribution of the cohesive term, which is a result of the plowing actions of the asperities of the harder counterface into the polymer. The energy required for the plowing action will depend primarily upon the tensile strength and the elongation before fracture (or toughness) of the polymer and the geometric parameters (height and the cutting angle) of the asperities on the counterface. The elastic hysteresis is another factor generally associated with the cohesive term for polymers that show large visco-elastic strains, such as in the case of rubbers and elastomers. Further, both the interfacial and the cohesive works would be dependent upon the prevailing interface and ambient temperatures, and the rate of relative velocity as these factors would in turn modify the polymer's other materials' parameters. Pressure has some effect on the interfacial friction as normal contact pressure tends to modify the shear strength of the interface layer by a relation given as

$$\tau = \tau_{\mathrm{o}} + \alpha_{\mathrm{p}} \qquad (4)$$

Total friction force is the sum of the forces required for interfacial and cohesive energy dissipations. Likewise, the distinction between interfacial and

Table 2.3 Comparative properties of various high performance polymers [47].

Properties	**Epoxy**	**Phenolics**	**Toughened BMI[1]**	**Bisox-phen[2] (40 : 60)**	**Cyanate ester**	**P-T resin[3]**	**Polybenzoxazine**
Density (g/cm^3)	1.2-1.25	1.24-1.32	1.2-1.3	1.3	1.1-1.35	1.25	1.19
Max use temperature (°C)	180	~200	200	250	150-200	300-350	130-280
Tensile strength (MPa)	90-120	24-25	50-90	91	70-130	42	100-125
Elongation (%)	3-4.3	0.3	3	1.8	0.2-0.4	2	2.3-2.9
Dielectric constant (1 MHz)	3.8-4.5	0.4-10	3.4-3.7	-	2.7-3.0	3.1	3-3.5
Cure temperature (°C)	RT-180	150-190	220-300	175-225	180-250	177-316	160-220
Cure shrinkage (%)	>3	0.002	0.007	<1	~3	~3	~0
TGA[4] onset (°C)	260-340	300-360	360-400	370-390	400-420	410-450	380-400
Tg (°C)	150-220	170	230-380	160-295	250-270	300-400	170-340
G_{IC}[5] (J/m^2)	54-100	-	160-250	157-223	-	-	168
K_{IC}[6] (MPa $m^{1/2}$)	0.6	-	0.85	-	-	-	0/94

[1] Bismaleimide (BMI),

[2] Bisoxazoline-phenolics (Bisox-phen),

[3] Phenolic-triazine resin (P-T resin),

[4] Thermogrvimetric analysis (TGA),

[5] Fracture energy (G_{IC})

[6] Fracture toughness plain-strain stress intensity factor (K_{IC})

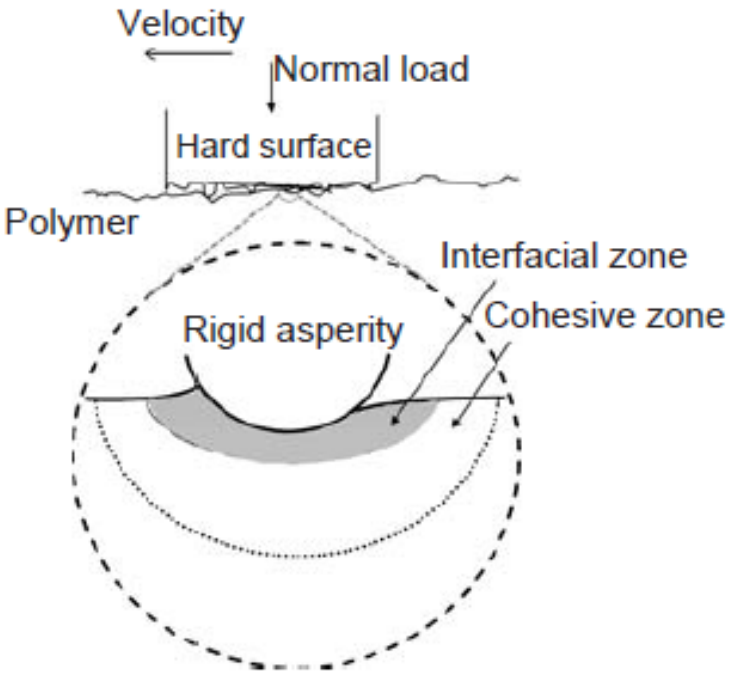

Figure 2.6 Two-term model of friction and wear processes.

cohesive wear processes arises from the extent of deformation in the softer material (usually polymer) by rigid asperity of the counterface. For interfacial wear, the frictional energy is dissipated mainly by adhesive interaction while for cohesive wear the energy is dissipated by adhesive and abrasive (sub-surface) interactions [50].

The implication of the above relation is that as the contact pressure increases, the shear stress would increase linearly leading to high friction. Eq. 4, as simple as it may look in the form, hides the very complex nature of polymer. Also, it does not include the temperature and the shear rate effects on the shear stress. In a normal sliding experiment, it is non-trivial to separate the two terms (interfacial and cohesive) and therefore most of the data available in the literature generally include

a combined effect. Often, the practice among experimentalists is to fix all other parameters and vary one parameter to study its effect on the overall friction coefficient for a polymer. Looking at the published data one can easily deduce that depending upon other factors, the friction is greatly influenced by the class of polymers viz. elastomers, thermosets and thermoplastics (semi-crystalline and amorphous). Semi-crystalline linear thermoplastic would give lowest coefficient of friction whereas elastomers and rubbers show large values. This is because of the molecular architecture of the linear polymers that helps molecules stretch easily in the direction of shear giving least frictional resistance.

2.3.2 Wear

The inevitable consequence of friction in a sliding contact is wear. Wear of polymers is a complex process and the explanation of the wear mechanism can be most efficiently given if we follow one of the three systems of classification. Depending on the classification, wear of a polymer sliding against a hard counterface may be termed as interfacial, cohesive, abrasive, adhesive, chemical wear, etc. Figure 2.7 describes the classification of polymer wear [50]. It is to be noted that, similar to the case of friction, polymer wear is also greatly influenced by the type (elastomer, amorphous, semi crystalline) of the polymer. These observations are in line with the idea that for polymers, surface hardness is not a controlling factor for wear resistance. In fact, high hardness of a polymer may be harmful for wear resistance in

dry sliding against hard counterface as hardness normally comes with low toughness for polymers. High extents of elongation at failure of a polymer means that the shear stress in a sliding event can be drastically reduced due to extensive plastic deformation of the polymer within a very thin layer close to the interface. This interfacial layer accommodates almost all of the energy dissipation processes and thus the bulk of the polymer undergoes minimal deformation or wear. Frictional heat generated at the interface is the major impediment to high wear life of the polymer. Thermosetting polymers though possess high hardness and strength among polymers, show very high wear rate and high coefficient of friction because of very

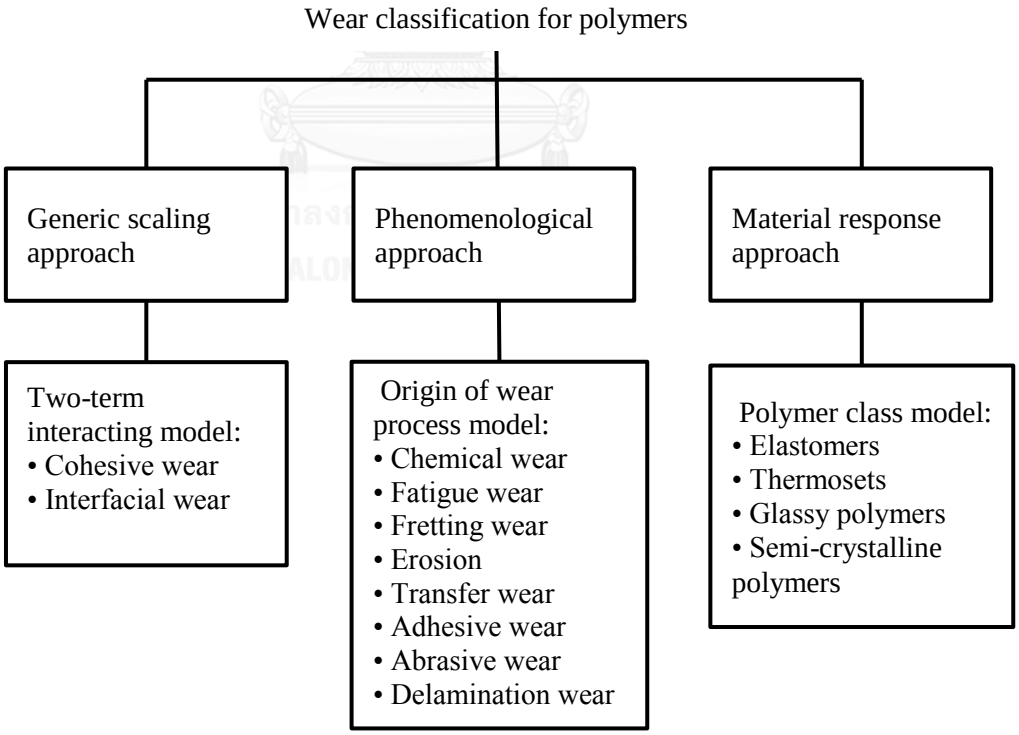

Figure 2.7 Simplified approach to classification of the wear of polymers.

low elongation at failure values. Thermosets are normally used in the form of composites as fiber strengthening can drastically reduce wear. Fiber strengthening sometimes improves the material's resistance to sub-surface crack initiation and propagation giving reduced plowing by the counterface asperities or fatigue cracking. Interface friction can also be optimized by adding a suitable percentage of a solid lubricant. This trend has led to much research in recent times on producing composite or hybrid materials for optimum wear and friction control using epoxy or phenolic resins as the matrix [51].

2.3.3 Tribology of polymer nanocomposites

The use of nano-particles in polymers for tribology performance enhancement started around mid-1990s and this area has become quite promising for the future as newer nanomaterials are being economically and routinely fabricated. In most of the cases, a polymer nanocomposite relies for its better mechanical properties on the extremely high interface area between the filler (nano-particles or nano-fibers) and the matrix (a polymer) [52]. High interface leads to a better bonding between the two phases and hence better strength and toughness properties over unfilled polymer or traditional polymer composites. For all polymer/nano-particle systems, there will be an optimum amount of the nanoparticles beyond which there will be a reduction in the toughness as the stiffness and strength increase. There are mainly two types of polymer

nanocomposites that have been tested for tribological performance. One type is where ceramic nano-particles, mainly metal and some non-metal oxide, have been added with the aim to improve load-bearing capacity and wear resistance of the material against the counterface. Examples of polymer nanocomposite systems of this type include fillers such as SiO_2, SiC, ZnO, TiO_2, Al_2O_3, Si_3N_4 and CuO in polymer matrices such as epoxy, PEEK, PTFE and PPS. The specific wear rates of these nanocomposites have been reported in the range 10 – 100 times lower than the specific wear rates of the polymers without fillers when optimum weight percent of the nano-particles is introduced. The role of nano-particles is to increase the load-bearing capacity of the material and thus the actual contact area is reduced leading to lower frictional stress for the nanocomposite. Also, the presence of nano-particles in the matrix improves the toughness to an extent that leads to lesser propensities for wear by sub-surface fatigue or asperity plowing actions. It has also been reported that the gain in wear resistance for nanocomposite could also be attributed to an increase in the thermal conductivity of the composite compared to the pristine polymer. The second type of polymer nanocomposite system is a polymer filled with carbon nanotubes (CNTs). CNT is an excellent material for reinforcing polymers as CNT shows very high strength and stiffness.

For both types of nanocomposites, the processing method has much significance in the improvement of mechanical and tribological performance of the

material. A suitable surface pre-treatment of the nano-particles can lead to less filler agglomeration and thus better bonding between the nano-particles and the matrix.

CHAPTER III
LITERATURE REVIEWS

I. Dueramae et al. (2013) [53] studied high thermal and mechanical properties enhancement obtained in highly filled polybenzoxazine nanocomposites with fumed silica. FT-IR spectroscopy was used to verify the molecular structures of nano-SiO_2, PBA-a, and 30 wt% nano-SiO_2-filled PBA-a as depicted in Figure 3.1(a–c), respectively. The new peak at 1075 cm^{-1} assigned to Si–O–C stretching was also clearly observed in Figure 3.1(c). The appearance of this absorption band is a clear evidence of the chemical bonding formed between the polybenzoxazine matrix and the nano-SiO_2 filler. The nanocomposites should provide a substantial reinforcing effect as a result of the chemical bonding between the two components.

The polymerization behaviors of benzoxazine monomers at different weight fractions of nano-SiO_2 were investigated by non-isothermal DSC as illustrated in Figure 3.2. The curing exotherms of these benzoxazine compounds exhibited thermal curability of benzoxazine resin without adding initiator or catalyst. No significant change in the exothermic peak position of the benzoxazine molding compounds were observed indicating that the nano-SiO_2 filler was relatively inert to the benzoxazine curing reaction. Moreover, the experiments revealed that the exothermic curing enthalpy decreased expectedly with increasing filler contents e.g. H = 188 J/g at 30wt% nano-SiO_2 content and H = 306 J/g for benzoxazine resin.

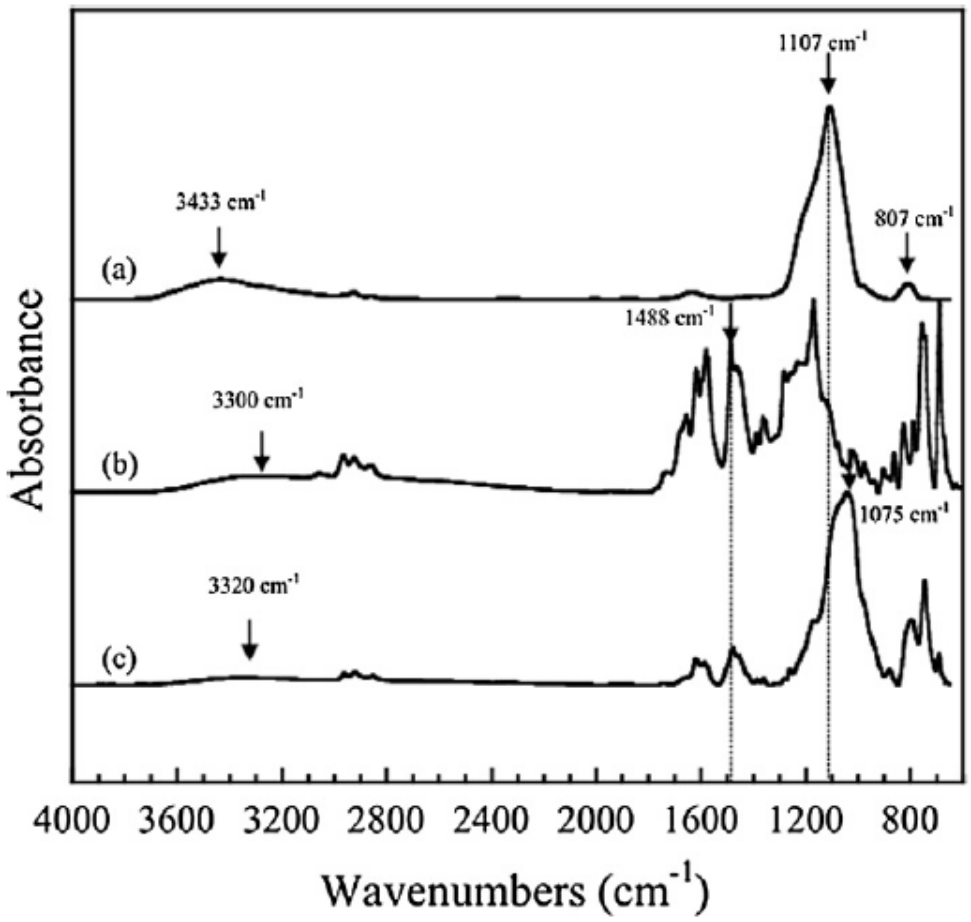

Figure 3.1 FT-IR spectra of (a) nano-silica, (b) polybenzoxazine and (c) 30 wt% nanosilica filled polybenzoxazine.

The autocatalytic curing behavior of benzoxazine resin can be explained by the generation of free phenol groups while the benzoxazine ring starts to ring-open. These phenol groups can actually accelerate further ring opening reaction of other monomers and the mechanism was not affected by the presence of the nano-SiO_2 filler used. The slightly acidic nature of the fumed silica nanoparticles due to the presence of surface silanol groups has been reported to exhibited some reactivity with hydroxyl groups [10]. The reaction of the O-H groups of the benzoxazine resin

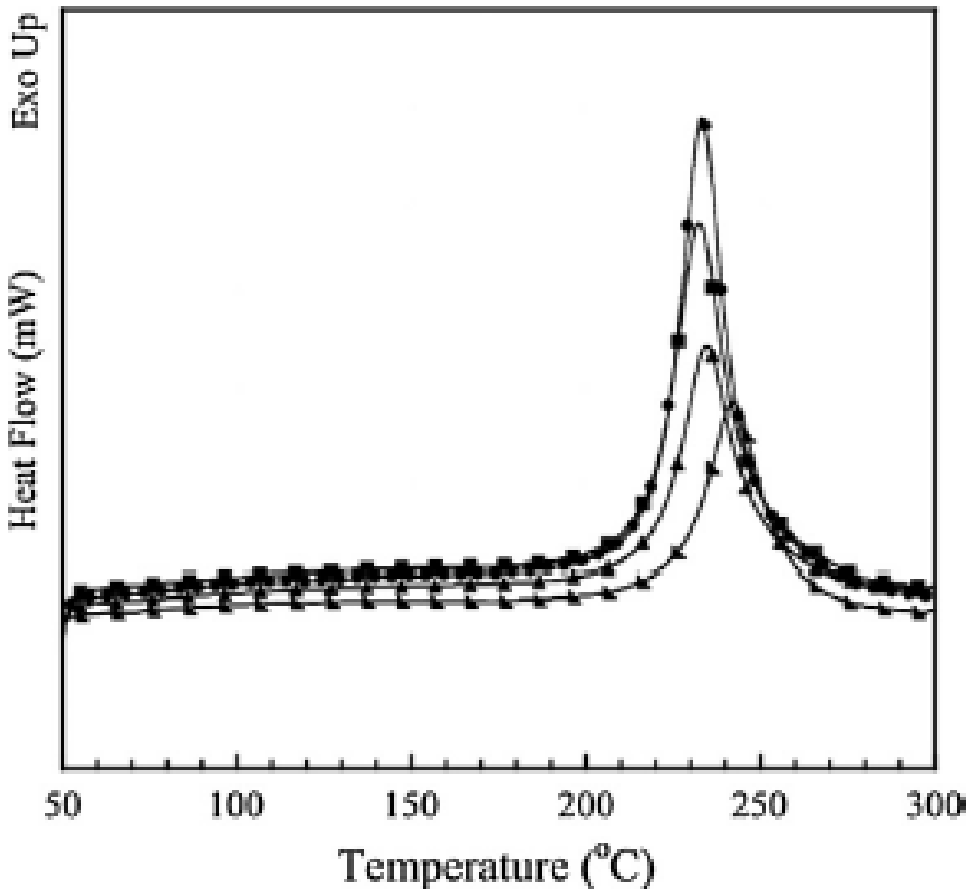

Figure 3.2 DSC thermograms of benzoxazine molding compound at different nano-SiO_2 contents: (●) PBA-a, (■) 10wt%, (♦) 15wt%, (▼) 20wt%, (▲) 25wt% and (◣) 30wt% nano-SiO_2-filled BA-a.

with the surface silanol groups of the nano-SiO_2 thus contributes to the observed curing authocatalytic behavior of the benzoxazine/nano-SiO_2 molding compounds. Figure 3.3 presented the variation of tan δ with temperature of the nano-SiO_2-filled PBA-a composite. The peak position of tan δ was used as T_g of the nanocomposites.

From the figure, It can be seen that the T_g of 201°C was observed at 30wt% of the nano-SiO_2-filled PBA-a while that of neat PBA-a was found to be 185°C.

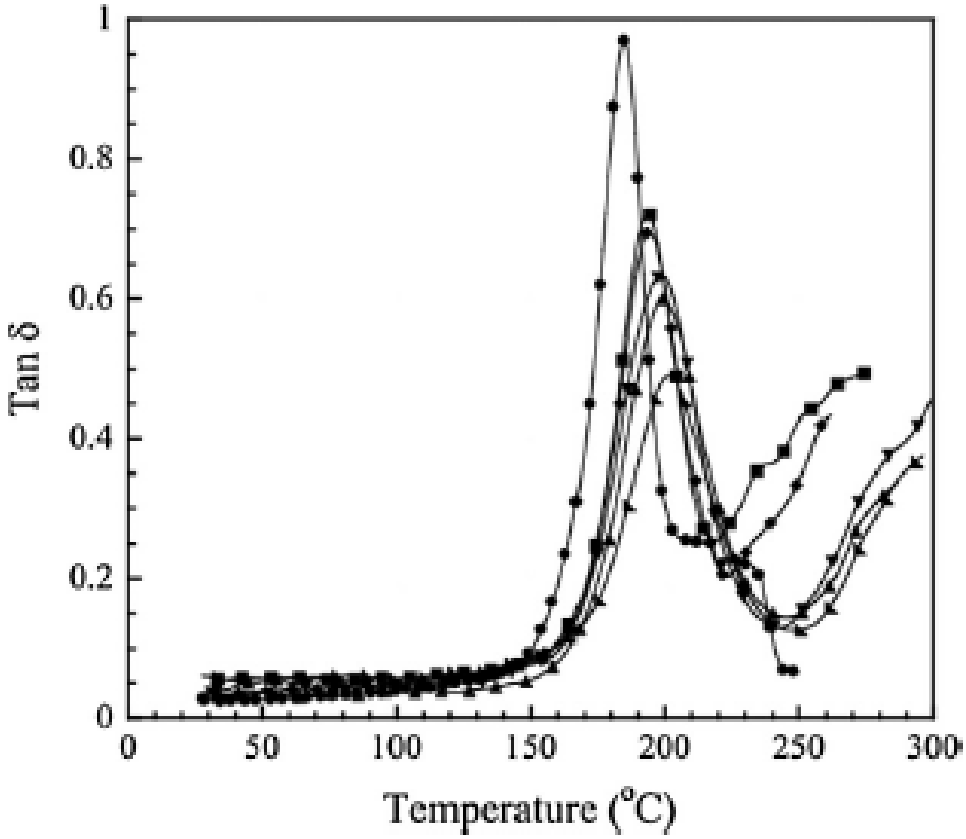

Figure 3.3 Mechanical damping factor of highly filled nanocomposites at different nano-SiO_2 contents: (●) PBA-a, (■) 10wt%, (♦) 15wt%, (▼) 20wt%, (▲) 25wt% and (◣) 30wt% nano-SiO_2-filled BA-a.

The enhancement of T_g of the nanocomposites was attributed to an ability of the nano-SiO_2 particles to substantially restrict the motion of the polybenzoxazine chains thus higher temperature is required to provide the requisite thermal energy for the occurrence of a glass transition in the nanocomposites. In addition, the huge surface

of the nano-SiO_2 as well as the strong interfacial interaction between the nano-SiO_2 and the polybenzoxazine were attributed to such strong restriction of the chains movements in the polybenzoxazine thus the substantial enhancement on its T_g.

H.-X. Yan et al (2013) [29] studied The tribological properties of Benzoxazine-Bismaleimides composites with functionalized nano-SiO_2. The friction coefficient of BOZ pure resin, BOZ-BMI resin and the composites with different amount of HBPSi-SiO_2 under dry conditions as a function of the sliding time is shown in Figure 3.4. Apparently, the frictional coefficient of BOZ-BMI resin is lower than BOZ pure resin during the sliding time, which demonstrates that the addition of BMI can decrease the frictional coefficient of BOZ. Moreover, the frictional coefficient of the composites decreases greatly by the addition of HBPSi-SiO_2, and the formation time of transform film on the surface of counterpart steel ring is also shortened. The transform film formation of BOZ pure resin and BOZ-BMI resin need much more time, and transform film is nonuniform, thus resulting in the instability of frictional coefficient. When the content of HBPSi-SiO_2 is 3.0 wt %, the composite not only has the lower frictional coefficient, but also exhibits a more stable frictional coefficient during the friction process than the composites with other content of HBPSi-SiO_2. Figure 3.5 gives the wear rate of BOZ pure resin, BOZ-BMI resin and the composites with different content of HBPSi-SiO_2. It can be concluded from the figure that BOZ-

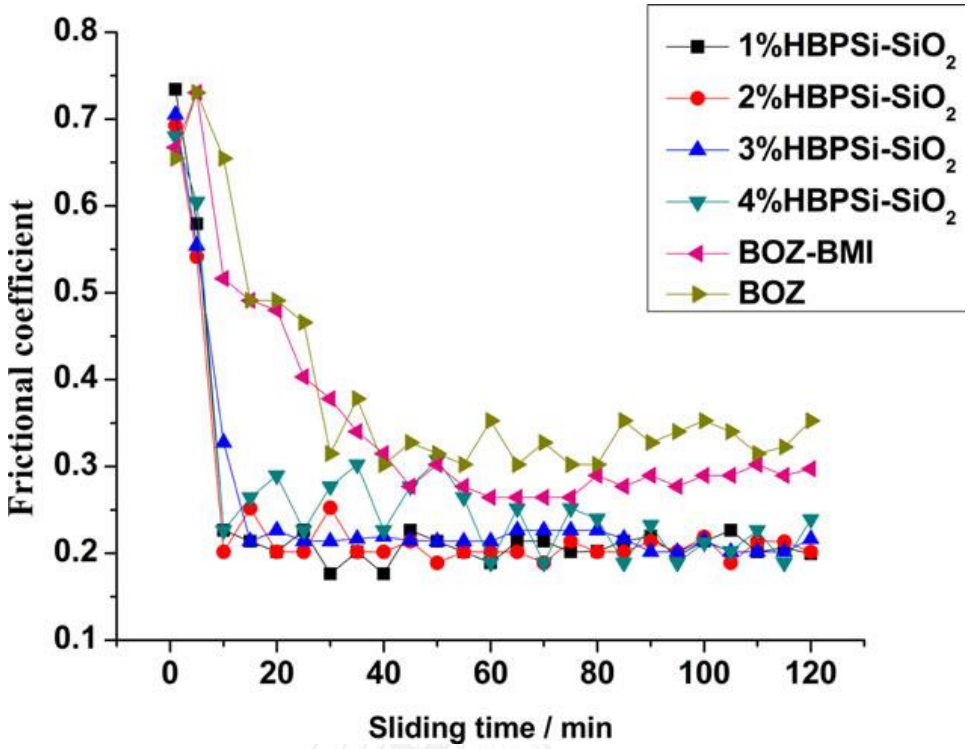

Figure 3.4 The friction coefficient of BOZ, BOZ-BMI, and the composites with different content HBPSi-SiO_2 (load: 196 N; sliding velocity: 0.42 m/s).

BMI resin exhibits lower wear rate than BOZ pure resin. The wear resistance of the composites is further improved by the addition of HBPSi-SiO_2. When the content of HBPSi-SiO_2 is 3.0 wt%, the lowest wear rate of the composites is merely 0.4 x 10^{-6} mm^3 N^{-1} m^{-1}, and decreases as much as 97.8% compared with BOZ-BMI resin. The tribological properties of a composite depend on the internal strength and lubricating property of both matrix and reinforcement [54]. However, HBPSi-SiO_2 has good self-lubrication properties due to their highly branched, nonentangled structure of HBPSi, which enable the homodisperse of particles in the matrix. Furthermore, the epoxy group on the surface of HBPSi-SiO_2 can form chemical bond with BOZ by ring

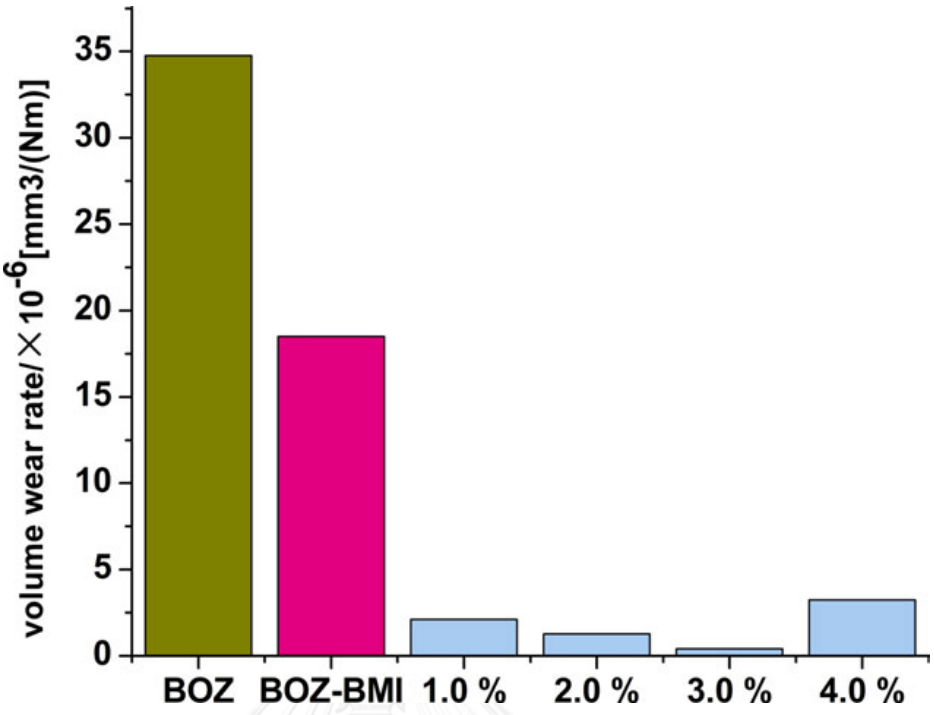

Figure 3.5 The volume wear rate of BOZ, BOZ-BMI, and the composites with different content HBPSi-SiO_2.

opening reaction (Figure 3.6). Consequently, the interfacial adhesion between HBPSi-SiO_2 particles and matrix is enhanced. However, when the amount of HBPSi-SiO_2 is excessive, HBPSi-SiO_2 entangled with each other, thus the advantages of HBPSi-SiO_2 cannot get into the full play. As a result, the tribology properties are also decrease. To confirm the conclusions above, the morphologies of the wear surfaces of BOZ pure resin, BOZ-BMI resin and its composite filled with 3.0 wt % HBPSi-SiO_2 are selected to investigate the wearing mechanisms. The SEM images of the wear surface the composites under the same testing condition are shown in Figure 3.7. Obvious cracks and plate-like flake away can be seen on the wear surface of BOZ pure resin

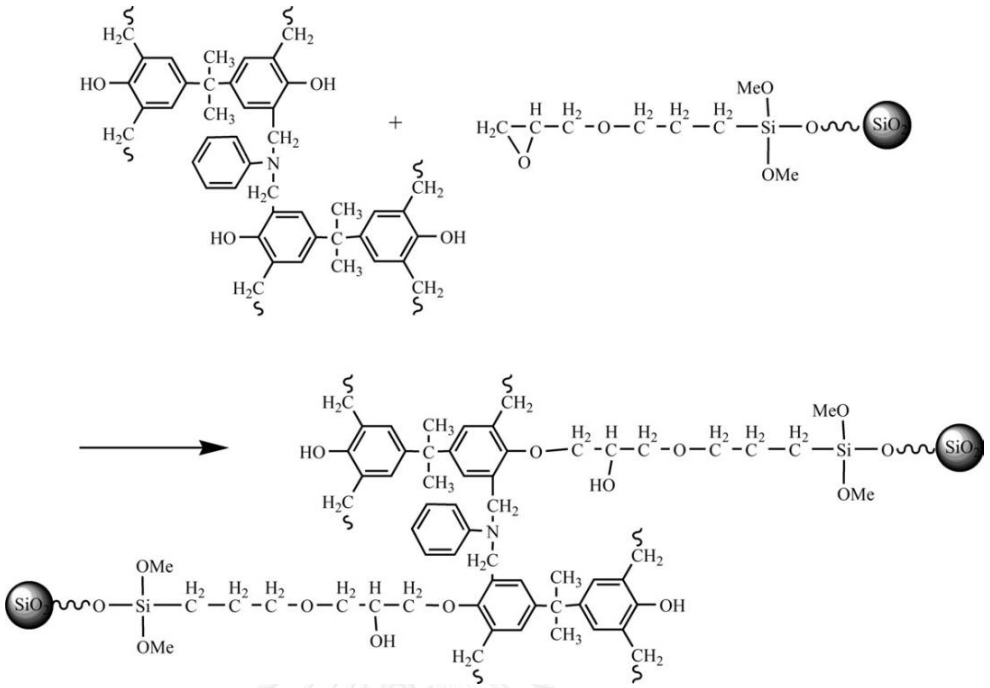

Figure 3.6 The reaction between HBPSi-SiO_2 and BOZ.

[Figure 3.7a)]. However, for the BOZ-BMI resin [Figure 3.7(b)], the cracks on the wear surface of the composites are much smaller in comparison with BOZ pure resin. The wear surfaces of the composites filled with 3.0 wt % HBPSi-SiO_2 [Figure 3.7(c)] is completely different. Compared with the BOZ pure resin and BOZ-BMI resin, the wear of the composites is much milder, which is the characteristic of abrasive wear mechanism, it is also indicates that the antiwear ability of the composite is reinforced by HBPSi-SiO_2. During the wear process of the composite, material transfer occurs and HBPSi-SiO_2 near the surface of resin matrix can be precipitated, then thin transfer film containing HBPSi-SiO_2 forms on the surface of counterpart steel ring. HBPSi-SiO_2 in the transfer film can play a role of ‘‘framework,’’ which inhibits the damage of the transfer film. Thus, the improvement of the wear resistance of the composites can

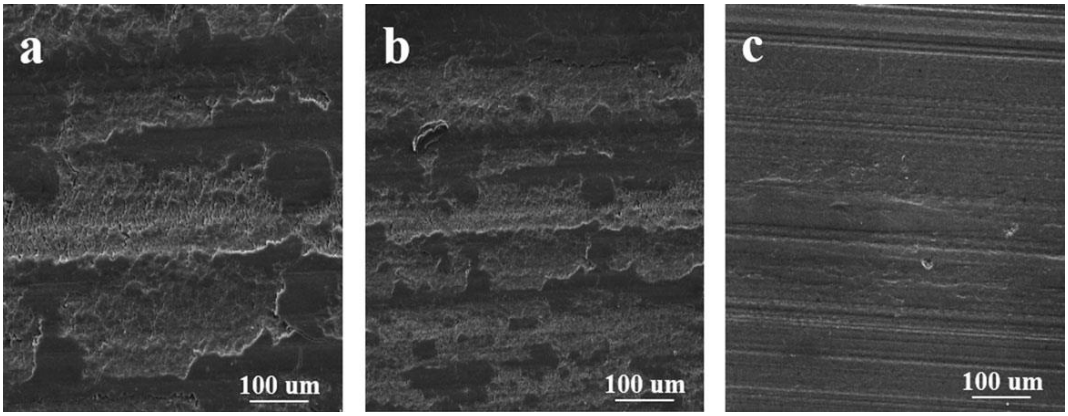

Figure 3.7 SEM of wear surface of BOZ, BOZ-BMI, and the composites with 3.0 wt % HBPSi-SiO_2 (a: BOZ; b: BOZ-BMI; c: composites with 3.0 wt%HBPSi-SiO_2).

be ascribed to the self-lubrication properties and ‘‘framework’’ role of HBPSi-SiO_2. In addition, the good dispersion of HBPSi-SiO_2 in the BOZ-BMI matrix possibly gives a uniform table and durable lubrication transfer film between the composite and the counterpart steel ring. The transfer film can protect the material during the sliding process, which results in lower frictional coefficient and higher wear resistance. These explanations are in agreement with the results described above that the content of 3.0 wt% HBPSi-SiO_2 composite possesses the highest wear resistance. The improved wear resistance of the content of 3.0 wt % HBPSi-SiO_2 composite can be attributed not only to the enhance functioning of BMI, but also to the fillers, especially to the HBPSi-SiO_2 homogeneously dispersed in resin matrix.

M.Q. Zhang et al. (2002) [33] studied Effect of particle surface treatment on the tribological performance of epoxy based nanocomposites. Figure 3.8 gives the

coefficient of friction of epoxy and its composites determined at the pressures 3 and 5 MPa under a constant sliding velocity v = 0.4 m/s. It is seen that the frictional coefficient of epoxy keeps almost unchanged when the pressure increases from 3 to 5 MPa. The frictional coefficients of nanosilica filled composites are lower than that of unfilled epoxy and decrease with increasing pressure. The lowest value of μ is recorded at a load of 5 MPa for SiO_2-g-PAAM/epoxy composites. These phenomena imply that nanosilica can improve the friction-reducing ability of the composites especially under higher load [55].

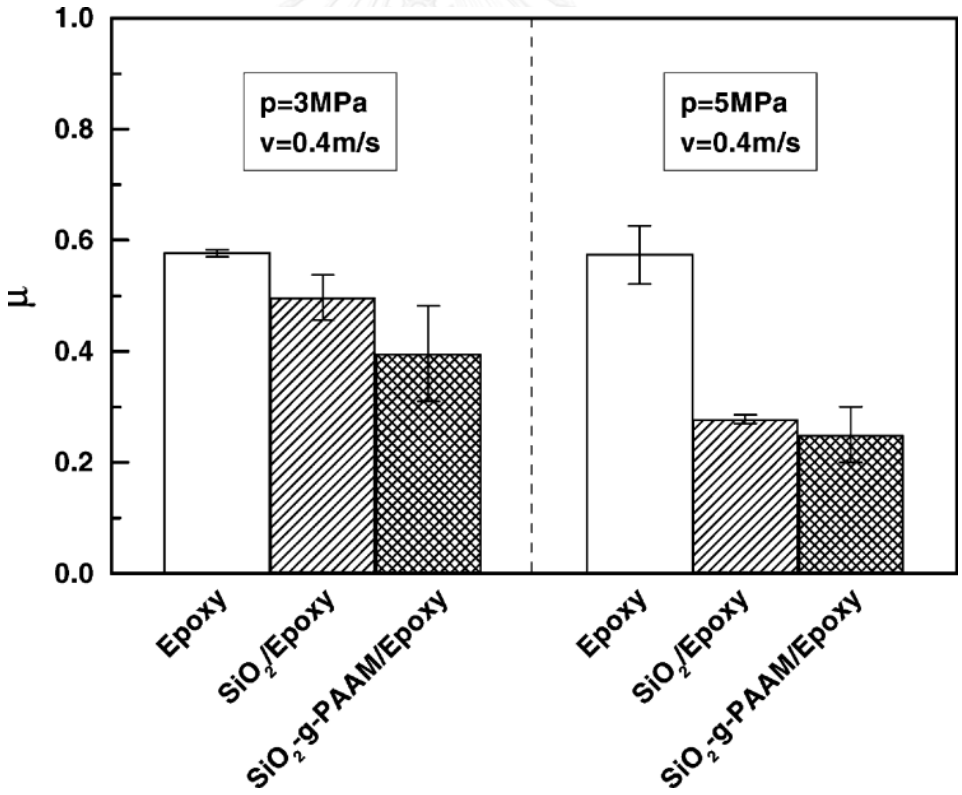

Figure 3.8 Frictional coefficient μ, of epoxy and its composites at 2.17 vol% nanosilica content.

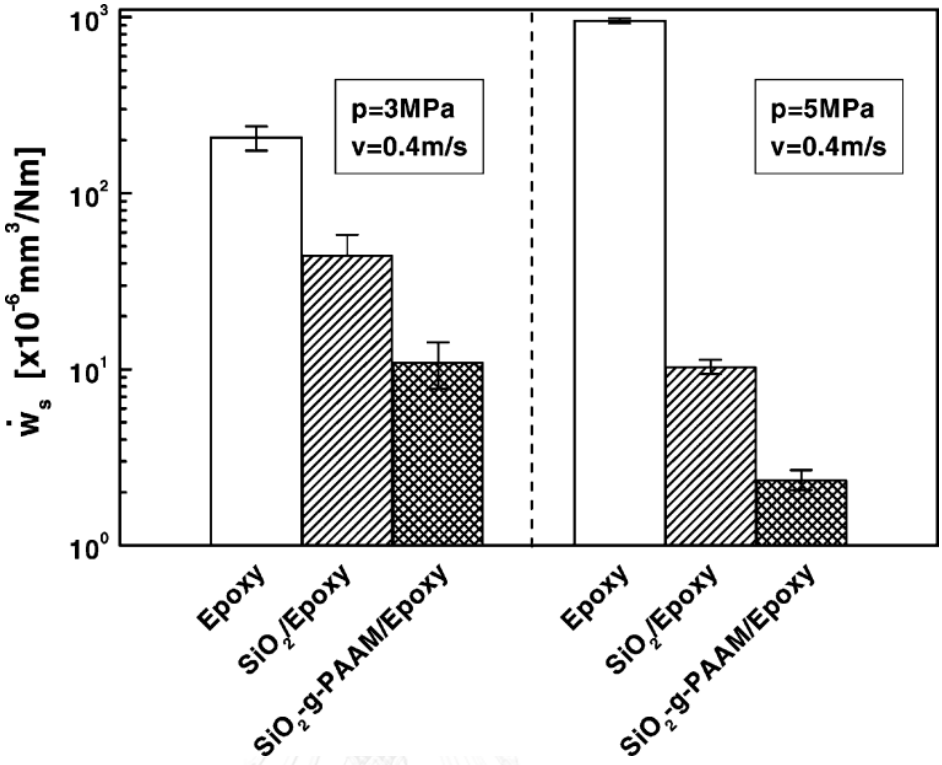

Figure 3.9 Specific wear rate ω_s of epoxy and its composites at 2.17 vol% filler content.

The introduction of grafting PAAM further enhances the role of the particles. The specific wear rates of the materials are exhibited in Figure 3.9. Nanocomposites evidence a much higher wear resistance compared to the neat epoxy. It is worth noting that, when micrometer SiO_2 particles (180 μm) are used, the filler content needed to acquire a significant decrease in wear rate of epoxy is as high as 40 wt% [56]. This is much higher than the amount added into the present systems (∼2 vol%). In view of applicability, the composites with such a high loading of micrometer particles are far from equal the nanocomposites characterized by lightweight. By comparing Figure 3.8 with Figure 3.9, it is seen that the decrement of

wear rate is greater than that of frictional coefficient when other conditions are the same. Silica nanoparticles seem to be more effective for improving the anti-wear property of the composites. Moreover, in the same way as it was observed for the materials' frictional coefficient μ, the additional surface modification of the nanoparticles helps to further decrease the wear rare of the composites. On the other hand, Figure 3.9 shows different pressure dependencies of the wear rate. With a rise in testing pressure, the wear loss of epoxy increases but that of the composites decreases.

C. Yan et al. (2010) [57] studied study of surface-functionalized nano-SiO_2/Polybenzoxazine composites. The ring-opening polymerization of BOZ monomers and with the modified nano-SiO_2 is shown in Figure 3.10. The microstructures of the SiO_2/PBOZ nanocomposites containing different amounts of

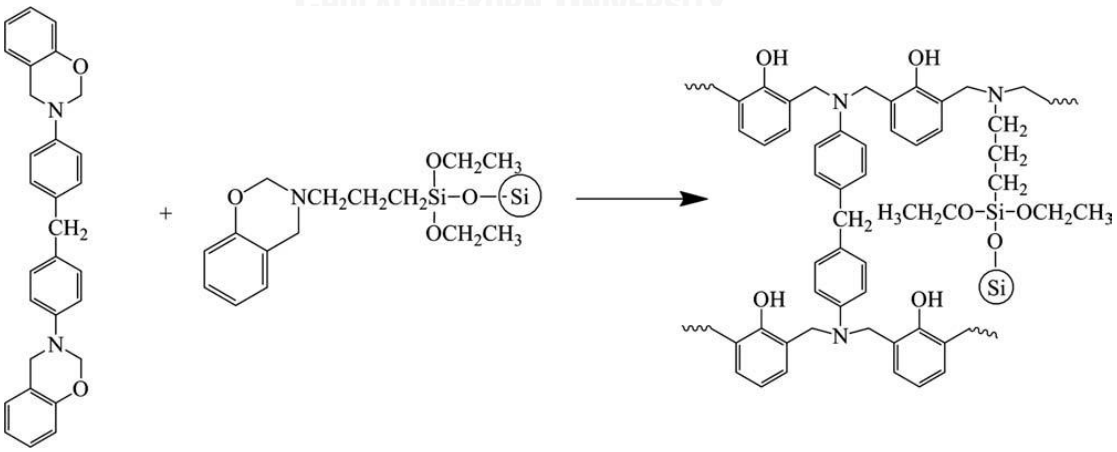

Figure 3.10 Ring-opening polymerization of BOZ monomer and modified nano-SiO_2.

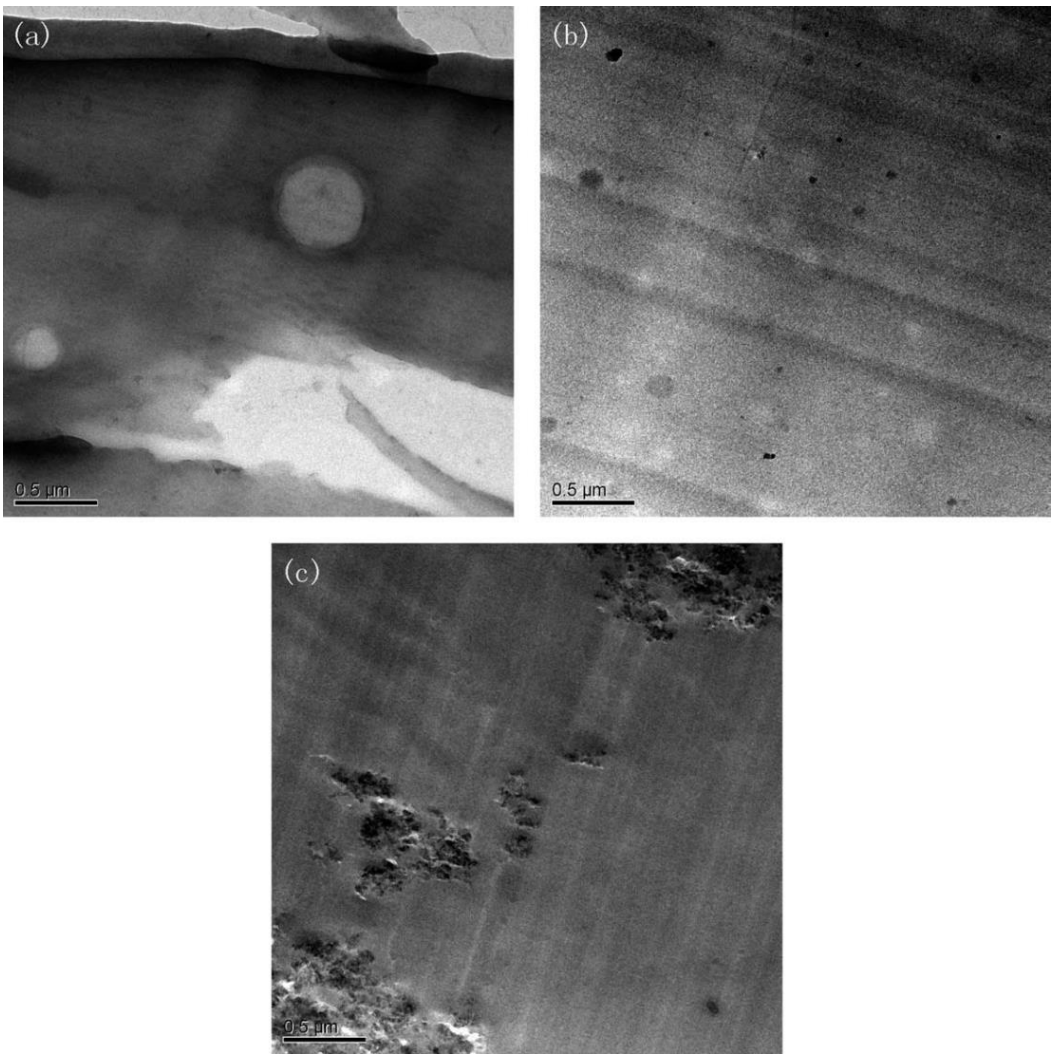

Figure 3.11 TEM images of the SiO_2/PBOZ nanocomposites with (a) 1 wt % nano-SiO_2; (b) 3 wt% nano-SiO_2; (c) 4wt % nano-SiO_2.

the nano-SiO_2 were investigated by TEM. The dispersions of the nano-$SiO_2$of the nanocomposites observed by TEM are shown in Figure 3.11. With the increasing in the nano-SiO_2 contents, nanoparticles become agglomerates very obviously when the loading is more than 3 wt%. When the loading is less than 3 wt%, nanoparticles

appear well dispersed in the matrix. The effect of the nano-SiO_2 contents on the glass transition temperature (T_g) of the PBOZ/SiO_2 nanocomposites is shown in Figure 3.12 clearly. The glass-transition temperatures were obtained from either the maximum of loss factor (tan δ) or loss modulus (E″), respectively. Although the values of T_g from tan d are higher than those from E″, the same trend of T_g is observed. The glass-transition temperatures of the nanocomposites are higher than that of the pristine PBOZ.

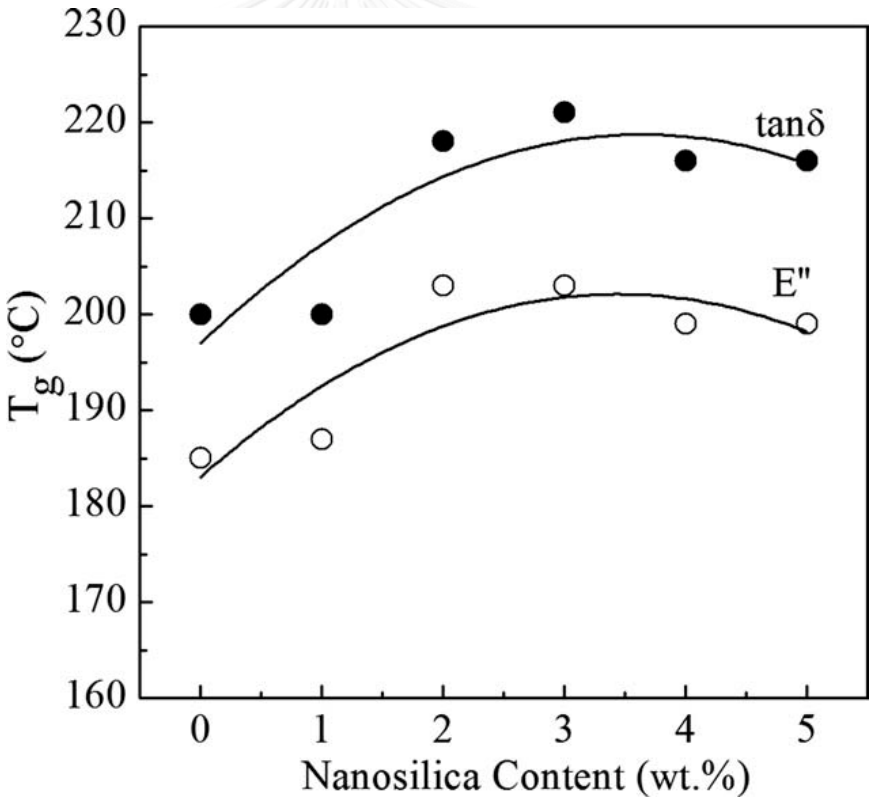

Figure 3.12 The effect of the nano-SiO_2 contents on the T_g of the SiO_2/PBOZ nanocomposites.

The T_g increases with the increase in the nano-SiO_2 contents until it reaches a maximum when nano-SiO_2 content is 3 wt%, then decreases when nano-SiO_2 content further increases. The aggregation of nano-SiO_2 in composites becomes evident after 3 wt% load, hence leads to the decrease of T_g. This phenomenon relies on the other competing fact, namely the interfacial bonding of nano-SiO_2 and the PBOZ matrix, which obviously prevails over the aggregation of nano-SiO_2 before 3 wt% load.

CHAPTER IV
EXPERIMENTAL

4.1. Materials

Benzoxazine monomer, bis(3-phenyl-3,4-dihydro-2H-1,3-benoxzinyl) isopropane (BA-a), was synthesized from 2,2′-bis(4-hydroxyphenyl)-propane (bisphenol-A) with aniline and formaldehyde. Bisphenol-A (polycarbonate grade) provided by Thai Polycarbonate Co., Ltd. (TPCC) was used as-received. Para-formaldehyde (AR grade) and aniline (AR grade) were purchased from Merck Ltd.

All of nanosilica was kindly supported by Evonik (Thailand) Ltd. Four grades of hydrophilic nanosilica including Aerosil OX50, Aerosil 90, Aerosil 150 and Aerosil 380. All grade of nanosilica has the density of 2.203 g/cm^3. These particles have surface areas of 50, 90, 150 and 380 m^2/g and primary particle sizes of 40, 20, 14 and 7 nanometers, respectively. Two grades of hydrophobic nanosilica including Aerosil R202 and Aerosil R972 were nanosilica after treated with polydimethylsiloxane and dimethyldichlorosilane, respectively. These particles have surface areas of 100 and 110 m^2/g and primary particle sizes of 14 and 16 nanometers, respectively. All of nanosilica is fluffy, white powder of amorphous structure.

4.2. Sample Preparations

The nanosilica powder was firstly dried at 120 $^{\circ}$C for 12 hours in an air-circulated oven and kept in a desiccator at room temperature. The benzoxazine resin

was well dry-mixed with nanosilica at a desired weight fraction. The molding compounds were prepared by using an internal mixer at temperature of 100 ^{o}C and a mixing speed of 40 rpm for 45 minutes. All molding compounds were thermally cured at 200 ^{o}C under hydraulic pressure of 15 MPa for 3 hours in compression molder. All composites were air-cooled to room temperature in the open mold and were cut into desired shapes before testing.

4.3. Sample characterizations

4.3.1. Density measurement

The density of nanosilica filled polybenzoxazine composites were measured by water displacement method according to ASTM D792-08 (Method A). All specimens were prepared in a rectangular shape of 50 mm×25 mm×2 mm and weighed both in air and in water.

The density was calculated using the following equation:

$$\rho = \frac{A}{A\text{-}B}\rho_0 \qquad (4.1)$$

Where ρ, ρ_o is density of the specimen and liquid at the given temperature, respectively (g/cm^3).

A, B is weight of the specimen in air and in liquid, respectively (g).

4.3.2. Fourier transform infrared spectroscopy (FTIR)

Fourier transform infrared spectra of polybenzoxazine, hydrophilic nanosilica, hydrophobic nanosilica and nanosilica filled polybenzoxazine composite were carried out on a Spectrum GX FTIR spectrometer from Perkin Elmer instrument. All obtained spectra were averaged from 128 scans at a resolution of 4 cm^{-1} within a spectral range of 4000-400 cm^{-1}.

4.3.3. Differential scanning calorimetry measurements

Curing behaviors of nanosilica filled polybenzoxazine molding compounds with different particle sizes and surface treatments at various contents were investigated by a differential scanning calorimeter (model DSC 1 Module) from Mettler Toledo. Approximately 3-5 mg of the molding compounds was placed in an aluminum pan with lid and characterized at heating rates of 10 $^{\circ}C$/min from 30 $^{\circ}C$ – 300 $^{\circ}C$ under nitrogen atmosphere (50 ml/min). The heat flow difference between reference blank and the sample pan was recorded.

4.3.4. Microhardness measurements

The microhardness of nanosilica filled polybenzoxazine composites was determined using Vickers hardness tester (Future-Tech Corp FM-700, Tokyo, Japan) at a constant load of 500 gf (4.9 N) and dwell time of 15 s. Diagonal length of the indentation was measured through a micrometric eyepiece with objective lens (50× magnification). Average values of six readings were reported as the microhardness of the samples.

4.3.5. Dynamic mechanical analysis

Dynamic mechanical analyzer (DMA, model DMA242) from NETZSCH, was used to investigate thermomechanical properties of the composite specimens. The dimension of each specimen was 50 mm × 10 mm × 2 mm. The test was performed under 3-point bending mode. The strain was applied sinusoidally with a frequency of 1 Hz, and the specimen was heated at a rate of 2 $^{\circ}$C/min from 30 to 250 $^{\circ}$C under nitrogen purging.

4.3.6. Morphology of nanosilica filled polybenzoxazine composite

Scanning electron microscopy (SEM) studies were performed using a Jeol JSM-6400, scanning electron microscope with the accelerating voltage of 10 kV. The worn surfaces of the materials were coated with thin gold using a JEOL ion sputtering device (model JFC-1200) for 4 min and then subjected to SEM observation.

4.3.7. Thermogravimetric analysis

Thermogravimetric analysis (TGA) of nanosilica filled polybenzoxazine composite was performed using Mettler Toledo STARe system TGA1 Module. Samples (10-15 mg) were heated from 30 to 850 $^{\circ}$C at dynamic heating rates of 20°C/min under nitrogen purge using a flow rate of 50 ml/min.

4.3.8. Coefficient of friction (COF) measurements

Coefficient of friction (COF) of nanosilica filled polybenzoxazine composites were carried out by using a pin-on-disc high-temperature tribometer (CSM Instruments, Switzerland). The pin was fixed in a holder on a loading lever arm. Normal load of 10 N was applied to the lever arm during the tests. The sliding velocity between the pin and the rotating discs was 0.366 m/s. The sliding distance

was calculated to be 1000 m. The environmental condition in the testing laboratory was 25 $^{\circ}$C.

4.3.9. Specific wear rate measurements

All nanosilica filled polybenzoxazine composites were weighed before and after test in high-temperature tribometer. Specific wear rate of nanosilica filled polybenzoxazine composites were calculated using the following equation

$$W_s = \frac{(W_1 - W_2) \times 10^3}{\rho \times P \times v \times t} \qquad (4.2)$$

Where W_s is specific wear rate of the sample (mm^3/Nm).

W_1, W_2 is weight of the sample before and after test, respectively (g).

ρ is density of the sample (g/cm^3)

P is applied normal load of tribometer (N)

v is sliding velocity of tribometer (m/s)

t is experimental time (s)

CHAPTER V
RESULTS AND DISCUSSION

5.1. Maximum packing density of nanosilica highly filled polybenzoxazine composite

The determination of density is important and highly sensitive measurement to evaluate the quality of samples, which provide insight into the nature of the particle dispersion within the polymer matrix as well as the presence of voids or air gaps in the specimen [53]. The specific density of nanosilica filled polybenzoxazine composites with different particle sizes and surface treatments at various contents of nanosilica is shown in Figure 5.1(a) and 5.1(b), respectively. The actual densities of the nanocomposites were calculated according to Eq. 4.1 and their theoretical densities were calculated according to Eq. 5.1 based on the reported the density of nanosilica of 2.203 g/cm^3 and density of polybenzoxazine of 1.19 g/cm^3.

$$\rho_c = \frac{1}{\frac{w_f}{\rho_f} + \frac{(1-w_f)}{\rho_m}} \quad (5.1)$$

where ρ_c, ρ_f, ρ_m are the composite density (g/cm^3), the filler density (g/cm^3) and the matrix density (g/cm^3), respectively and w_f is the filler weight fraction. From Figure 5.1(a) and 5.1(b), the measured nanocomposite density was

clearly observed to exhibit a linear relationship following the rule of mixture with relatively high accuracy (straight line). The actual density of the composite was similar to the theoretical density thus implying negligible void or air gap in the composites samples. The maximum packing density referred to as the maximum filler content filled in the composite which their theoretical and actual densities are equal. The maximum packing density of nanosilica filled polybenzoxazine composites (Figure 5.1(a)) were 20, 25, 40 and 45 wt% or 11.9, 15.3, 26.5 and 30.7 vol% of nanosilica content with nanoparticle size of 7, 14, 20 and 40 nm, respectively. The attempt to add nanosilica at 23, 28, 43 and 48 wt% for composite with nanoparticle size of 7 nm, 14 nm, 20 nm and 40 nm, respectively, resulted in a lower in the observed composite packing density than the theoretical density which was likely due to the presence of void or air gap in the nanocomposite. Moreover, it can be observed that smaller particle size of nanosilica provided less maximum packing density of the nanocomposite compared to the nanocomposite with larger particle size. It is due to a higher surface area and a lower mass particle of smaller size of silica [58].

Moreover, the maximum packing density of polybenzoxazine filled nanosilica after treated with polydimethylsiloxane (PDMS) and dimethyldichlorosilane (DDS) were 30 wt% and 30 wt% of nanosilica content as displayed in Figure 5.1(b). It can be seen that both surface treatment of nanosilica provided equal maximum packing

density of both nanocomposite, which is due to the similar surface area of those two treated nanosilica.

Furthermore, the highly filled nanosilica in various composite systems has been reported [2, 59]. Goertzen and Kessler investigated the maximum packing density of nanosilica filled cyanate ester system which was reported to be 20.7 vol% using 40 nm of nanosilica and only up to 3.4 vol% with nanosilca size of 12 nm [2]. Zhang et al. reported that the maximum packing density of nanosilica filled epoxy system was up to only 14 vol% using nanosilica particle size of 25 nm [59]. However, the maximum packing densities of those two nanocomposite systems i.e. nanosilica filled cyanate ester and nanosilica filled epoxy were relatively lower than that of nanosilica filled polybenzoxazine composite compared to the composite with the same nanosilica size. Therefore, it could be concluded that benzoxazine resin accommodated the greater filler content than other thermosetting polymer which is due to the much lower melt viscosity of benzoxazine resin among the others.

5.2. Spectroscopic properties of nanosilica filled polybenzoxazine nanocomposites

FT-IR spectroscopy was used to verify the chemical interaction between nanosilica particle and polybenzoxazine matrix. Figure 5.2(a) shows spectrum of hydrophilic nanosilica which exhibited the characteristic peaks at about 1110 cm^{-1},

assigned to the asymmetric stretching vibrations of siloxane groups (Si–O–Si), whereas the band at 811 cm^{-1} is attributed to the symmetric stretching of Si–O–Si. Moreover, a broad peak at 3426 cm^{-1} is attributed to hydroxyl groups (symmetric stretching –OH-) attached to a silicon atom on the nanosilica surface [53, 60]. Figure 5.2(b) shows FT-IR spectrum of benzoxazine monomer with a characteristic peak at 1497 cm^{-1} due to tri-substituted benzene ring, whereas the peak at 947 and 1233 cm^{-1} assigned to C-O-C stretching mode of benzoxazine ring. The spectrum of benzoxazine molding compound filled with nanosilica showed the characteristic peaks at 1110 cm^{-1}, which is the asymmetric stretching vibrations of siloxane groups (Si–O–Si) in nanosilica particle, while the band at 1497 cm^{-1} and 947 cm^{-1} is attributed to tri-substituted benzene ring and C-O-C stretching mode of benzoxazine ring in benzoxazine monomer as observed in Figure 5.2(c). Figure 5.2(d) shows FTIR spectrum of polybenzoxazine with a characteristic peak at 1488 cm^{-1} which assigned to tetra-substituted benzene ring that led to the formation of a phenolic hydroxyl group-based polybenzoxazine structure. The FTIR spectrum of the 45 wt% of nanosilica filled polybenzoxazine is presented in Figure 5.2(e). From this Figure, the new peak at 1073 cm^{-1} assigned to Si-O-C stretching was apparently observed in Figure 5.2(e). The appearance of this absorption band is a clear evidence of the chemical bonding formed between the polybenzoxazine matrix and the nanosilica. Agag and Takeichi reported the peak of Si-O-C stretching at 1087cm^{-1} to follow the formation reaction

of silica nanoparticles from the starting benzoxazine resin and silanes [22]. Dueramae et al also observed the peak of Si-O-C stretching at 1075 cm^{-1} to confirm the formation reaction of silica nanoparticles and benzoxazine matrix [53]. Therefore, the chemical bonding between the nanosilica and the polybenzoxazine matrix should provide a substantial reinforcing effect to the nanosilica filled polybenzoxazine composite.

In addition, FTIR spectra of nanosilica after chemical treatment and their composites were also observed. The spectrum of nanosilica after treated with polydimethylsiloxane (PDMS) and dimethyldichlorosilane (DDS) showed the characteristic peaks at about 1110 cm^{-1}, which is due to the asymmetric stretching vibrations of siloxane groups (Si–O–Si), whereas the band at 805 cm^{-1} is attributed to the symmetric stretching of Si–O–Si, while the band at 2935 cm^{-1} is attributed to the asymmetric stretching of C-H as observed in Figure 5.3(a) and 5.3(b). Figure 5.3(c) and 5.3(d) show FTIR spectrum of polybenzoxazine with a characteristic peak at 1488 cm^{-1} due to tetra-substituted benzene ring that led to the formation of a phenolic hydroxyl group-based polybenzoxazine structure, whereas the peak at 1110 cm^{-1} assigned to the asymmetric stretching vibrations of siloxane groups (Si–O–Si) in nanosilica. However, the peak of Si-O-C stretching at 1073 cm^{-1} was not observed in nanocomposite of DDS and PDMS silica, which exhibited no chemical bonding

between the nanosilica particle of both surface treatment and the polybenzoxazine matrix.

5.3. Curing characteristics of nanosilica filled benzoxazine molding compounds

The curing reaction of benzoxazine molding compound with different nanosilica particle sizes and surface treatments at various contents of nanosilica were investigated by non-isothermal differential scanning calorimetry as shown in Figure 5.4(a) and 5.4(b). From the DSC thermograms, the single exothermic peak of the curing reaction in each nanosilica particle size and surface treatment was observed. From the Figure, the curing exotherms of these benzoxazine compounds presented thermal curability of benzoxazine resin without adding catalyst for the polymerization process. The exothermic peak of the neat benzoxazine resin was found at 228 $^{\circ}$C. In Figure 5.4(a), the positions of the exothermic peaks of the benzoxazine molding compound with different nanosilica particle sizes at 20wt% nanosilica content were located at 228, 225, 224 and 226 $^{\circ}$C at particle size of 7, 14, 20 and 40 nm, respectively. Furthermore, the effect of untreated and surface treatment of nanosilica (similar particle size) on curing characteristic of benzoxazine compounds was investigated. In Figure 5.4(b), the exothermic peaks of the benzoxazine molding compound filled with 20 wt% of untreated and treated

nanosilica were observed to be 225, 227 and 226 °C at untreated silica (14 nm), PDMS treated silica and DDS treated silica, respectively. It can be concluded that no significant change in the exothermic peak position of the benzoxazine molding compound with different particle sizes and surface treatment was observed thus indicating the particle size and surface treatment of nanosilica is not influenced to the benzoxazine curing reaction. Moreover, the exothermic curing enthalpy of the neat benzoxazine resin was measured to be 280 J/g. The exothermic curing enthalpies of the benzoxazine molding compound were measured to be 201, 208, 195 and 197 J/g at silica particle size of 7, 14, 20 and 40 nm, respectively whereas the exothermic curing enthalpies of the benzoxazine molding compound were found to be 208, 202 and 199 J/g at untreated silica (14 nm), PDMS treated silica and DDS treated silica, respectively. From the results, the exothermic curing enthalpies also not significantly change with different particle sizes and surface treatment of nanosilica.

The polymerization behaviors of benzoxazine molding compound with 40 nm of untreated nanosilica at various contents were investigated by DSC as shown in Figure 5.5. From this Figure, the exothermic curing enthalpy was measured to be 280 J/g for neat benzoxazine resin. The exothermic curing enthalpies of benzoxazine molding compounds were measured to be 273, 244, 197 and 130 J/g at nanosilica content of 3, 10, 20 and 45 wt%, respectively. The result indicated that the

exothermic curing enthalpy of benzoxazine molding compound decreased with increasing nanosilica content. Figure 5.6(a) and 5.6(b) show the polymerization behaviors of benzoxazine molding compound with PDMS treated silica and DDS treated silica at various nanosilica contents. The exothermic curing enthalpies of benzoxazine molding compounds were found to be 280, 251, 203 and 163 J/g at silica PDMS content of 0, 10, 20 and 30 wt%, respectively. In Figure 5.6(b), the curing enthalpies of benzoxazine molding compound with DDS treated silica were measured to be 280, 255, 208 and 161 J/g at nanosilica content of 0, 10, 20 and 30 wt%, respectively. The exothermic curing enthalpies of benzoxazine molding compound with PDMS treated silica and DDS treated silica were also decreased with increasing nanosilica content as same as untreated nanosilica.

5.4. Microhardness of nanosilica filled polybenzoxazine nanocomposites

Microhardness is generally investigated as one of the most important factors that are related to the abrasion and wear resistance of composite materials [61]. Abrasion and wear are especially important in such applications as plastic bearings, floor covering materials, and friction material [52]. Rigid fillers are normally much harder than plastics as measured by most tests, so it is not surprising that such fillers increase the microhardness of the composite over that of the polymer. The microhardness values of nanosilica filled polybenzoxazine composite with untreated

silica at various contents are shown in Figure 5.7(a). The microhardness of the nanosilica composites was found to increase with increasing nanosilica content. At 40 nm of untreated nanosilica, the microhardness of the nanocomposite was improved from 405 MPa of the neat polybenzoxazine to 409, 433, 480 and 625 MPa at nanosilica content of 3, 10, 20 and 45 wt%, respectively. The microhardness of the nanosilica composites was measured to be 525, 536, 603 and 625 MPa at their maximum packing density of composite filled with nanosilica size 7, 14, 20 and 40 nm, respectively. A large increase in microhardness is attributed to a much higher hardness of the nanosilica (10,784 MPa) [36] compared to that of the neat polybenzoxazine (405 MPa). The improvement of microhardness value is attributed to the homogeneous dispersion of the nanofiller in the polybenzoxazine matrix and to the strong filler-polymer interactions with decreasing in interparticle distance when the amount of the filler increases [53]. Moreover, the microhardness of the nanocomposites was also found to increase with decreasing size of the nanosilica. Comparing at the same nanosilica content of 20 wt%, the microhardness of the nanocomposites was determined to be 525, 506, 492 and 480 MPa for nanosilica sizes of 7, 14, 20 and 40 nm, respectively. The behavior suggests good interfacial property between the nanosilica and polybenzoxazine matrix. This result is consistent with the observation by FTIR spectra in Figure 5.2(e) that silica nanoparticles can form covalent bond through ether linkages as a result of

polycondensation reaction of the hydroxyl group in the nanosilica and phenol moieties in the polybenzoxazine.

In Figure 5.7(b), the microhardness values of nanosilica filled polybenzoxazine composite with different nanosilica surface treatment were observed to be 506, 432 and 465 MPa at untreated silica (14 nm), PDMS treated silica and DDS treated silica, respectively. The microhardness values of nanocomposite filled DDS treated silica was higher than that of nanocomposite filled with PDMS treated silica which was due to the hardness of PDMS treated silica lower than DDS treated silica as a result from long polymeric chain in PDMS. Comparing between nanoscomposites filled with untreated and treated nanosilica, the microhardness of the nanocomposites filled untreated nanosilica has higher than treated nanosilica. This is due to nanocomposites filled untreated nanosilica can form chemical bonding between the untreated nanosilica and the polybenzoxazine matrix which should provide better interfacial interaction between the untreated nanosilica and the polymer matrix than the treated nanosilica and the polymer matrix (as discussed in Section 5.2).

In addition, our polybenzoxazine nanocomposites showed better improvement in microhardness than epoxy/nanosilica comparing at the same filler content. The microhardness value of epoxy composite increased from about 177 MPa for the neat epoxy to 218 MPa for 25wt% (15 vol%) nanosilica nanocomposite

with nanosilica particle size 25 nm [62]. In case of UA/TMPTA, the hardness value increased from 320 MPa for the neat UA/TMPTA to 490 MPa for the UA/TMPTA filled with 40 wt% of 20 nm nanosilica.

5.4.1. Modeling studies of microhardness of nanosilica filled polybenzoxazine nanocomposites

The increment of the microhardness value of nanosilica filled polybenzoxazine composite with 40 nm nanosilica particle size was observed to be of an exponential type and can be predicted by Halpin-Tsai model as can be seen in Figure 5.8. Another simplest theoretical model to predict the microhardness of particle-reinforced polymer composites is the simple rule of mixture (ROM) as represent by Eq. 5.2. As shown in Figure 5.8, the absolute upper bound would be given by rule of mixture (ROM), where a constant strain is assumed in each of the phases. This is more suitable, however, for composites with unidirectional reinforcement. A wide gap exists between the experimental data and the microhardness predicted from this model. This can be attributed to the surface coating of nanosilica particle with a film of matrix and hence, preventing direct particle-particle contact. Moreover, due to much lower maximum packing factor of the nanosilica particle under applied pressure, nanocomposites could not resist the indent penetration in proportion of nanosilica content.

Haipin-Tsai model is a semi-empirical relationship that takes into account the aspect ratio of the reinforcing particles [61]. This model has shown good fitting for modulus due to it takes into account the aspect ratio of the reinforcing particles [63]. Therefore, Halpin-Tsai equation was applied for microhardness by replacing symbol of modulus with hardness as shown in Equation 5.3

$$H_c = H_f V_f + H_m V_m \quad \text{ROM} \quad (5.2)$$

$$Hc = Hm\,[(1 + \xi\eta V_f) / (1 - \eta V_f)] \quad \text{Halpin – Tsai} \quad (5.3)$$

$$\eta = [(H_f/H_m - 1) / (H_f/H_m + \xi)]$$

Where H_c, H_f, H_m are the hardness of the composite, particle, and matrix respectively, V_f, and V_m are the volume fractions of the particle and matrix respectively. ξ is an adjustable parameter. The upper bound is obtained when ξ = infinite and lower bound when ξ = 0. The values of ξ depend on the geometry and packing of the particles as well as on the direction of the load relative to the orientation of anisotropic particles, especially with the aspect ratio *(w/t)* of the particles, where *w* the length of the particle and *t* is its thickness. Halpin and Kardos [64] suggested that a shape factor of ξ = 2*w/t* is used for calculating the microhardness of a polymer with particles reinforcement. For the spherical particles used in this work the aspect ratio *(w/t)* = 1, hence ξ = 2 will be used.

5.5. Dynamic mechanical properties of the polybenzoxazine nanocomposites

Storage modulus is an important material parameter for measuring stiffness and elasticity of polymeric materials. Figure 5.9(a) and (b) show the storage modulus (E') of nanosilica filled polybenzoxazine composites with different particle sizes and surface treatment at various contents of nanosilica. From the Figure, the storage modulus of untreated nanosilica filled polybenzoxazine composite at its glassy state (35°C) was observed to systematically increase with increasing nanosilica content. For example, the storage modulus of the nanocomposite with 40 nm of nanosilica was 6.1, 6.4, 7.0 and 11.5 GPa at nanosilica content of 3, 10, 20 and 45 wt%, respectively. It was likely due to the high stiffness of the nanosilica which can substantially increase the storage modulus of the polybenzoxazine composite. The strong reinforcement also implies substantial interfacial interaction between the nanosilica and the polybenzoxazine matrix. At the same nanosilica content, the value of storage modulus of the nanocomposite tended to increase with decreasing size of the nanosilica. The modulus value of the nanosilica composites was measured to be 8.0, 7.5, 7.3 and 7.0 GPa at content 20 wt% of nanosilica content with particle size of 7, 14, 20 and 40 nm, respectively. The phenomenon suggested the better reinforcing effect of the smaller size of the nanosilica due to its much larger interfacial surface area. In addition, Figure 5.9(b) shows the modulus values of nanosilica filled

polybenzoxazine composite with different surface treatment. The storage modulus of nanocomposite was observed to be 7.5, 6.9 and 7.2 GPa at 20 wt% of untreated nanosilica (14 nm), PDMS treated silica and DDS treated silica, respectively. The modulus values of nanocomposite filled DDS treated silica was higher than that of nanocomposite filled PDMS treated silica which was due to the stiffness of PDMS treated silica lower than DDS treated silica, corresponding to the microhardness value of both nanocomposites. Comparing between nanocomposites filled with untreated and treated nanosilica, the storage modulus of the nanocomposites filled untreated nanosilica was higher than that of treated nanosilica. This is due to the formation of a strong interface between the hydroxyl groups of the nanosilica and the phenolic hydroxyl groups of the polybenzoxazine as discussed earlier in the spectroscopic analysis of the samples. Moreover, the storage modulus of nanosilica filled polybenzoxazine composite was enhanced from 5.9 GPa for the neat polybenzoxazine to 8.0, 8.3, 10.7 and 11.5 GPa at its maximum packing density of each nanosilica size of 7, 14, 20 and 40 nm, respectively, which accounted to be about 36, 41, 81 and 95% enhancement in the polybenzoxazine stiffness. The values are also substantially higher than that of nanosilica filled cyanate ester at its maximum nanosilica content as reported by Goertzen and Kessler [2]. The authors reported the modulus values of nanosilica filled cyanate ester using particle sizes of 12 and 40 nm at the filler loading of up to 3.4 and 20.7% by volume which was

enhanced from the neat cyanate ester boutof a 2.7 GPa. Furthermore, the maximum packing density of nanosilica filled epoxy system was observed by Johnsen et al [65]. They reported the maximum packing density of nanocomposite filled with 20 nm nanosilica size at 20.2 wt% or 13.4 vol%. The modulus value of nanosilica filled epoxy composite was enhanced from 2.96 GPa for the neat epoxy to 3.85 GPa at maximum packing density of nanocomposite, which represents an increase of 30% over the unfilled system. The greater enhancement of the storage modulus observed in nanosilica filled polybenzoxazine composite than in epoxy and cyanate ester composite systems as compared in Table 5.1 suggests the greater interaction between the nanosilica and the polybenzoxazine matrix than that in epoxy and cyanate ester resins [2, 62, 65, 66]. These results suggest that benzoxazine resin is a highly effective adhesive for the nanosilica filler.

5.5.1. Modeling studies of modulus of nanosilica highly filled polybenzoxazine composites

There are many proposed theoretical models used to predict the properties of particulate filled polymers [61]. In our study, isostrain model (rule of mixtures), isostress model (or Reuss average), Mori-Tanaka and Kerner models are evaluated to predict the modulus of the highly nanosilica filled polybenzoxazine composites. The isostress model assumes that the matrix and filler are stressed equally while the

isostrain model assumes that a strain is constant in each of the phases. In the Mori-Tanaka method, it is assumed that only the two phases exist (matrix and reinforcement) and are perfectly bonded to each other. The effective storage modulus for a composite reinforced by spherical particles based on the Mori-Tanaka method could be predicted by the relationship

$$E_c = \frac{9\overline{K}_c\overline{G}_c}{3\overline{K}_c + \overline{G}_c} \tag{5.4}$$

Where E_c, K_c and G_c are the effective storage modulus, bulk modulus, and shear modulus of nanocomposites, respectively.

The values of K_C and G_C can be expressed as follows:

$$\overline{K}_c = \overline{K}_m + \frac{V_f\overline{K}_m(\overline{K}_f - \overline{K}_m)}{\overline{K}_m + \beta_2(1-V_f)(\overline{K}_f - \overline{K}_m)} \tag{5.5}$$

$$\overline{G}_c = \overline{G}_m + \frac{V_f\overline{G}_m(\overline{G}_f - \overline{G}_m)}{\overline{G}_m + \beta_1(1-V_f)(\overline{G}_f - \overline{G}_m)} \tag{5.6}$$

$$\beta_1 = \frac{2(4-5v_m)}{15(1-v_m)} \tag{5.7}$$

$$\beta_2 = 3 - 5\beta_1 \tag{5.8}$$

Where V_f is volume fraction of nanoparticle

v_m, K_m, G_m are Poisson's ratio, bulk modulus, shear modulus of matrix, respectively.

K_f, G_f are bulk modulus, shear modulus of filler, respectively.

This model is based on a low concentration of micrometer-scale or larger filler embedded in the matrix. The interactions between the filler and the matrix, as well as the filler between filler are not considered. Finally, another usually used model for estimating the modulus of composite containing spherical particles is the Kerner equation, generalized by Lewis and Nielsen [61] and given by

$$\frac{E_c}{E_m} = \frac{1+ABV_f}{1-B\varphi V_f} \tag{5.9}$$

Where A is a constant (it is usually referred as k_E - 1, where k_E is the Einstein coefficient), which depends on the geometry of the filler phase and the Poisson's ratio for the matrix (ϑ). B is also a constant that takes into account the relative modulus between the filler and the polymer matrix. Constants A (for spherical particles) and B are given by

$$A = \frac{7-5\vartheta}{8-10\vartheta} \tag{5.10}$$

$$B = (\frac{E_f}{E_m} - 1)/(\frac{E_f}{E_m} + A) \tag{5.11}$$

The factor φ is the maximum packing fraction of the filler into the matrix. It can be estimated using the following relation:

$$\varphi = 1 + \frac{1-\emptyset_m}{\emptyset_m^2} V_f \tag{5.12}$$

Where E_f , E_m are the storage modulus of filler and matrix, respectively.

ϕ_m is the maximum packing fraction

5.5.2. Comparison between experimental results and model prediction

All constants for the fillers and matrix used in the model calculations are listed in Table 5.2. Figure 5.10 shows the comparison of the isostress model, isostrain model (rule of mixtures), Mori-Tanaka and Kerner models to the experimental data for the storage modulus of composite filled with nanosilica size 40 nm as a function of volume percentage of fillers. The absolute upper bound would be given by an isostrain model (rule of mixtures) of the composite. The isostress model (or Reuss average) gives a theoretical lower bound for the composite modulus. The Mori-Tanaka model was found to be good agreement with the experimental data at low volume fraction up to 5.7 vol% of fillers. The Mori-Tanaka model assumes that only two phases exist in composite (matrix and reinforcement), and that they are perfectly joined to each other. The existence of interfacial phase between particle and matrix was not considered in this model, which this model does not also consider the interaction between the fillers which is critical at high filler loading. Typically, the Mori-Tanaka approach has been used to accurately predict the overall properties of composites with filler size in micrometer scale or larger [12]. As seen in Figure 5.10,

the experimental data is fitted to the value obtained by Kerner model. In the analysis, we used three different values for the fitting of the maximum packing fraction: ϕ_m = 0.632 (for random close packing without agglomeration), ϕ_m = 0.601 (for random loose packing without agglomeration), and ϕ_m = 0.37 (for random close packing with agglomeration) [53]. The best fit for the storage modulus of our nanocomposites was found when the maximum packing fraction for random close packing without agglomeration of the nanosilica, ϕ_m = 0.632, is used with A = 1.088. The values for both parameters (ϕ_m and A) suggest no agglomeration in the system. If the particles are strong aggregates, the factor A becomes higher as can observe in alumina filled epoxy nanocomposites system [66]. At the same ϕ_m = 0.632, the best fit of alumina filled epoxy nanocomposites system is found when A has value of at least 3, which can indicate that the higher values of the constant A are an indication for the existent of agglomerates.

5.6. Glass transition temperature (T_g) of nanosilica highly filled polybenzoxazine composites

Glass transition temperature (T_g) of nanosilica filled polybenzoxazine composite was observed from the peak position of tan δ. T_g of nanocomposite at various nanosilica contents and each silica particle size was shown in Figure 5.11(a). The T_g of the nanocomposite was higher than that of the neat polybenzoxazine

which was observed to be 185 ^{o}C. The T_g of nanosilica filled polybenzoxazine composite was found to increase with increasing nanosilica contents. For example at 40 nm of nanosilica, The T_gs of the nanocomposites were investigated to be 186, 188, 192 and 203 ^{o}C at nanosilica content of 3, 10, 20 and 45 wt%, respectively. The improvement of T_g of the polybenzoxazine with an addition of the nanosilica filler is attributed to an ability of the nanosilica particles to substantially restrict the motion of the polybenzoxazine chains thus higher temperature is required to provide the requisite thermal energy for the occurrence of a glass transition in the nanocomposites [53]. The T_g of the nanocomposite of 197, 199, 202 and 203 ^{o}C was attained at the maximum packing density of the composite filled with nanosilica size of 7, 14, 20 and 40 nm, respectively. Moreover, at fixed 20 wt% content, The T_g of the nanocomposite increased with decreasing the size of nanosilica. The T_gs of the nanosilica filled polybenzoxazine composites were measured to be 197, 196, 194 and 192 ^{o}C with particle size of 7, 14, 20 and 40 nm, respectively, which is due to the fact that the smaller size of nanosilica has a higher surface area than larger size of nanosilica. This characteristic generally promotes better interfacial interaction between the filler and the polymer matrix.

In addition, the T_g of polybenzoxazine composite filled with different surface treatment of nanosilica was shown in Figure 5.11(b). T_g of nanocomposite filled with surface treated nanosilica was also found to increase with increasing nanosilica

content. At fixed content 20 wt%, the T_g of nanocomposite was found to be 196, 192 and 194 ^{o}C with untreated silica (14 nm), PDMS treated silica and DDS treated silica, respectively. Comparing between nanocomposites filled with surface treated silica, the T_g of nanocomposite filled with DDS treated silica was higher than that of nanocomposite filled with PDMS treated silica as PDMS treated silica was covered by long polymeric chain of PDMS resulting in a higher free volume than DDS filled silica. It is well known that the free volume influence to T_g of nanocomposite. Moreover, The T_g of nanocomposite with untreated silica is higher than nanocomposite with treated silica. It is due to untreated silica possessed a lower free volume than treated silica which is attributed to the formation of a strong interface between the hydroxyl groups of the untreated silica and the phenolic hydroxyl groups of the polybenzoxazine as discussed in Section 5.2.

In comparison to other silica filled nanocomposite systems, negligible change in T_g of composite was observed in the nanosilca filled cyanate ester composite [2, 66]. Furthermore, T_g of nanosilica filled epoxy systems was even found to decrease with the nanosilica loadings with various size of nanosilica as seen in Table 5.1.

5.7. Thermal stability of nanosilica filled polybenzoxazine composites

Thermal stability determined via degradation temperature at 5 % weight loss ($T_{d,5}$) of nanosilica filled polybenzoxazine composite with each silica particle size at various nanosilica contents is exhibited in Figure 5.12(a). The $T_{d,5}$ of the untreated nanosilica composites was found to increase with increasing nanosilica content. For 40 nm of nanosilica, The $T_{d,5}$s of the nanocomposites improved from 325 ^{o}C for the neat polybenzoxazine to 327 ,333 ,342 and 365 ^{o}C at nanosilica content of 3, 10, 20 and 45 wt%, respectively. The $T_{d,5}$s of the nanocomposites at their maximum packing density were observed to be 357, 358, 364 and 365 ^{o}C with nanosilica particle size of 7, 14, 20 and 40 nm, respectively. The substantial enhancement of $T_{d,5}$ of nanosilica filled polybenzoxazine composite is attributed to the shielding effect of nanosilica filler which can serve as a good thermal cover layer, avoiding the direct thermal decomposition of the polymeric matrix by heat [53]. Moreover, the $T_{d,5}$ of nanocomposites was found to increase with decreasing size of the nanosilica as shown in Figure 5.12(a). At 20 wt% of nanosilica filled polybenzoxazine composite, the $T_{d,5}$ of the nanocomposites was measured to be 357, 351, 346 and 342 ^{o}C with nanosilica size of 7, 14, 20 and 40 nm, respectively. This is due to the finer particle has a higher surface area than bigger particle that supports better interfacial interaction between the filler and the polymer matrix.

In addition, Figure 5.12(b) exhibits $T_{d,5}$ of nanosilica filled polybenzoxazine composite with different surface treatment of silica. The $T_{d,5}$ of the nanosilica composites was found to be 351, 341 and 344 ^{o}C at 20 wt% of untreated nanosilica (14 nm), PDMS treated silica and DDS treated silica, respectively. The $T_{d,5}$ of nanocomposite filled DDS treated silica was higher than that of nanocomposite filled with PDMS treated silica which is attributed to thermal stability of DDS treated silica is better than PDMS treated silica [67]. Comparing between composites filled with untreated and treated nanosilica, the $T_{d,5}$ of the nanocomposites filled untreated silica is higher than that of nanocomposite filled treated silica. This is due to the formation of a strong interface between the hydroxyl groups of the untreated silica and the phenolic hydroxyl groups of the polybenzoxazine, which should provide better interfacial interaction between the untreated silica and the polymer matrix.

5.8. Tribological properties of nanosilica filled polybenzoxazine composites

Tribological properties of nanosilica filled polybenzoxazine composites including coefficient of friction, specific wear rate and worn surface of nanocomposite are such important factors for friction material characterization.

5.8.1. Coefficient of friction (COF) of nanosilica filled polybenzoxazine composites

Coefficient of friction (COF) is an important parameter for measuring friction of polymeric materials which using as a friction material. Figure 5.13(a) shows COF of nanosilica filled polybenzoxazine composites with different particle sizes at various contents of nanosilica. The COF of the nanosilica composites was found to increase with addition of nanosilica. For example, at 40 nm nanosilica , the COF of the composite enchanced from 0.483 for the neat polybenzoxazine to 0.492, 0.525, 0.581 and 0.665 at nanosilica content of 3, 10, 20 and 45 wt%, respectively. Moreover, the COF of nanocomposite was observed to be 0.646, 0.655, 0.662 and 0.665 at its maximum packing density of nanosilica filled polybenzoxazine composite with particle size 7, 14, 20 and 40 nm, respectively. The improved COF with increasing nanosilica content was because the hard nanosilica particles can be separated from the polybenzoxazine matrix during wear test, resulting in scratch effect on the nanocomposite materials and thus COF of the nanosilica filled polybenzoxazine composites increased. In addition, COF of the nanocomposites was observed to be 0.646, 0.625, 0.604 and 0.581 at 20 wt% of nanosilica with particle size of 7, 14, 20 and 40 nm, respectively. It can be seen that COF of the nanocomposite filled with smaller size of nanosilica was higher than that of nanocomposite filled with larger size of nanosilica. This is due to smaller transfer

films occurred from composite with smaller particle size as evidenced in Figure 5.16. Furthermore, COF of nanosilica filled polybenzoxazine composites with different surface treatment at various contents of nanosilica as shown in Figure 5.13(b). The COF of nanocomposite was found to be 0.625, 0.560 and 0.585 at 20 wt% of nanosilica with untreated silica (14 nm), PDMS treated silica and DDS treated silica, respectively. The COF of nanocomposite filled DDS treated silica was higher than that of nanocomposite filled with PDMS treated silica. Comparing between nanocomposites filled with untreated and treated nanosilica, the COF of nanocomposites filled with untreated silica is higher than that of nanocomposites filled with treated silica. This is due to the more transfer film of the polybenzoxazine filled with treated nanosilica. Moreover, these results were in agreement with the result of poly(ethylene) terephthalate filled with nanoalumina particles in which smaller alumina particle resulted in higher COF of composites [68].

5.8.2. Specific wear rate of nanosilica filled polybenzoxazine composites

Specific wear rate is one of important factor for friction material which it indicate amount of wear debris of specimens after test by tribometer. It also indicates wear resistant of specimens which can be calculated by Eq. 4.2. Specific wear rate of nanosilica filled polybenzoxazine composites with different particle sizes at various contents of nanosilica is shown in Figure 5.14(a). The specific wear rate of nanosilica composite was found to decrease with increasing nanosilica content. It

was also found that the addition of nanosilica at different particle size i.e.7, 14, 20 and 40 nm into the polybenzoxazine matrix significantly reduced the specific wear rate of nanosilica composite. For example, at 40 nm of nanosilica, specific wear rate reduced from $9.27x10^{-4}$ mm^3/Nm for the neat polybenzoxazine to $7.34x10^{-4}$, $5.53x10^{-4}$, $2.35x10^{-4}$ and $1.01x10^{-4}$ mm^3/Nm at nanosilica content of 3, 10, 20 and 45 wt%, respectively. In addition, the specific wear rate of nanosilica filled polybenzoxazine composite was found to be $1.13x10^{-4}$, $1.10x10^{-4}$, $1.05x10^{-4}$ and $1.01x10^{-4}$ mm^3/Nm at its maximum packing density of nanocomposite with nanosilica size of 7, 14, 20 and 40 nm, respectively. Moreover, the specific wear rate of nanosilica filled polybenzoxazine composite decreases with decreasing nanosilica particle size as shown in Figure 5.14(a). The specific wear rate of the nanosilica composites was found to be $1.13x10^{-4}$, $1.59x10^{-4}$, $1.90x10^{-4}$ and $2.35x10^{-4}$ mm^3/Nm at 20 wt% of nanosilica with particle size of 7, 14, 20 and 40 nm, respectively. This is due to the different of wear mechanism in nanocomposite which the neat polybenzoxazine showed adhesive wear on its worn surface. The composites with nanosilica particle presented adhesive and abrasive wear which abrasive wear was more observed with increasing nanosilica content. The abrasive wear was showed a ploughing groove on worn surface of specimen. The adhesive wear was represented by a plastic deformation on worn surface of specimen which the specific wear rate of plastic deformation was higher than that of ploughing groove as seen in Figure 5.15.

This result was inversely related with microhardness which the hardness values of the nanocomposite increased with decreasing particle size of nanosilica. It can be seen that the microhardness of our nanocomposite is an important factor related to wear resistance as similarly observed in zirconium oxide filled PMMA composites [69]. This also indicates that the nanosilica with particle sizes in the range of 7 - 40 nm is very effective particle in reducing the specific wear rate of the composite. Moreover, smaller size nanosilica seemed to be more effective in reduction of the specific wear rate of the composite which is consistent with the results of epoxy filled with uniform sized spherical silica particles with diameter of 120 or 510 nm [70].

In addition, the specific wear rate of nanosilica filled polybenzoxazine composites with different surface treatment of silica is shown in Figure 5.14(b). The specific wear rate of nanosilica composite with different surface treatment was also found to decrease with increasing nanosilica content. The specific wear rate of nanocomposite was found to be 1.59×10^{-4}, 5.74×10^{-4} and 4.66×10^{-4} mm^3/Nm at 20 wt% of untreated nanosilica (14 nm), PDMS treated silica and DDS treated silica, respectively. The specific wear rate of nanocomposite filled with DDS treated silica was lower than that of nanocomposite filled with PDMS treated silica which was due to the longer polymer chain of PDMS resulting in the lower interaction between polymer matrix and PDMS treated silica. The result of specific wear rate of the

composite is corresponded to the result of microhardness of the nanocomposites. Comparing between nanocomposites filled with untreated and treated nanosilica, the specific wear rate of the nanocomposites filled with untreated silica is lower than that of nanocomposites filled with treated silica. This is due to the formation of a strong interface between the hydroxyl groups of the nanosilica and the phenolic hydroxyl groups of the polybenzoxazine as discussed earlier in the spectroscopic analysis of the samples.

5.8.3. Worn surfaces of nanosilica filled polybenzoxazine composite

Worn surfaces are surface of specimens after test by tribometer, which specimens are sliding against hard material with applied loading. The worn surfaces of each specimen show wear mechanisms of composite, which influenced to COF and specific wear rate. Worn surfaces of the neat polybenzoxazine and nanosilica filled polybenzoxazine composite with different particle size at various contents was observed by scanning electron microscopy (SEM) as presented in Figure 5.15. Figure 5.15(a) shows worn surface of the neat polybenzoxazine which small cracks across the wear track which occurred due to the brittle nature of the polybenzoxazine as well as large plastic deformation with numbers of tracks were observed. With an increasing in nanosilica content, a plastic deformation on the worn surface of the composite decreased whereas a ploughing groove on the worn surface increased as seen in Figure 5.15(b-e). Moreover, none of a plastic deformation was noticed on the

worn surface of 45 wt% of silica filled polybenzoxazine composite as seen in Figure 5.15(e). There observed on worn surface of the nanocomposites related to the specific wear rate in which a lower plastic deformation of the composite provided a lower specific wear rate of the composites, which is due to the interaction between silica and polybenzoxazine matrix.

Figure 5.16(a)-(d) shows the effect of the particle size at 20 wt% of nanosilica on the wear behavior of the nanosilica filled polybenzoxazine composite. As a result, a plastic deformation on the worn surface of the nanocomposite decreased with a decreasing of particle size of nanosilica. On the other hand, a ploughing groove on the worn surface was observed to increase with a larger particle size. The results of worn surface of the nanocomposite also related to the specific wear rate of the composite in which a lower particle size of nanosilica in the composite provided a lower value of specific wear rate. It was due to the fact that the smaller size of nanosilica has a higher surface area than larger size of nanosilica. This characteristic generally promotes better interfacial interaction between the filler and the polymer matrix.

Worn surface of nanosilica filled polybenzoxazine composite with PDMS and DDS treated silica at various nanosilica contents is presented in Figure 5.17 and 5.18, respectively. As seen, no obvious difference in worn surface of the two surface treated silica filled polybenzoxazine composite was noticed. Futhermore, a smaller

plastic deformation on the worn surface of both type of surface treated silica in the composites was observed with increasing silica content up to 30 wt%. In comparison to the untreated silica filled polybenzoxazine composite with the same amount of silica as seen in Figure 5.19, a much plastic deformation was noticed on the worn surface of surface treated silica filled polybenzoxazine composites resulting in a higher in specific wear rate of the composites filled with surface treated silica. This is due to the formation of a strong interface between the hydroxyl groups of the untreated silica and the phenolic hydroxyl groups of the polybenzoxazine, which should provide better interfacial interaction between the untreated silica and the polymer matrix. Transfer film on steel pin surface of nanocomposite filled untreated silica was observed in figure 5.19(e). From figure 5.19(f), the surface treatment of nanosilica in composite led to more formation of transfer film on steel pin surface. In addition, comparing between nanoscomposites filled with untreated and treated of nanosilica, worn surface of the nanocomposites filled treated nanosilica was more obvious plastic deformation than untreated nanosilica were observed. This is due to the nanocomposites filled treated silica form more transfer film than nanocomposite filled untreated silica, which it was confirmed by SEM micrograph of steel pin after sliding against those nanocomposite as shown in Figure 5.19(e) and 5.19(f).

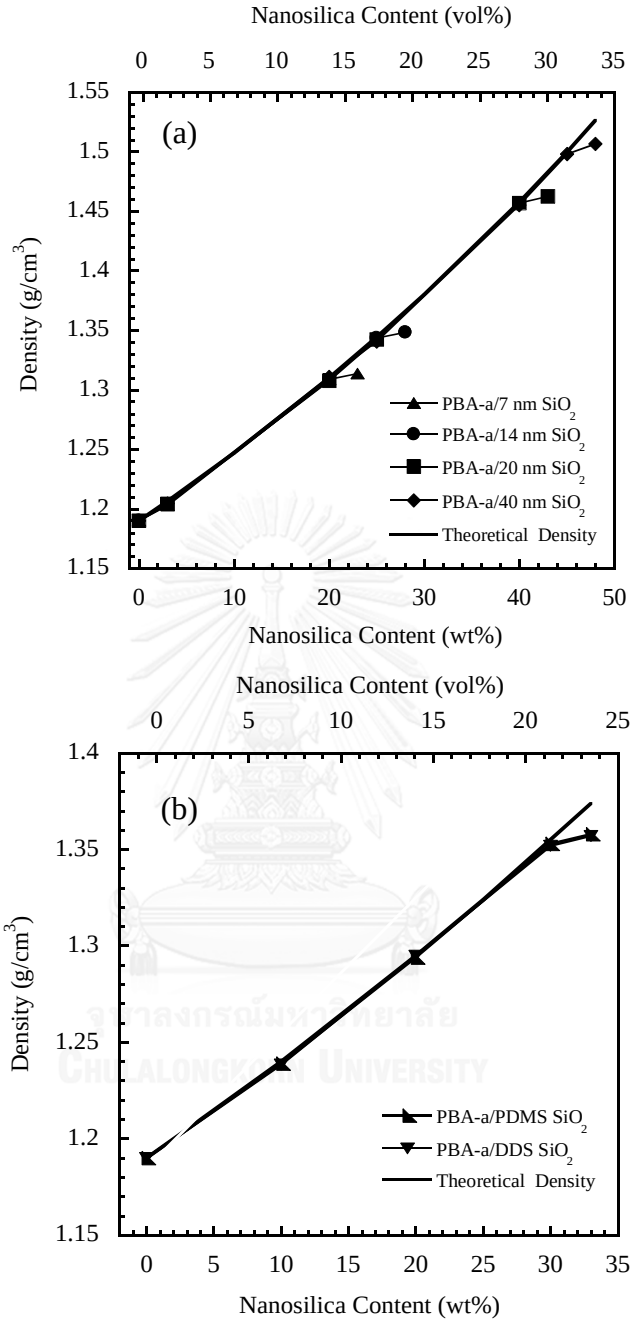

Figure 5.1 Maximum packing density of nanosilica filled polybenzoxazine composite with different nanosilica (a) particle size and (b) surface treatment. (-) theoretical density (▲) 7 nm, (●) 14 nm, (■) 20 nm, (♦) 40 nm, (▼) DDS treated silica and (◣) PMDS treated silica.

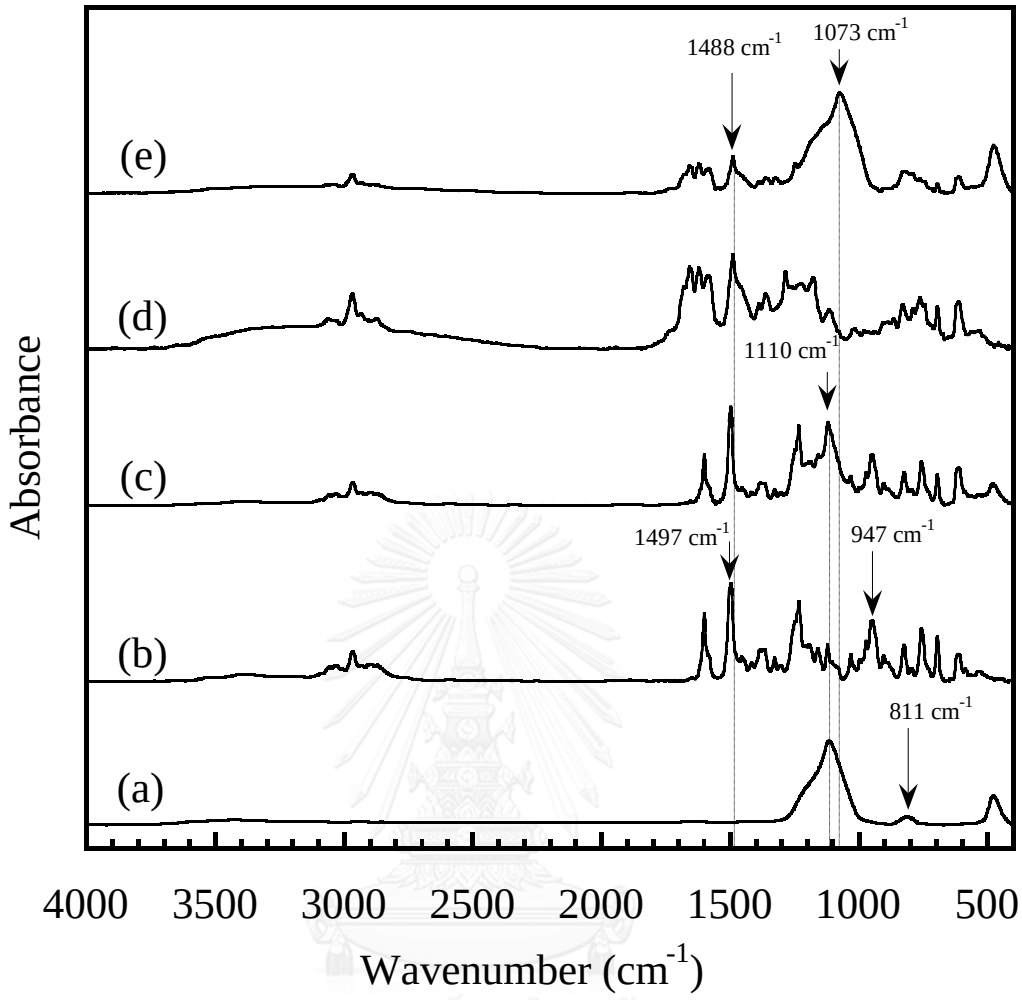

Figure 5.2 FT-IR spectra of (a) hydrophilic nanosilica, (b) benzoxazine monomer, (c) benzoxazine molding compound filled with nanosilica at content of 45 wt%, (d) polybenzoxazine and (e) polybenzoxazine composite filled with nanosilica at 45 wt%.

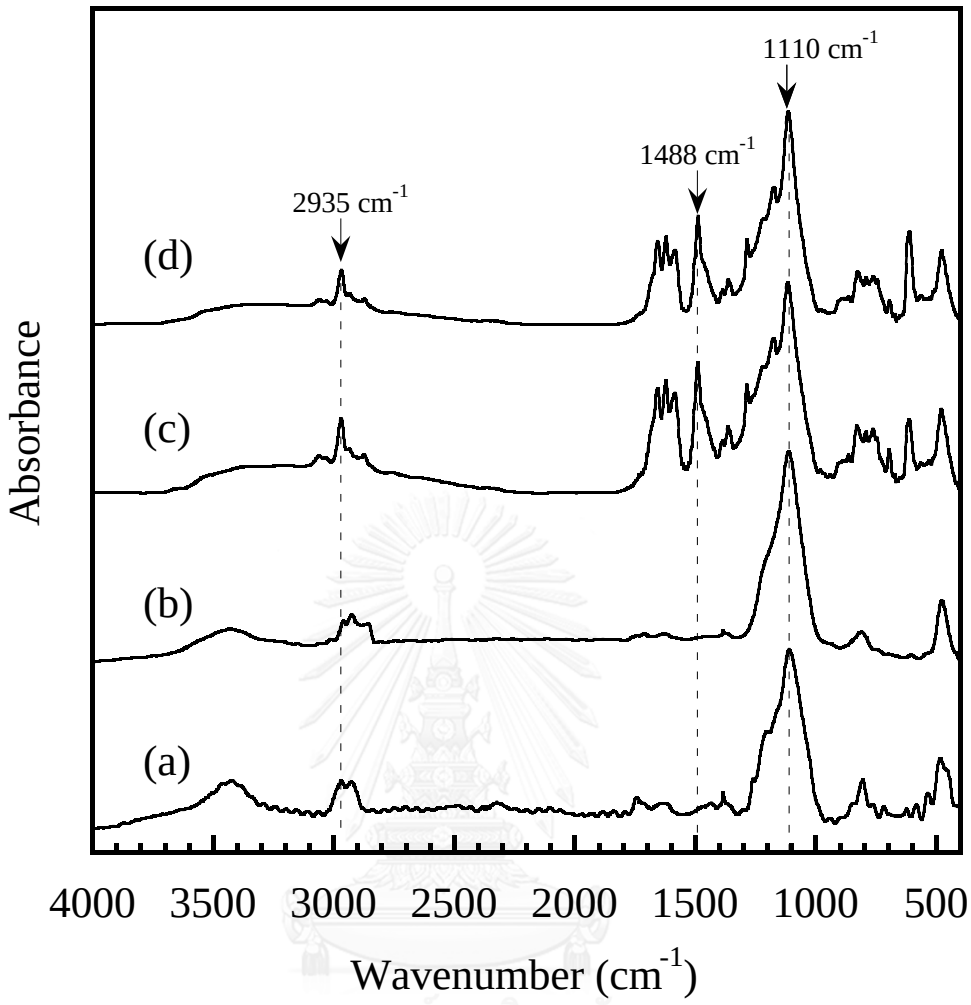

Figure 5.3 FT-IR spectra of (a) nanosilica after treated with polydimethylsiloxane (PDMS), (b) nanosilica after treated with dimethyldichlorosilane (DDS), nanosilica filled polybenzoxazine composite with (c) DDS treated silica and (d) PDMS treated silica.

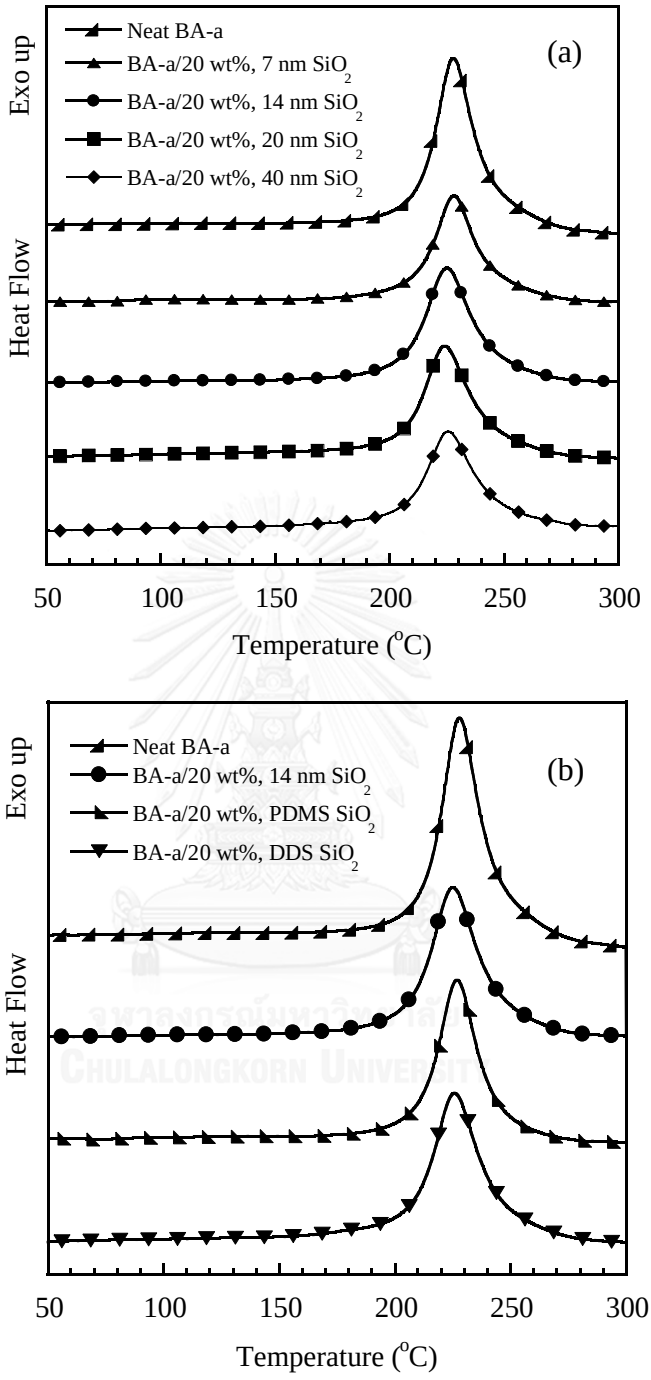

Figure 5.4 DSC thermograms of benzoxazine molding compound (a) particle sizes and (b) surface treatment at various contents of nanosilica : (◢) neat BA-a (▲) 7 nm, (●) 14 nm, (■) 20 nm, (♦) 40 nm, (▼) DDS treated silica and (◣) PDMS treated silica.

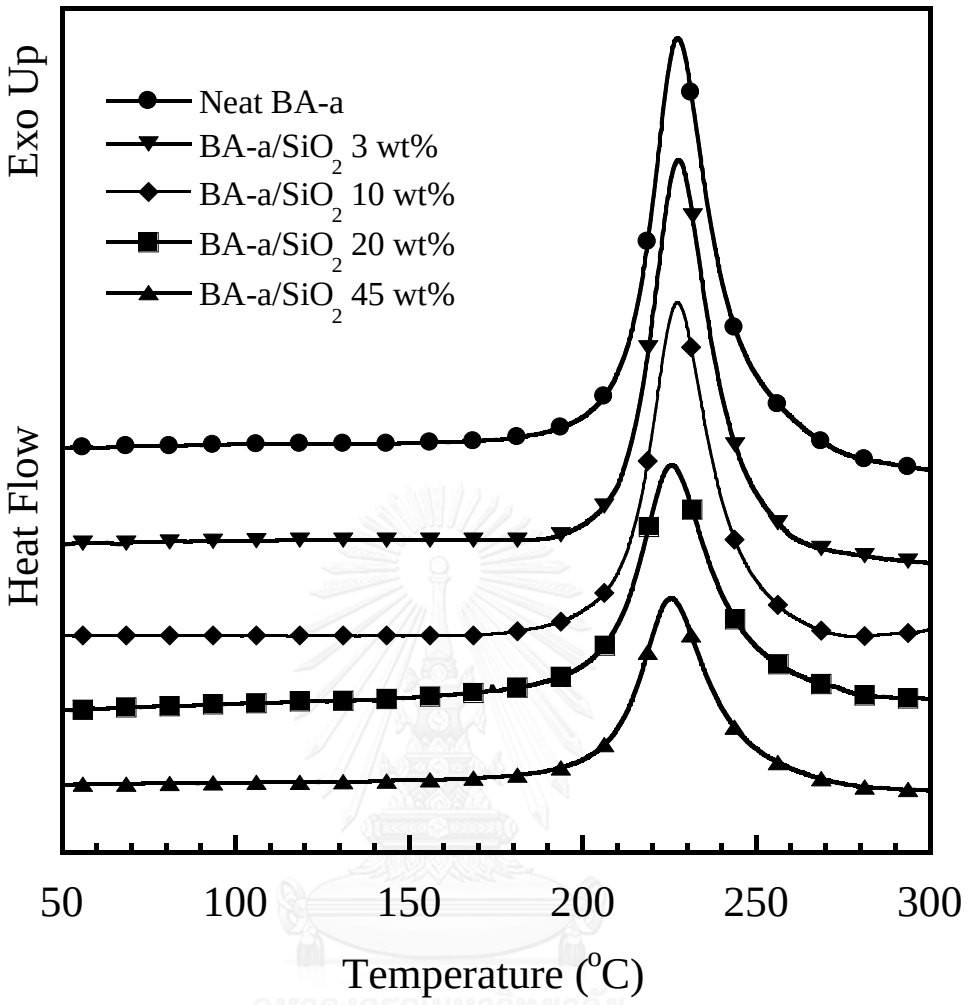

Figure 5.5 DSC thermograms of benzoxazine molding compound with nanosilica particle size 40 nm at different nanosilica contents: (●) neat BA-a, (▼) 3 wt%, (♦) 10 wt%, (■) 20 wt% and (▲) 45 wt%.

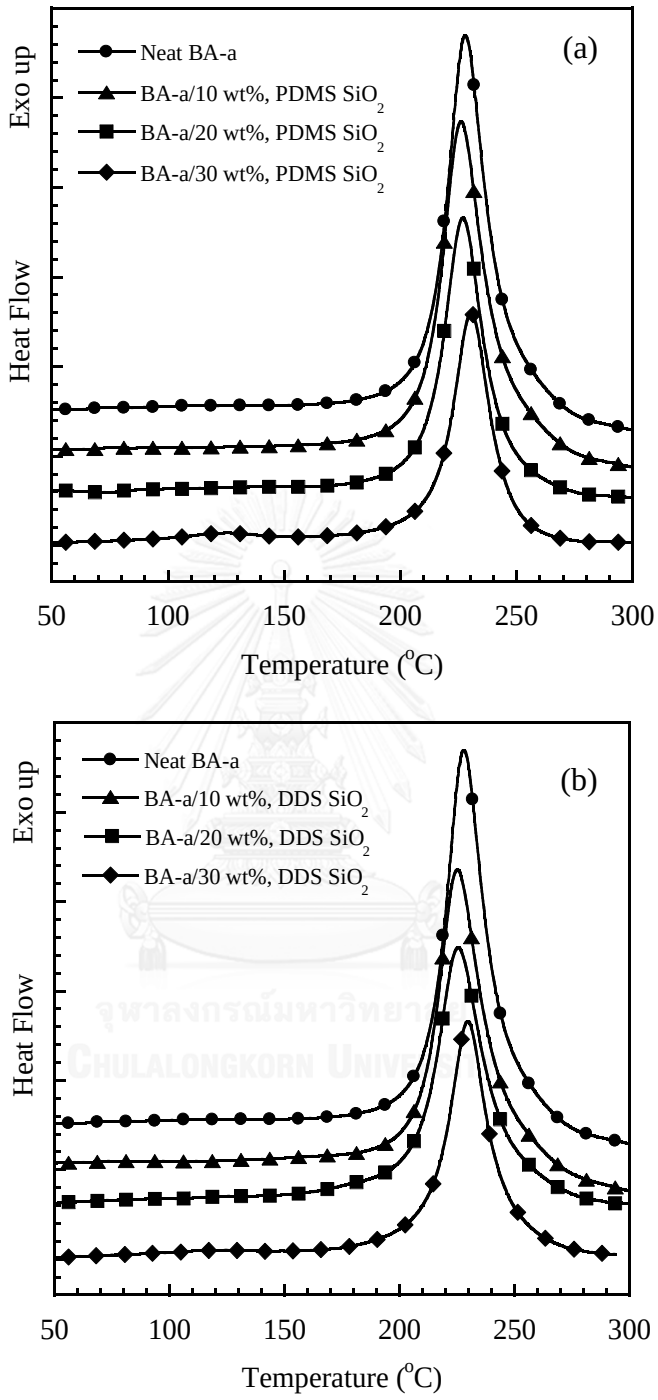

Figure 5.6 DSC thermograms of benzoxazine molding compound with (a) PDMS treated silica and (b) DDS treated silica at various nanosilica contents: (●) neat BA-a, (▲) 10 wt%, (■) 20 wt% and (♦) 30 wt%.

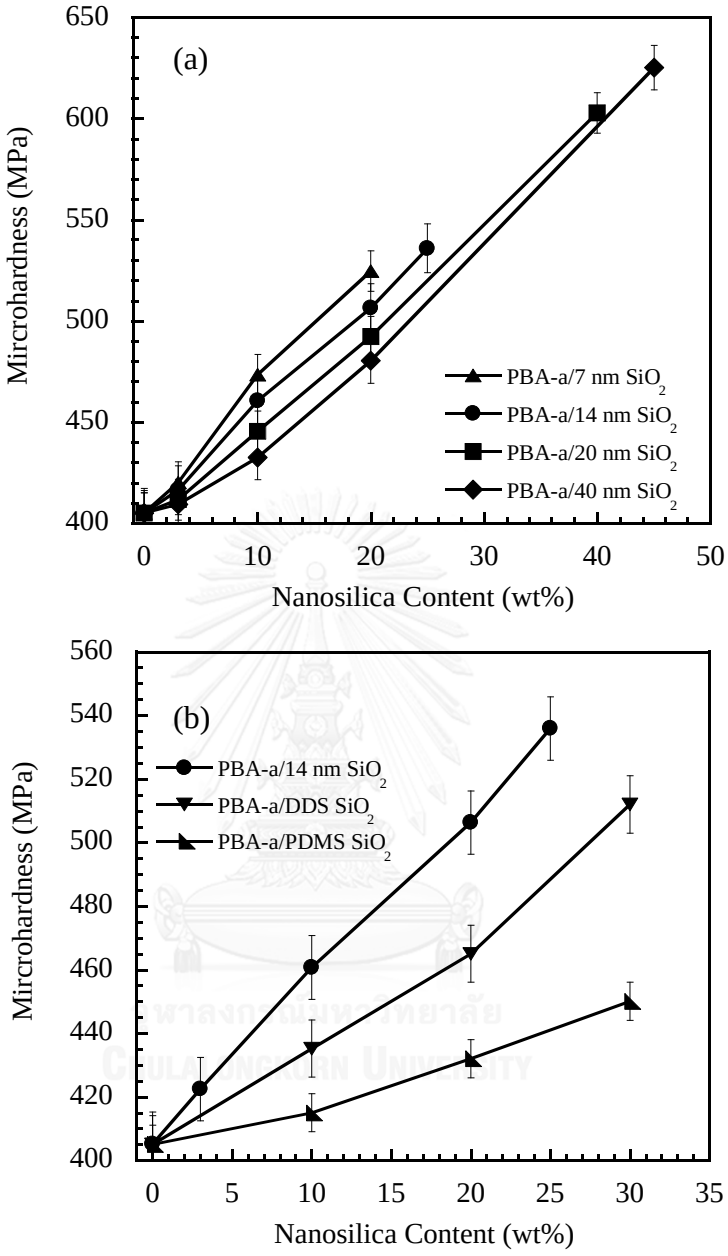

Figure 5.7 Microhardness of nanosilica filled polybenzoxazine composite (a) particle sizes and (b) surface treatment at various contents of nanosilica : (▲) 7 nm, (●) 14 nm, (■) 20 nm, (♦) 40 nm, (▼) DDS treated silica and (◣) PDMS treated silica.

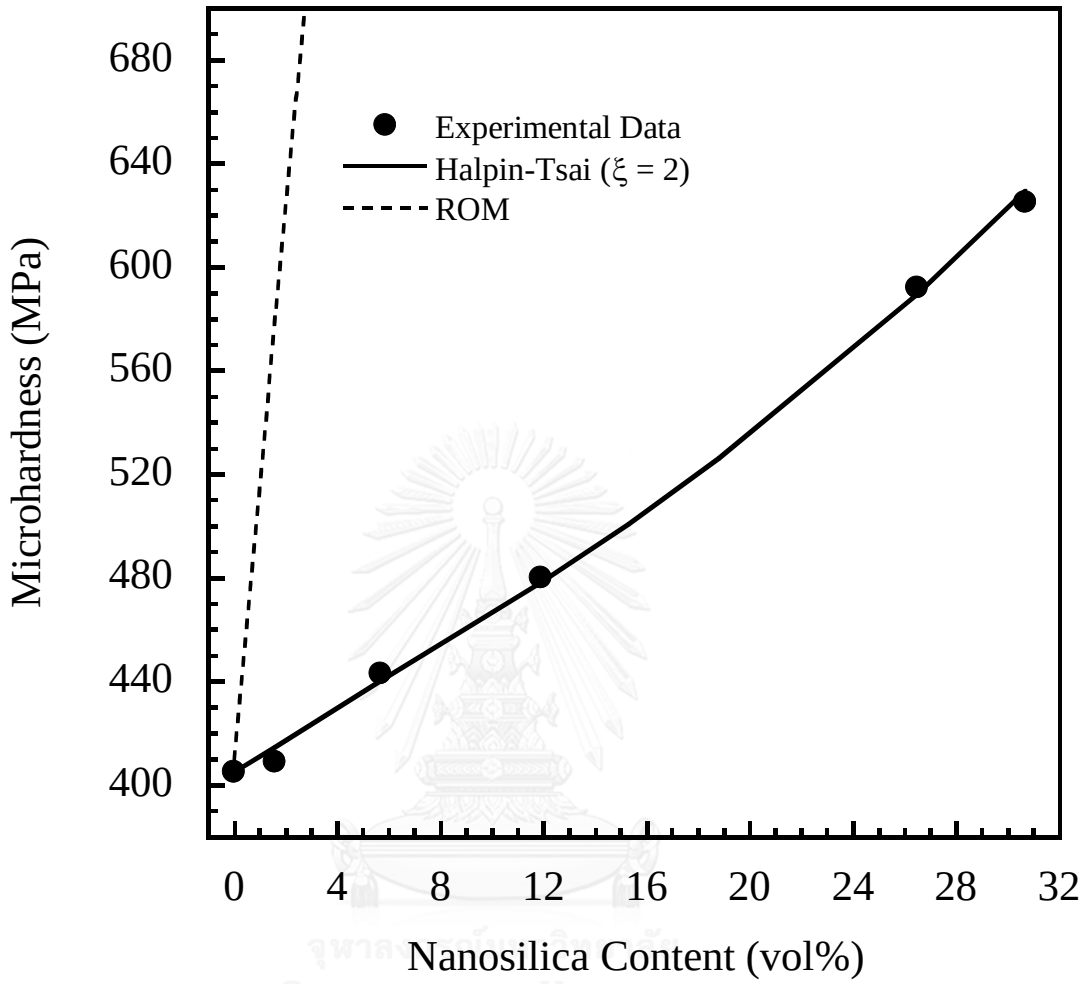

Figure 5.8 Microhardness value as a function of volume content of 40 nm nanosilica filled polybenzoxazine composite.

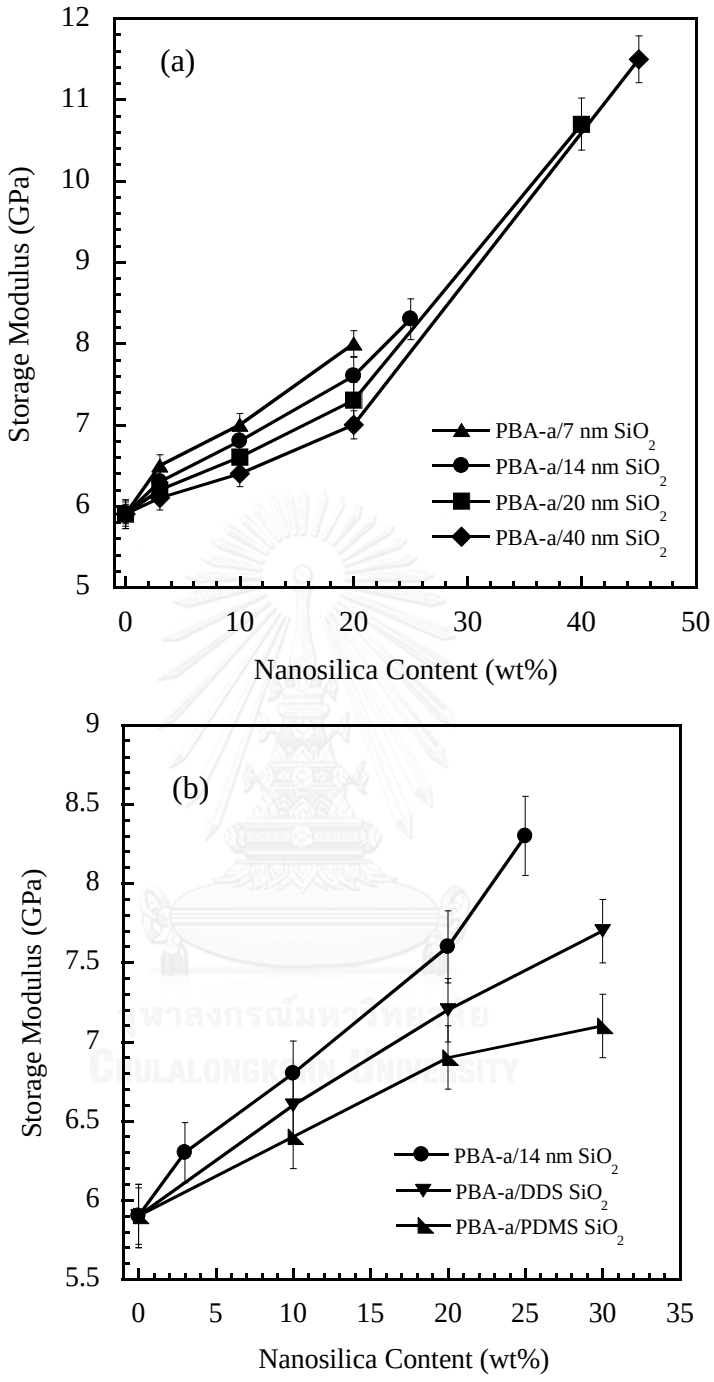

Figure 5.9 Storage modulus at 35 oC of nanosilica filled polybenzoxazine composite (a) particle sizes and (b) surface treatment at various contents of nanosilica: (▲) 7 nm, (●) 14 nm, (■) 20 nm, (♦) 40 nm, (▼) DDS treated silica and (◣) PDMS treated silica.

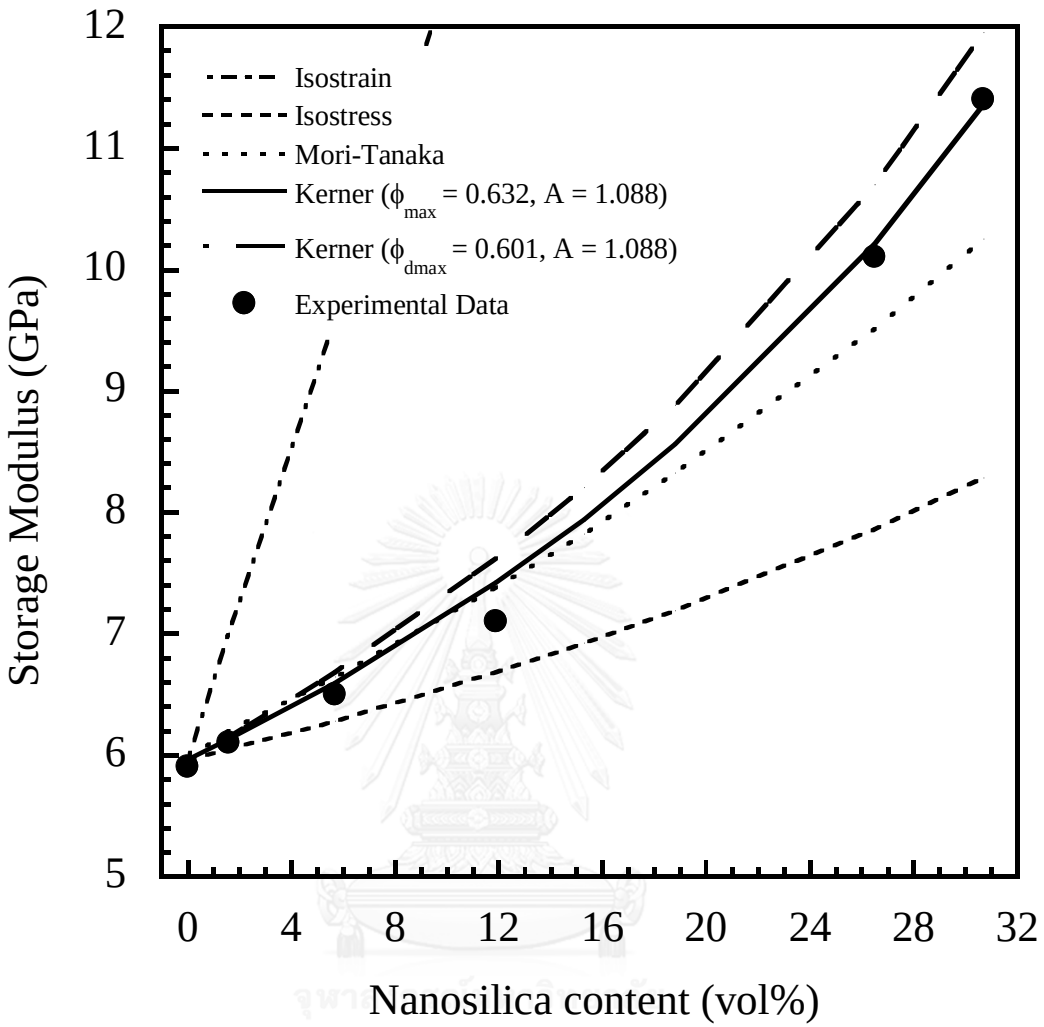

Figure 5.10 Storage modulus at 35oC versus volume content of 40 nm nanosilica filled polybenzoxazine composite.

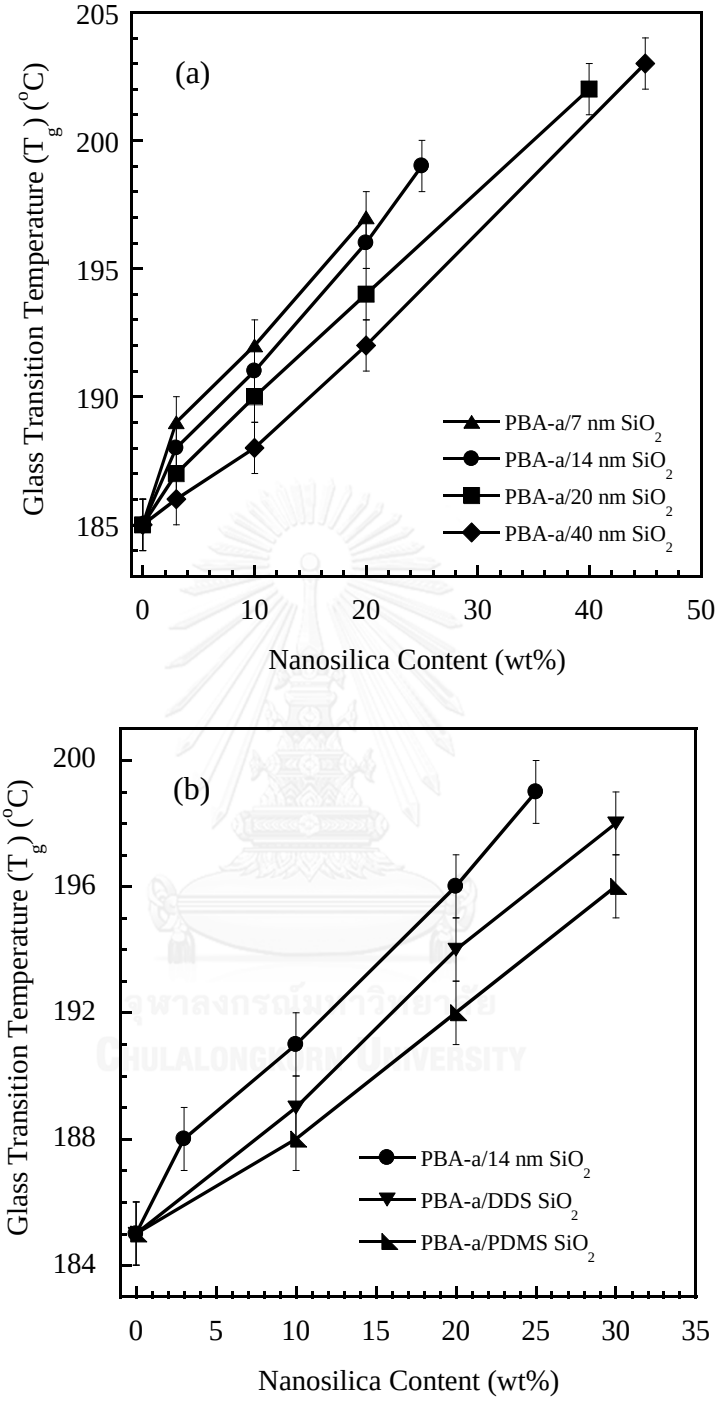

Figure 5.11 Glass transition temperature (T_g) of nanosilica filled polybenzoxazine composite (a) particle sizes and (b) surface treatment at various contents of nanosilica : (▲) 7 nm, (●) 14 nm, (■) 20 nm, (♦) 40 nm, (▼)DDS treated silica and (◣) PDMS treated silica.

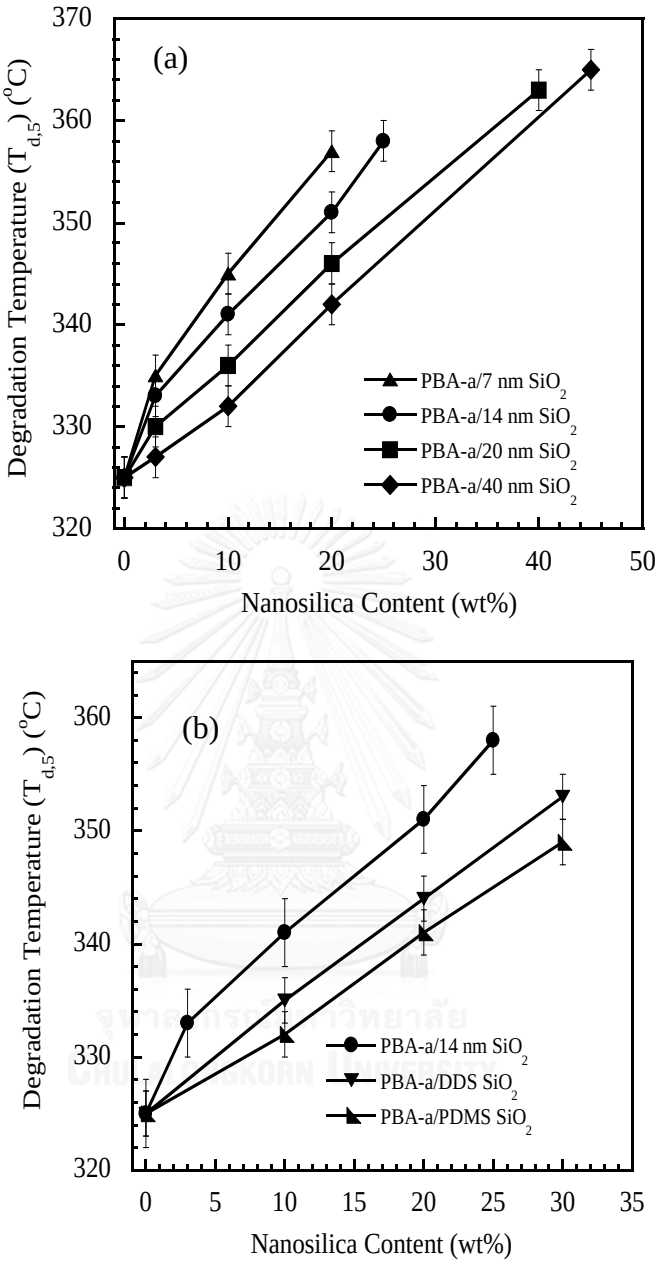

Figure 5.12 Degradation temperature at 5 % weight loss ($T_{d,5}$) of nanosilica filled polybenzoxazine composite (a) particle sizes and (b) surface treatment at various contents of nanosilica : (▲) 7 nm, (●) 14 nm, (■) 20 nm, (♦) 40 nm, (▼)DDS treated silica and (◣) PDMS treated silica.

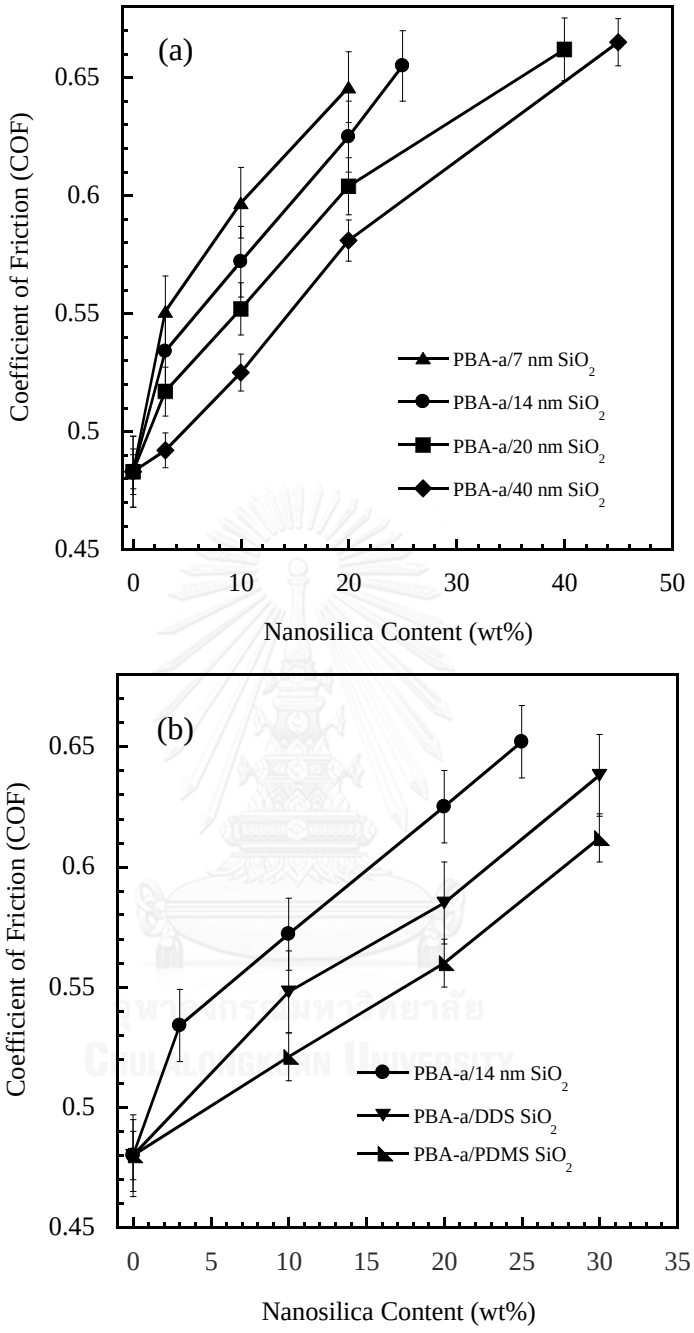

Figure 5.13 Coefficient of friction (COF) of nanosilica filled polybenzoxazine composites (a) particle sizes and (b) surface treatment at various contents of nanosilica : (▲) 7 nm, (●) 14 nm, (■) 20 nm, (♦) 40 nm, (▼)DDS treated silica and (◣) PDMS treated silica.

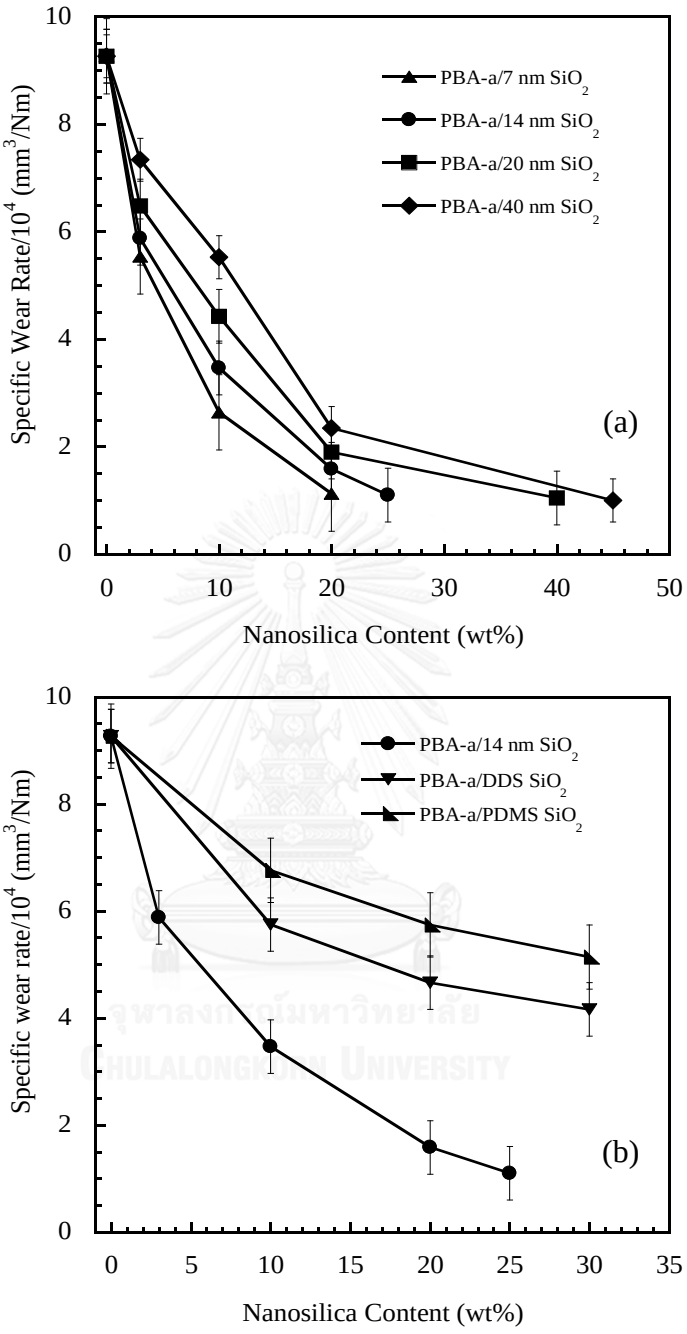

Figure 5.14 Specific wear rate of nanosilica filled polybenzoxazine composites (a) particle sizes and (b) surface treatment at various contents of nanosilica: (▲) 7 nm, (●) 14 nm, (■) 20 nm, (♦) 40 nm, (▼)DDS treated silica and (◣) PDMS treated silica.

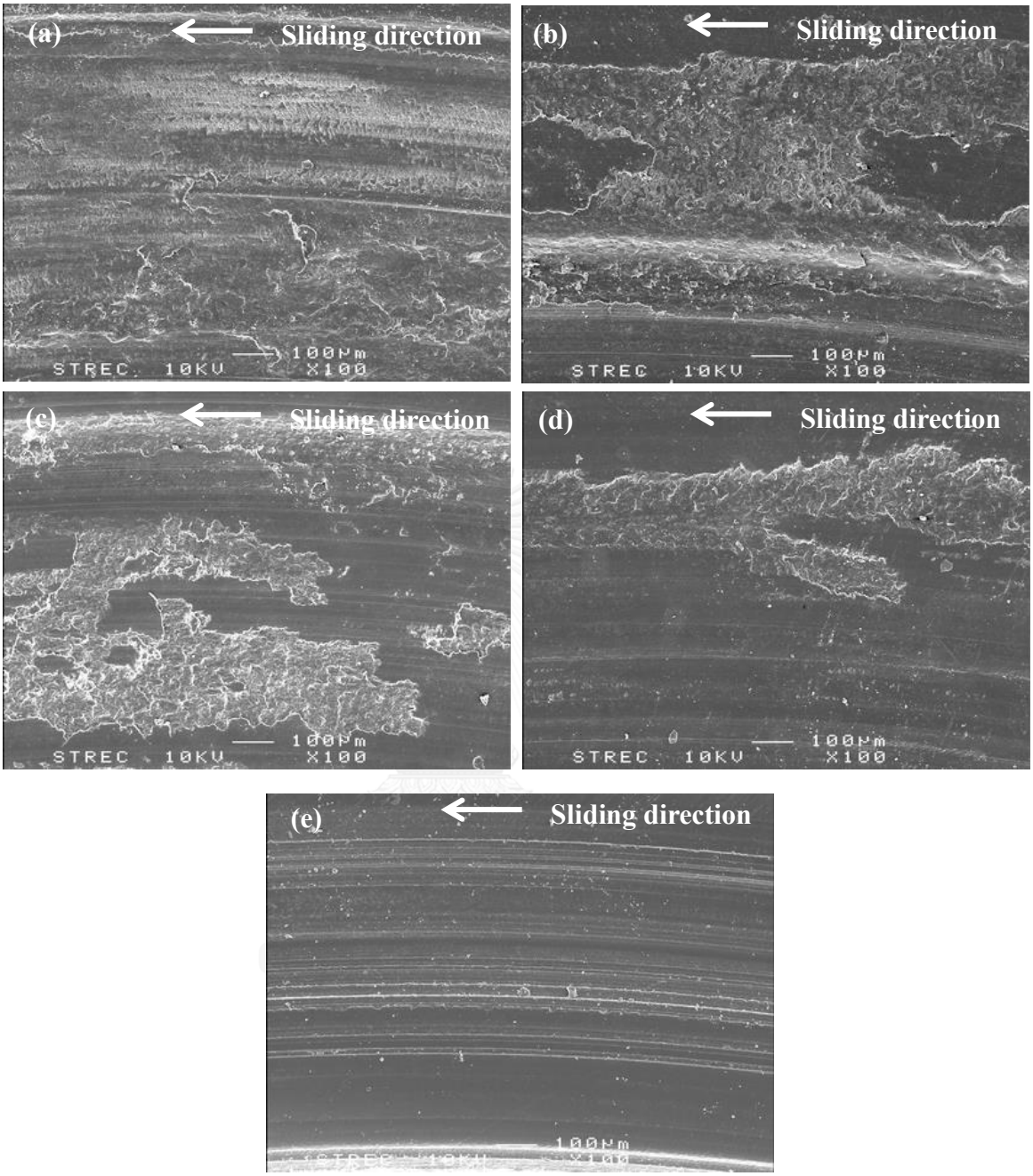

Figure 5.15 Worn surface of nanosilica filled polybenzoxazine composite with particle size 40 nm at various nanosilica contents: (a) 0 wt%, (b) 3 wt%, (c) 10 wt%, (d) 20 wt% and (e) 45 wt%.

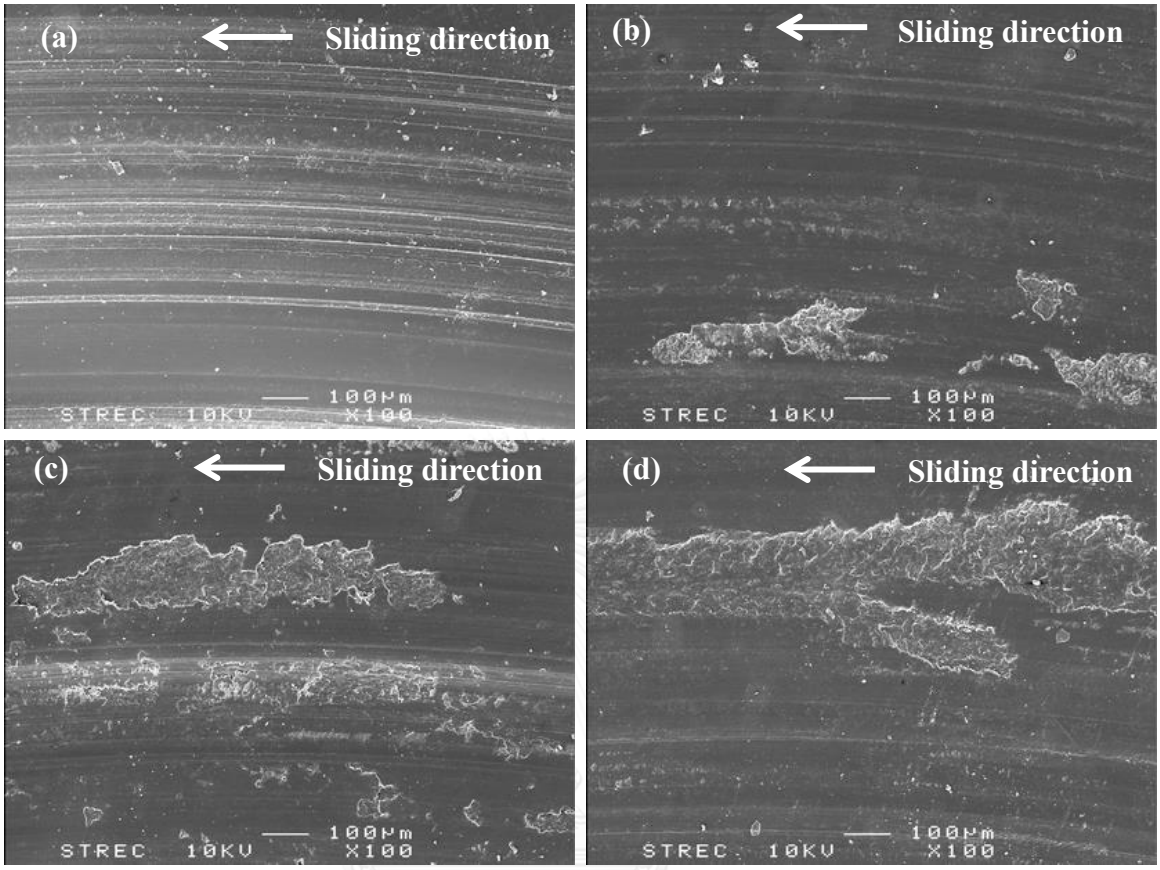

Figure 5.16 Worn surface of nanosilica filled polybenzoxazine composite at fixed content 20 wt% with various nanosilica particle sizes: (a) 7 nm, (b) 14 nm, (c) 20 nm and (d) 40 nm.

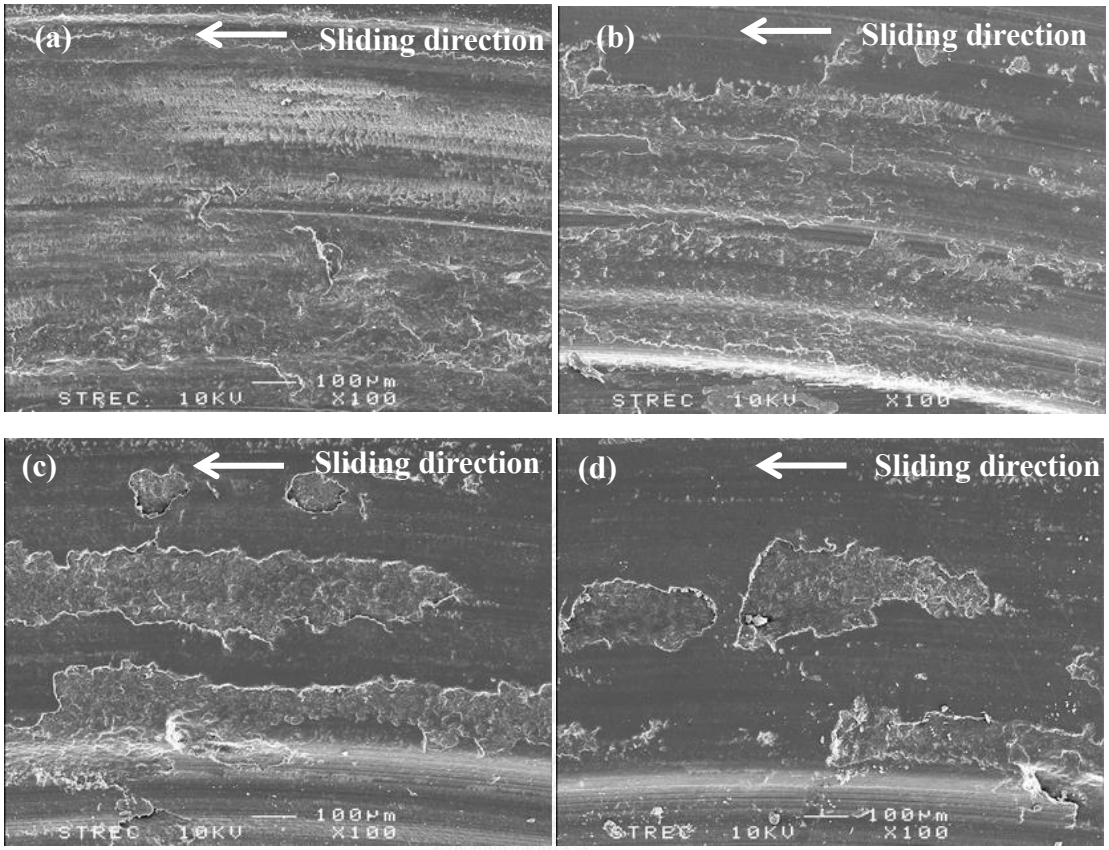

Figure 5.17 Worn surface of nanosilica filled polybenzoxazine composite with PDMS treated silica at various nanosilica content: (a) PBA-a, (b) 10 wt%, (c) 20 wt% and (d) 30 wt%.

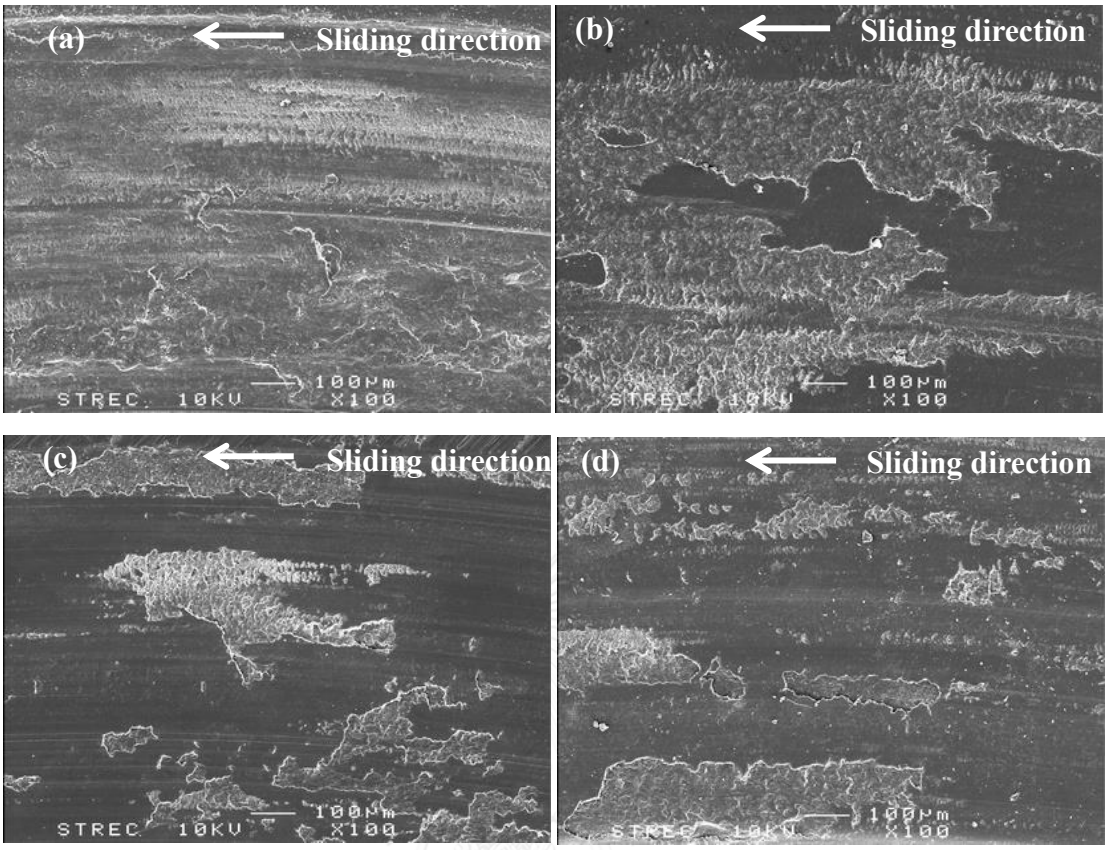

Figure 5.18 Worn surface of nanosilica filled polybenzoxazine composite with DDS treated silica at various nanosilica content: (a) PBA-a, (b) 10 wt%, (c) 20 wt% and (d) 30 wt%.

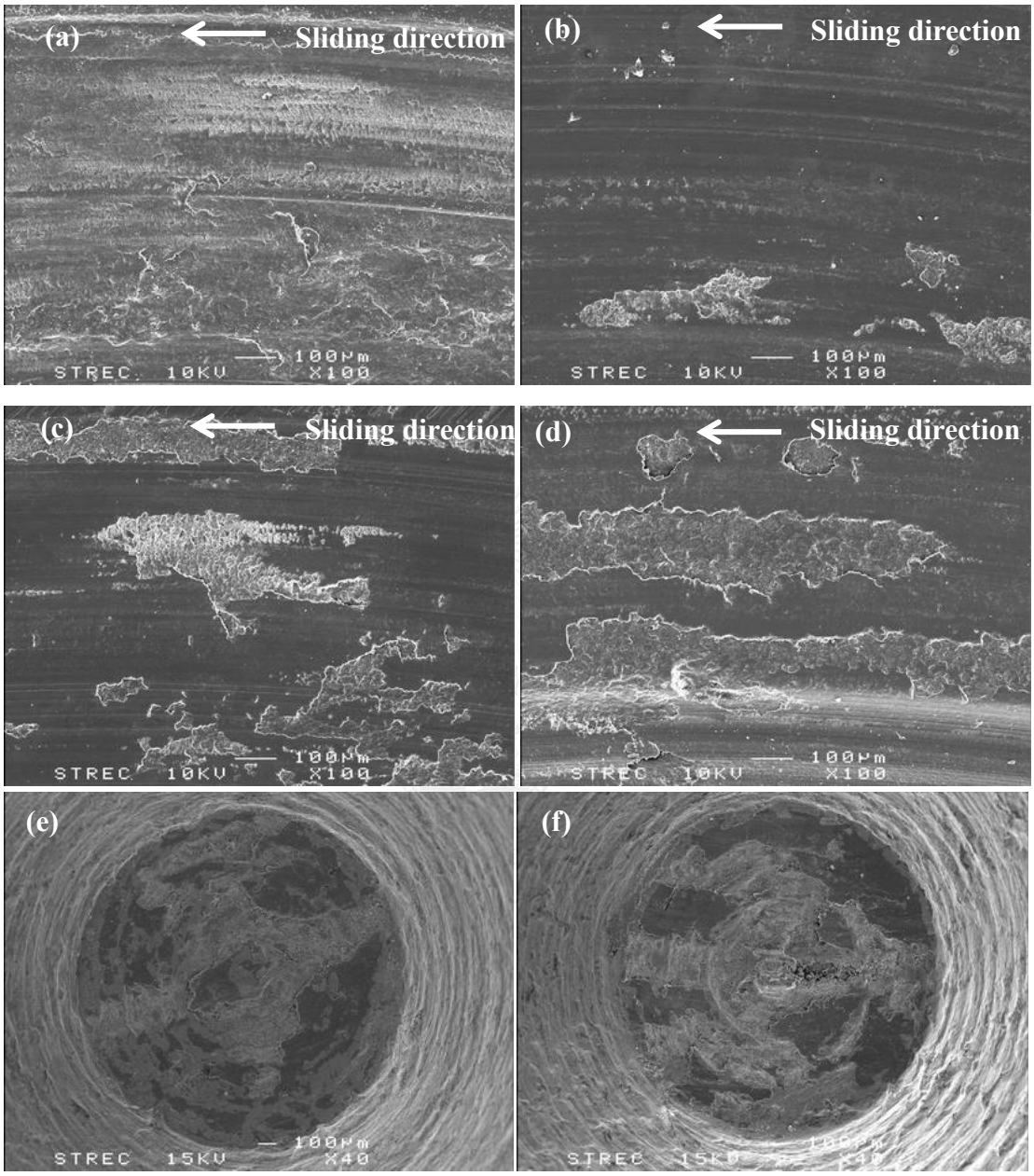

Figure 5.19 Worn surface of nanosilica filled polybenzoxazine composite at fixed content 20 wt% with different surface treatment of nanosilica : (a) PBA-a, (b) silica 14 nm, (c) DDS treated silica and (d) PDMS treated silica. SEM micrograph of steel pin after sliding against nanocomposite filled with (e) silica 14 nm (untreated) and (f) treated surface silica.

Table 5.1. Mechanical property comparison of polymer matrix filled with nanosilica composite at maximum packing density with various particle sizes.

Matrix	**Maximum Filler Content (vol%)**	**Particle Size (nm)**	**Storage Modulus**		**ΔT_g^* (^oC)**	**Reference**
			Absolute value (GPa)	**Enhancement (%)**		
PBA-a	30.7	40	11.5	94.9	+18	-
	26.5	20	10.7	81.4	+17	-
	18.3	14	8.3	40.7	+14	-
Epoxy	14	25	4.2	31.8	-17	[62]
	13.4	20	3.9	30	-3	[65]
UA/TMPTA	26.5	20	5.0	56.2	-	[66]
Cyanate ester	20.7	40	4.8	75	+4	[2]
	3.4	12	3.1	15	+1	[2]

*$\Delta T_g = T_g$ of composite - T_g of matrix

Table 5.2. Material parameters used in composite models predictions.

Parameters	**Symbol**	**Value**	**Reference**
Bulk modulus of polybenzoxazine, GPa	K_m	4.12	[45]
Bulk modulus of nanosilica, GPa	K_f	35.35	[42]
Shear modulus of polybenzoxazine,GPa	G_m	2.4	[45]
Shear modulus of nanosilica, GPa	G_f	29.9	[42]
Storage modulus of polybenzoxazine, GPa	E_m	5.95	[45]
Storage modulus of nanosilica, GPa	E_f	70	[42]
Poisson's ratio of polybenzoxazine	v_m	0.29	[45]
Poisson's ratio of nanosilica	v_f	0.17	[42]

CHAPTER VI
CONCLUSIONS

Nanocomposites of polybenzoxazine filled with nanosilica of various particle size and surface treatment were prepared by compression molding at various nanosilica loadings. Thermal, mechanical and tribological properties of the nanocomposites were systematically characterized for friction materials application. The maximum packing densities of untreated nanosilica-filled polybenzoxazine composites were 20, 25, 40 and 45 wt% for the nanosilica particle sizes of 7, 14, 20 and 40 nm, respectively. Mechanical and thermal properties of the untreated nanosilica filled polybenzoxazine composites such as storage modulus, microhardness, glass transition temperature and degradation temperature at 5% weight loss showed a substantial enhancement from the neat polybenzoxazine. Moreover, the values were found to increase with decreasing the size of nanosilica. The increment of the microhardness value of nanosilica filled polybenzoxazine composite was observed to be of an exponential type and can be predicted by Halpin-Tsai model. Furthermore, the storage modulus of nanocomposite filled with various nanosilica contents is well fitted by the generalized Kerner equation. FTIR spectra confirmed the bond formation of Si-O-C between silanol group of untreated nanosilica and polybenzoxazine. The coefficient of friction of polybenzoxazine filled

with smaller nanosilica size was higher than that of the composite with larger nanosilica size.

The increment of nanosilica content in composite was found to improve the coefficient of friction of the composite at each nanosilica particle size. The specific wear rate of the nanocomposite was found to decrease with increasing nanosilica content. At same content, the specific wear rate of the nanocomposite increased with increasing size of nanosilica. In addition, the maximum packing densities of treated nanosilica filled polybenzoxazine composites were measured to be 30 wt%. The composite with untreated nanosilica provided higher mechanical and thermal properties including specific wear rate and coefficient of friction compared to those of composite with treated nanosilica due to the chemical bond formation between the untreated nanosilica and the polybenzoxazine.

Moreover, the composite is attractive as a friction material for high thermal and mechanical properties, high coefficient of friction and very low specific wear rate. The composite for use as a friction material should has the chemical bond formation between the filler and the polymer matrix which should provide better interfacial interaction between the filler and the polymer matrix. The chemical bonding also provide a substantial reinforcing effect to the nanosilica filled polybenzoxazine composite such as thermal and mechanical properties.

REFERENCES

[1] Jajam, K.C. and Tippur, H.V., Quasi-static and dynamic fracture behavior of particulate polymer composites: A study of nano- vs. micro-size filler and loading-rate effects. Composites Part B: Engineering, 2012. 43(8): p. 3467-3481.

[2] Goertzen, W.K. and Kessler, M.R., Dynamic mechanical analysis of fumed silica/cyanate ester nanocomposites. Composites Part A: Applied Science and Manufacturing, 2008. 39(5): p. 761-768.

[3] Preghenella, M., Pegoretti, A., and Migliaresi, C., Thermo-mechanical characterization of fumed silica-epoxy nanocomposites. Polymer, 2005. 46(26): p. 12065-12072.

[4] Lin, L.-Y. and Kim, D.-E., Tribological properties of polymer/silica composite coatings for microsystems applications. Tribology International, 2011. 44(12): p. 1926-1931.

[5] Lai, S.-Q., Li, T.-S., Wang, F.-D., Li, X.-J., and Yue, L., The effect of silica size on the friction and wear behaviors of polyimide/silica hybrids by sol–gel processing. Wear, 2007. 262(9–10): p. 1048-1055.

[6] Kang, Y., Chen, X., Song, S., Yu, L., and Zhang, P., Friction and wear behavior of nanosilica-filled epoxy resin composite coatings. Applied Surface Science, 2012. 258(17): p. 6384-6390.

[7] Chen, Q., Xu, R., and Yu, D., Multiwalled carbon nanotube/polybenzoxazine nanocomposites: Preparation, characterization and properties. Polymer, 2006. 47(22): p. 7711-7719.

[8] Chrissafis, K., Paraskevopoulos, K.M., Stavrev, S.Y., Docoslis, A., Vassiliou, A., and Bikiaris, D.N., Characterization and thermal degradation mechanism of isotactic polypropylene/carbon black nanocomposites. Thermochimica Acta, 2007. 465(1–2): p. 6-17.

[9] Policandriotes, T. and Filip, P., Effects of selected nanoadditives on the friction and wear performance of carbon-carbon aircraft brake composites. Wear, 2011. 271(9-10): p. 2280-2289.

[10] Vaziri, H.S., Omaraei, I.A., Abadyan, M., Mortezaei, M., and Yousefi, N., Thermophysical and rheological behavior of polystyrene/silica nanocomposites: Investigation of nanoparticle content. Materials & Design, 2011. 32(8–9): p. 4537-4542.

[11] Periadurai, T., Vijayakumar, C.T., and Balasubramanian, M., Thermal decomposition and flame retardant behaviour of SiO2-phenolic nanocomposite. Journal of Analytical and Applied Pyrolysis, 2010. 89(2): p. 244-249.

[12] Goertzen, W.K. and Kessler, M.R., Thermal expansion of fumed silica/cyanate ester nanocomposites. Journal of Applied Polymer Science, 2008. 109(1): p. 647-653.

[13] Chrissafis, K., Paraskevopoulos, K.M., Papageorgiou, G.Z., and Bikiaris, D.N., Thermal and dynamic mechanical behavior of bionanocomposites: Fumed silica nanoparticles dispersed in poly(vinyl pyrrolidone), chitosan, and poly(vinyl alcohol). Journal of Applied Polymer Science, 2008. 110(3): p. 1739-1749.

[14] Ishida, H. and Koenig, J.L., The reinforcement mechanism of fiber-glass reinforced plastics under wet conditions: A review. Polymer Engineering & Science, 1978. 18(2): p. 128-145.

[15] Ishida, H. and Koenig, J.L., Fourier transform infrared spectroscopic study of the silane coupling agent/porous silica interface. Journal of Colloid and Interface Science, 1978. 64(3): p. 555-564.

[16] Frenzel, H., Silane coupling agents. Von EDWIN P. PLUEDDEMAHN. New York/London: Plenum Press 1982. IX, 235. Acta Polymerica, 1983. 34(10): p. 666-666.

[17] L, M.K. Silanes and other coupling agents. in International Symposium on Silanes and other Adhesion Promoters. 2009. Utrecht; Boston: VSP.

[18] Krysztafkiewicz, A. and Rager, B., Hydrated silicas modified by nonsilane pro-adhesion compounds. Journal of Adhesion Science and Technology, 1999. 13(3): p. 393-415.

[19] Impens, N.R.E.N., Van Der Voort, P., and Vansant, E.F., Silylation of micro-, meso- and non-porous oxides: A review. Microporous and Mesoporous Materials, 1999. 28(2): p. 217-232.

[20] Daniels, M.W. and Francis, L.F., Silane adsorption behavior, microstructure, and properties of glycidoxypropyltrimethoxysilane-modified colloidal silica coatings. Journal of Colloid and Interface Science, 1998. 205(1): p. 191-200.

[21] Chu, L., Daniels, M.W., and Francis, L.F., Use of (Glycidoxypropyl)trimethoxysilane as a Binder in Colloidal Silica Coatings. Chemistry of Materials, 1997. 9(11): p. 2577-2582.

[22] Agag, T. and Takeichi, T., Synthesis and characterization of benzoxazine resin-SiO2 hybrids by sol-gel process: The role of benzoxazine-functional silane coupling agent. Polymer, 2011. 52(13): p. 2757-2763.

[23] Rimdusit, S., Jubsilp, C., and Tiptipakorn, S., Polybenzoxazine Alloys, in Alloys and Composites of Polybenzoxazines: Properties and Applications. 2013, Springer Singapore: Singapore. p. 29-46.

[24] Yagci, Y., Kiskan, B., and Ghosh, N.N., Recent advancement on polybenzoxazine—A newly developed high performance thermoset. Journal of Polymer Science Part A: Polymer Chemistry, 2009. 47(21): p. 5565-5576.

[25] Almaslow, A., Ratnam, C.T., Ghazali, M.J., Talib, R.J., and Azhari, C.H., Effects of electron-beam and sulfur crosslinking of epoxidized natural rubber on the friction performance of semimetallic friction materials. Composites Part B: Engineering, 2013. 54(0): p. 377-382.

[26] Almaslow, A., Ghazali, M.J., Talib, R.J., Ratnam, C.T., and Azhari, C.H., Effects of epoxidized natural rubber–alumina nanoparticles (ENRAN) composites in semi-metallic brake friction materials. Wear, 2013. 302(1–2): p. 1392-1396.

[27] Wu, Y., Zeng, M., Jin, H., Xu, Q., Lu, L., Wang, J., and Hou, S., Effects of Glass-to-Rubber Transition on the Friction Properties of ZrO2 Reinforced Polybenzoxazine Nanocomposites. Tribology Letters, 2012. 47(3): p. 389-398.

[28] Wu, Y., Jin, H., Hou, S., and Zeng, M., Effects of glass-to-rubber transition on the temperature, load and speed sensitivities of nano-ZrO2 reinforced polybenzoxazine. Wear, 2013. 297(1–2): p. 1025-1031.

[29] Yan, H.X., Jia, Y., Li, M.L., and Li, T.T., The tribological properties of benzoxazine-bismaleimides composites with functionalized nano-SiO2. Journal of Applied Polymer Science, 2013. 129(6): p. 3150-3155.

[30] Kurihara, S., Idei, H., Aoyagi, Y., and Okumura, N., *Thermosetting Resin Material* 2010, Google Patents.

[31] Kurihara, S., Idei, H., Aoyagi, Y., and Kuroe, M., *Binder Resin For Friction Material, Binder Resin Composition For Friction Material, Composite Material For Friction Material Containing The Same, Friction Material And Production Method Thereof*, 2012, Google Patents.

[32] Wu, Y., Zeng, M., Yu, L., and Fan, L., Synergistic effect of nano- and micrometer-size ceramic fibers on the tribological and thermal properties of automotive brake lining. Journal of Reinforced Plastics and Composites, 2010. 29(18): p. 2732-2743.

[33] Zhang, M.Q., Rong, M.Z., Yu, S.L., Wetzel, B., and Friedrich, K., Effect of particle surface treatment on the tribological performance of epoxy based nanocomposites. Wear, 2002. 253(9–10): p. 1086-1093.

[34] Callister, W.D., Materials Science And Engineering: An Introduction. 2007: John Wiley & Sons.

[35] Zou, H., Wu, S., and Shen, J., Polymer/Silica Nanocomposites: Preparation, Characterization, Properties, and Applications. Chemical Reviews, 2008. 108(9): p. 3893-3957.

[36] Platzer, N., Handbook of fillers for plastics, Harry S. Katz and John V. Milewski, Eds., Van Nostrand Reinhold, New York, 1987, 467 pp. Journal of Polymer Science Part C: Polymer Letters, 1988. 26(6): p. 274-274.

[37] Barthel, H., Rösch, L., and Weis, J., Fumed Silica - Production, Properties, and Applications, in Organosilicon Chemistry II. 2008, Wiley-VCH Verlag GmbH. p. 761-778.

[38] Kim, H.C.a.D., G. D. , Encyclopedia of Nanoscience and Nanotechnology. 2005, New York: Taylor & Francis.

[39] Jana, S.C. and Jain, S., Dispersion of nanofillers in high performance polymers using reactive solvents as processing aids. Polymer, 2001. 42(16): p. 6897-6905.

[40] Fu, S.-Y., Feng, X.-Q., Lauke, B., and Mai, Y.-W., Effects of particle size, particle/matrix interface adhesion and particle loading on mechanical properties of particulate–polymer composites. Composites Part B: Engineering, 2008. 39(6): p. 933-961.

[41] Mottola, H.A. and Steinmetz, J.R., Chemically modified surfaces: proceedings of the Fourth Symposium on Chemically Modified Surfaces, Chadds Ford, Pennsylvania, USA, July 31-August 2, 1991. 1992: Elsevier.

[42] Takeichi, T., Zeidam, R., and Agag, T., Polybenzoxazine/clay hybrid nanocomposites: influence of preparation method on the curing behavior and properties of polybenzoxazines. Polymer, 2002. 43(1): p. 45-53.

[43] Ishida, H., *Process for preparation of benzoxazine compounds in solventless systems*, 1996, Google Patents.

[44] Rimdusit, S., Tiptipakorn, S., Jubsilp, C., and Takeichi, T., Polybenzoxazine alloys and blends: Some unique properties and applications. Reactive and Functional Polymers, 2013. 73(2): p. 369-380.

[45] Ishida, H. and Agag, T., Handbook of Benzoxazine Resins. 2011: Elsevier Science.

[46] Ning, X. and Ishida, H., Phenolic materials via ring-opening polymerization of benzoxazines: Effect of molecular structure on mechanical and dynamic mechanical properties. Journal of Polymer Science Part B: Polymer Physics, 1994. 32(5): p. 921-927.

[47] Nair, C.P.R., Advances in addition-cure phenolic resins. Progress in Polymer Science, 2004. 29(5): p. 401-498.

[48] Schallamach, A., Abrasion of rubber by a needle. Journal of Polymer Science, 1952. 9(5): p. 385-404.

[49] Briscoe, B., Wear of polymers: an essay on fundamental aspects. Tribology International, 1981. 14(4): p. 231-243.

[50] Briscoe, B.J. and Sinha, S.K., Wear of polymers. Proceedings of the Institution of Mechanical Engineers, Part J: Journal of Engineering Tribology, 2002. 216(6): p. 401-413.

[51] Friedrich, K., Lu, Z., and Hager, A.M., Recent advances in polymer composites' tribology. Wear, 1995. 190(2): p. 139-144.

[52] Briscoe, B.J. and Sinha, S.K. Tribology of Polymeric Nanocomposites (Second Edition). 2013, Oxford: Butterworth-Heinemann.

[53] Dueramae, I., Jubsilp, C., Takeichi, T., and Rimdusit, S., High thermal and mechanical properties enhancement obtained in highly filled polybenzoxazine nanocomposites with fumed silica. Composites Part B: Engineering, 2014. 56(0): p. 197-206.

[54] Liu, L., Gu, A., Fang, Z., Tong, L., and Xu, Z., The effects of the variations of carbon nanotubes on the micro-tribological behavior of carbon nanotubes/bismaleimide nanocomposite. Composites Part A: Applied Science and Manufacturing, 2007. 38(9): p. 1957-1964.

[55] Wang, Q., Xue, Q., and Shen, W., The friction and wear properties of nanometre SiO2 filled polyetheretherketone. Tribology International, 1997. 30(3): p. 193-197.

[56] Chapter 3 Improvement of Lubricity, in Tribology Series, Y. Yukisaburo, Editor. 1990, Elsevier. p. 143-202.

[57] Yan, C., Fan, X., Li, J., and Zhiqi Shen, S., Study of surface-functionalized nano-SiO2/polybenzoxazine composites. Journal of Applied Polymer Science, 2011. 120(3): p. 1525-1532.

[58] German, R.M., Particle Packing Characteristics. 1989: Metal Powder Industries Federation.

[59] Zhang, H., Zhang, Z., Friedrich, K., and Eger, C., Property improvements of in situ epoxy nanocomposites with reduced interparticle distance at high nanosilica content. Acta Materialia, 2006. 54(7): p. 1833-1842.

[60] Chen, H., Zhou, S., Gu, G., and Wu, L., Study on Modification and Dispersion of Nano-silica. Journal of Dispersion Science and Technology, 2005. 26(1): p. 27-37.

[61] Landel, R.F. and Nielsen, L.E., Mechanical Properties of Polymers and Composites, Second Edition. 1993: Taylor & Francis.

[62] Zhang, H., Tang, L.-C., Zhang, Z., Friedrich, K., and Sprenger, S., Fracture behaviours of in situ silica nanoparticle-filled epoxy at different temperatures. Polymer, 2008. 49(17): p. 3816-3825.

[63] Goyal, R.K., Tiwari, A.N., and Negi, Y.S., Microhardness of PEEK/ceramic micro- and nanocomposites: Correlation with Halpin–Tsai model. Materials Science and Engineering: A, 2008. 491(1–2): p. 230-236.

[64] Halpin, J.C. and Kardos, J.L., The Halpin-Tsai equations: A review. Polymer Engineering & Science, 1976. 16(5): p. 344-352.

[65] Johnsen, B.B., Kinloch, A.J., Mohammed, R.D., Taylor, A.C., and Sprenger, S., Toughening mechanisms of nanoparticle-modified epoxy polymers. Polymer, 2007. 48(2): p. 530-541.

[66] Zhang, H., Zhang, H., Tang, L., Zhang, Z., Gu, L., Xu, Y., and Eger, C., Wear-resistant and transparent acrylate-based coating with highly filled nanosilica particles. Tribology International, 2010. 43(1–2): p. 83-91.

[67] Ferch, H., The Use of Hydrophobic AEROSIL in the Coatings Industry. Technical Bulletin Pigments, 1987. 18.

[68] Bhimaraj, P., Burris, D., Sawyer, W.G., Toney, C.G., Siegel, R.W., and Schadler, L.S., Tribological investigation of the effects of particle size, loading and crystallinity on poly(ethylene) terephthalate nanocomposites. Wear, 2008. 264(7–8): p. 632-637.

[69] Akinci, A., Sen, S., and Sen, U., Friction and wear behavior of zirconium oxide reinforced PMMA composites. Composites Part B: Engineering, 2014. 56: p. 42-47.

[70] Xing, X.S. and Li, R.K.Y., Wear behavior of epoxy matrix composites filled with uniform sized sub-micron spherical silica particles. Wear, 2004. 256(1–2): p. 21-26.

APPENDIX

VITA